3. Darstellung einzelner Studienergebnisse

3.1 Blockade des Mineralokortikoid-Rezeptors in einem Angiotensin II-abhängigen Tiermodell

Klinische Daten belegen den therapeutischen Nutzen einer Blockade des MR zusätzlich zur Hemmung der Angiotensin II-Wirkung. Die Wirkmechanismen von Aldosteron und seinem Rezeptor sind bisher nicht vollständig verstanden. Wir untersuchten deshalb den Effekt einer alleinigen Blockade des MR beim Angiotensin II-induzierten Endorganschaden. Für die Experimente nutzten wir ein Rattenmodell mit aktiviertem Renin-Angiotensin-Aldosteron-System (RAAS), welches Blutdruck-unabhängig einen kardiovaskulären Endorganschaden entwickelt [25,26]. Die Tiere sind für das humane Renin und das humane Angiotensinogen transgen (dTGR). Die daraus resultierenden Angiotensin II-Spiegel sind in Herz, Nieren und Plasma im Vergleich zu nicht-transgenen Sprague-Dawley-Ratten drei- bis fünffach erhöht. Bei diesen Tieren werden neben einem erhöhten Blutdruck ausgeprägte Gefäßveränderungen mit Gefäßhypertrophie und –verschlüssen beobachtet. Sie sterben im Alter von 7 bis 9 Wochen und haben zu diesem Zeitpunkt eine schwere linksventrikuläre Hypertrophie und eine ausgeprägte Albuminurie. Eine alleinige Blutdrucksenkung ohne Renin- bzw. Angiotensin II-Inhibition kann diese Veränderungen nicht aufhalten, während die Blockade der Wirkungen von Renin oder Angiotensin II den Endorganschaden verhindert (dTGR; **Abb. 5**).

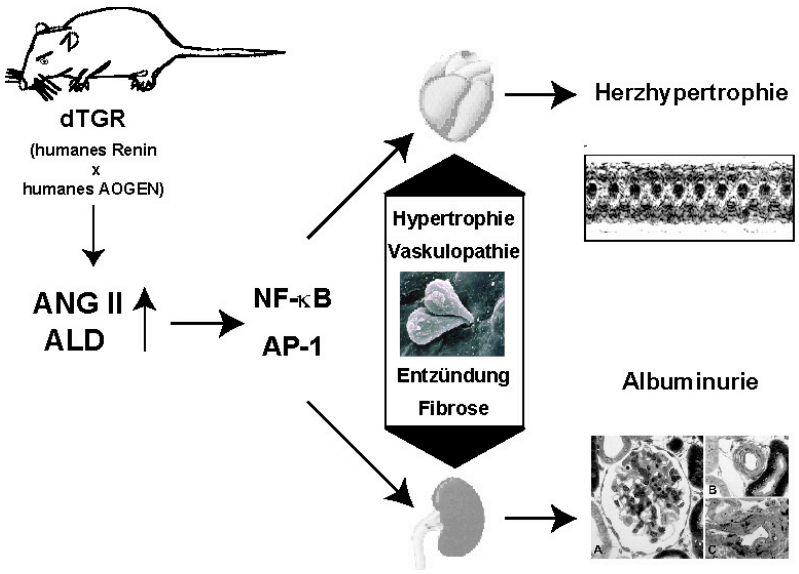

Abbildung 5: Phänotyp der dTGR (doppeltransgene Ratte). dTGR entwickeln schwere entzündlich-fibrotische Veränderungen in ihren Gefäßen (zu sehen sind Leukozytenadhäsion und Transmigration in die Gefäßwand von dTGR), zusätzlich eine ausgeprägte linksventrikuläre Hypertrophie (hier im Echokardiogramm ablesbar) und Niereninsuffizienz (abgebildet ist die Histologie aus der Niere mit fokaler Fibrose im Glomerulum (A) und Hypertrophie von kleinen Arterien (B, C); ANG II: Angiotensin II, ALD: Aldosteron, NF-κB: *nuclear factor-kappaB*, AP-1: *activated protein 1*).

Wir verglichen in dieser Studie Spironolakton-behandelte dTGR mit Valsartan-behandelten oder unbehandelten dTGR. Dazu wurden gleichaltrige, nicht-transgene Sprague-Dawley-Ratten untersucht. Das Studienschema ist in **Abbildung 6** zusammengefasst.

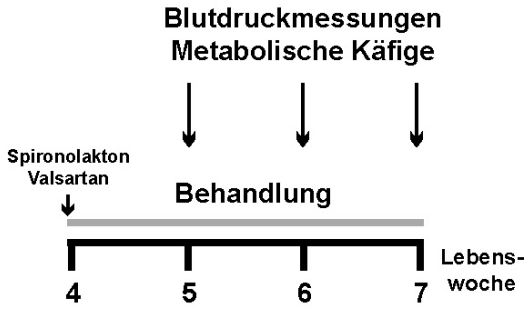

Abbildung 6: Design der Spironolakton-Studie

3.1.1 Einfluss auf Mortalität, Blutdruck, Herz- und Nierenfunktion

Bei unbehandelten dTGR ergab sich bis zur 7. Woche eine Mortalität von 45 %. Spironolakton reduzierte diese um 90%, während die Valsartan-behandelten Tiere und die Ratten aus der nicht-transgenen Kontrollgruppe bis zum Ende der Studie überlebten **(Abb. 7**).

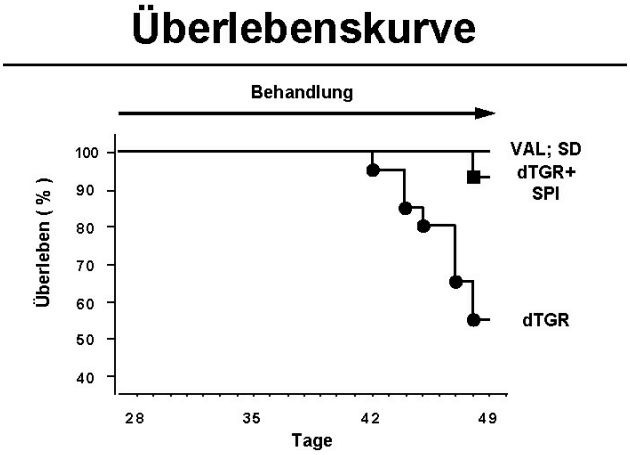

Abbildung 7: Spironolakton (Spi) steigert das Überleben in dTGR (VAL: Valsartan; SPI: Spironolakton; SD Sprague-Dawley: nicht-transgene Kontrollratten).

Spironolakton reduzierte den Blutdruck nur geringfügig, führte jedoch wie Valsartan zur Reduktion von Herzhypertrophie und Albuminurie. Spironolakton verhinderte den Endorganschaden partiell, während eine Valsartanbehandlung den Endorganschaden komplett verhinderte.

In einer ähnlich aufgebauten Studie untersuchten wir die Wirkung des spezifischen MR-Blockers Eplerenon im gleichen Tiermodell. Auch Eplerenon reduzierte die Mortalität und verhinderte die Ausbildung von Herzhypertrophie und diastolischer Dysfunktion am Herzen (**Reprint 3**; s.u.).

3.1.2 Wirkmechanismen durch die Blockade des Mineralokortikoid-Rezeptors

Zum Verständnis der zugrunde liegenden protektiven Mechanismen der Blockade des MR in dem Angiotensin II-abhängigen Tiermodell untersuchten wir die Plasmaspiegel von Aldosteron, die Histologie von Herz und Nieren, die Infiltration von Entzündungszellen und die Ablagerung von Bindegewebe in diesen Organen, die RNA-Expression von Wachstumsfaktoren und die Aktivität der Transkriptionsfaktoren AP-1 und NF-κB. Dabei waren die Plasmaspiegel von Aldosteron in den unbehandelten dTGR deutlich höher als in allen anderen Gruppen. Für die hohen Plasmaaldosteronspiegel ist zum einen das bei unbehandelten Tieren stark aktivierte RAAS verantwortlich; die Renin- und die Aldosteronspiegel korrelieren mit dem Krankheitsgrad der Ratten und präfinale dTGR weisen besonders hohe Hormonspiegel auf. Eine weitere mögliche Erklärung ist der verzögerte hepatische Abbau von Aldosteron durch das Rechtsherzversagen. In beiden Behandlungsgruppen fanden sich weniger infiltrierende Entzündungszellen und eine verminderte Ablagerung von Kollagen, Fibronektin und Laminin in Herz und Nieren. In dTGR war die mRNA-Expression von bFGF (*basic fibroblast growth factor*) deutlich erhöht. An Spironolakton-behandelten Tieren beobachteten wir eine Reduktion der bFGF-Überexpression um 75 %. Bei Valsartan-behandelten Tieren war die bFGF-Expression mit der von gesunden Kontrolltieren vergleichbar. Sowohl Spironolakton als auch Valsartan reduzierten die Bindungsaktivität der Transkriptionsfaktoren AP-1 (*activated protein-1*) und NF-κB (*nuclear factor-kappaB*).

Schlussfolgerung: Der MR vermittelt den Angiotensin II-induzierten Endorganschaden. Die zugrunde liegenden Mechanismen sind vom Blutdruck

unabhängig. Eine wichtige Rolle spielen der Wachstumsfaktor bFGF und die Transkriptionsfaktoren AP-1 und NF-κB.

Reprint 1

Fiebeler A, Schmidt F, Muller DN, Park JK, Dechend R, Bieringer M, Shagdarsuren E, Breu V, Haller H, Luft FC. Mineralocorticoid receptor affects AP-1 and nuclear factor-kappab activation in angiotensin II-induced cardiac injury.

***Hypertension*. 2001;37:787-93.**

Mineralocorticoid Receptor Affects AP-1 and Nuclear Factor-κB Activation in Angiotensin II–Induced Cardiac Injury

Anette Fiebeler,* Folke Schmidt,* Dominik N. Müller,* Joon-Keun Park, Ralf Dechend, Markus Bieringer, Erdenechimeg Shagdarsuren, Volker Breu, Hermann Haller, Friedrich C. Luft

Abstract—Aldosterone is implicated in cardiac hypertrophy and fibrosis. We tested the role of the mineralocorticoid receptor in a model of angiotensin II–induced cardiac injury. We administered spironolactone (SPIRO; 20 mg · kg^{-1} · d^{-1}), valsartan (VAL; 10 mg · kg^{-1} · d^{-1}), or vehicle to rats double transgenic for the human renin and angiotensinogen genes (dTGR). We investigated basic fibroblast growth factor (bFGF), platelet-derived growth factor, transforming growth factor-β_1, and the transcription factors AP-1 and nuclear factor (NF)-κB. We used immunohistochemistry, electrophoretic mobility shift assays, and TaqMan RT-PCR. Untreated dTGR developed hypertension, cardiac hypertrophy, vasculopathy, and fibrosis with a 50% mortality rates at 7 weeks. SPIRO and VAL prevented death and reversed cardiac hypertrophy, while only VAL normalized blood pressure. Both drugs prevented vasculopathy. bFGF was markedly upregulated in dTGR, whereas platelet-derived growth factor-B and transforming growth factor-β_1 were little changed. VAL and SPIRO suppressed this upregulation. Both AP-1 and NF-κB were activated in dTGR compared with controls. VAL and SPIRO reduced both transcription factors and reduced bFGF, collagen I, fibronectin, and laminin in the interstitium. These findings show that aldosterone promotes hypertrophy, cardiac remodeling, and fibrosis, independent of blood pressure. The effects involve AP-1, NF-κB, and bFGF. Mineralocorticoid receptor blockade downregulates these effectors and reduces angiotensin II–induced cardiac damage. **(*Hypertension*. 2001; 37[part 2]:787-793.)**

Key Words: angiotensin ■ nuclear factors ■ receptors, mineralocorticoid ■ spironolactone

In a recent study, patients with heart failure after myocardial infarction exhibited a 30% reduced mortality rates with mineralocorticoid receptor blockade compared with control subjects.[1] A direct relationship has been shown between death and serum aldosterone concentrations in heart failure patients.[2] After myocardial infarction, the renin-angiotensin-aldosterone system contributes to cardiac remodeling; local tissue angiotensin (Ang) II and aldosterone are increased.[3,4] The effects of aldosterone on the kidney are well recognized; however, less appreciated are the facts that aldosterone also induces collagen, fibronectin, and laminin and contributes directly to fibrosis.[5–7] Vascular smooth muscle and endothelial cells respond to aldosterone with increased ITP, $[Ca^{2+}]_i$, and protein kinase C activity, as well as with ion channel activation. Aldosterone-induced genes include the G protein K-Ras and several serum glucocorticoid kinase proteins.[8] Furthermore, genes important for cell cycle progression, such as c-*myc*, c-*fos*, and c-*jun*, are upregulated by aldosterone.[8] Aldosterone-induced cardiac fibrosis can be prevented with spironolactone (SPIRO), as well as with Ang II type 1 receptor (AT_1) blockade.[9] We investigated the effect of SPIRO in rats harboring the human renin and angiotensinogen genes (dTGR). They produce Ang II locally and develop hypertension and severe end-organ damage.[10]

Methods

Four-week-old male dTGR (n=20) and age-matched Sprague-Dawley (SD; n=10) rats were investigated after due approval. The dTGR line and characteristics have been described previously.[11] In the treatment groups (15 per group), dTGR rats received drugs for 3 weeks. Either SPIRO (20 mg · kg^{-1} · d^{-1} IP) or valsartan (VAL) (10 mg · kg^{-1} · d^{-1} PO) was administered. Immunohistochemical studies were performed as described previously.[12] Antibodies were purchased against monocyte/macrophages (ED-1; Serotec), rabbit anti-mouse IgG (DAKO), collagen I (South Bio ABS), fibronectin (Paesel), bFGF (Transduction Laboratories), and transforming growth factor (TGF)-β_1 (Santa Cruz). Nuclear extracts, electrophoretic mobility shift assay (EMSA), and supershift assay for nuclear factor (NF)-κB and AP-1 were performed according to a protocol described earlier.[12] Briefly, 10 μg total heart homogenates was incubated in binding reaction medium [0.66 μg poly(dI/dC), 1 μg BSA, 1 mmol/L DTT, 20 mmol/L HEPES, pH 8.4, 60 mmol/L KCl, and 8% Ficoll] with 0.5 ng of ^{32}P-dATP end-labeled oligonu-

Received October 25, 2000; first decision December 4, 2000; revision accepted December 14, 2000.

From the Franz Volhard Clinic and Max Delbrück Center, Medical Faculty of the Charité, Humboldt University of Berlin, and Department of Medicine-Nephrology, Hoffmann La Roche Inc, Basel, Schwitzerland; and Hannover Medical School, University of Hannover, Germany.

*These authors contributed equally to this work.

Correspondence to Dr Friedrich C. Luft, Franz Volhard Clinic, Wiltberg Str 50, 13125 Berlin, Germany. E-mail luft@fvk-berlin.de

Hypertension **is available at http://www.hypertensionaha.org**

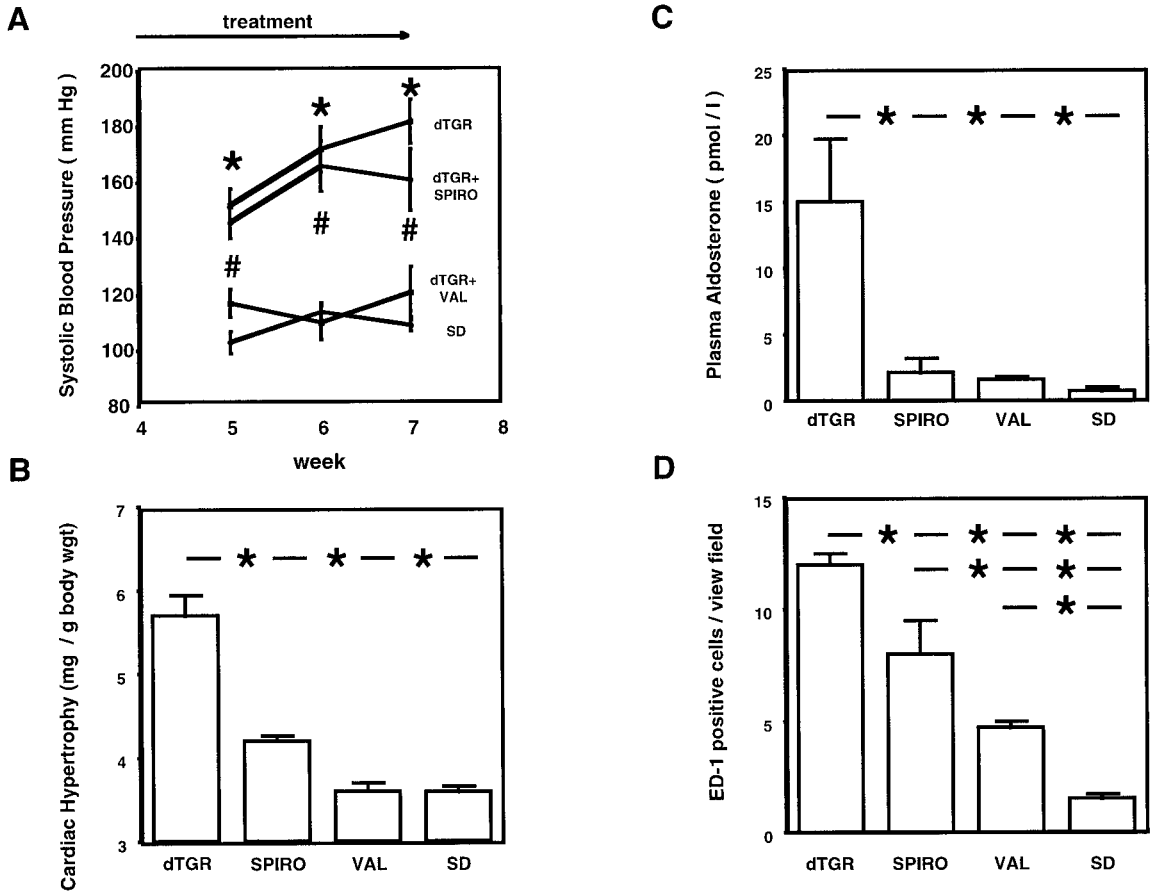

Figure 1. Systolic blood pressure (A), cardiac index (B), and plasma aldosterone concentrations (C) from vehicle-treated dTGR rats, SPIRO-treated dTGR rats, VAL-treated dTGR rats, and vehicle-treated SD rats. SPIRO had a marginal blood pressure-reducing effect compared with VAL treatment. Cardiac index and plasma aldosterone levels were both reduced by SPIRO and VAL treatment. D, Quantified data for ED-1–positive cell infiltration and amelioration with SPIRO and VAL.

cleotide, containing the NF-κB–binding site from the MHC enhancer (H2K: 5′-gatcCAGGGCTGGGGATTCCCCATCTCCACAGG)or containing the consensus sequence for AP-1 (Santa Cruz) (5′-GAT CGA ACT GAC CGC CCG CCG CCC GT-3′). In competition assays, 50 ng unlabeled H2K or AP-1 oligonucleotides was used. Nuclear extracts were supershifted with antibodies against the NF-κB subunits p50 and p65 and the AP-1 subunits c-*fos* and c-*jun*, respectively (all antibodies from Santa Cruz). For RT-PCR, RNA was isolated according to the TRIZOL protocol (Gibco Life Technology). Primers were synthesized (BioTez) for the following sequences: GAPDH, c-*fos*, basic fibroblast growth factor (bFGF), platelet-derived growth factor (PDGF)-B, TGF-β_1, and aldosterone synthase. Real-time quantitative RT-PCR was performed with the TaqMan system (PE Biosystems). Forty cycles of PCR were performed according to the EZ-RT-PCR TaqMan kit protocol instructions with Mangan concentrations of 3 μmol/L for GAPDH; 4 μmol/L for PDGF-B, TGF-β_1, and bFGF; and 2 mmol/L for aldosterone synthase. The sequences were GAPDH-F, AAGCTGGTCATCAATGGGAAAC; GAPDH-R, ACCCCATTT-GATGTTAGCGG; GAPDH-P, CATCACCATCTTCCAG-GAGCGCGCGAT; bFGF-F, GGAGTTGTGTCCATCAAGGGA; bFGF-R, AGCAGCCGTCCATCTTCCT; bFGF-P, TGTGTGC-GAACCGGTACCTGGCT; TGF-β_1-F, TCCCAAACGTCGAGGT-GAC; TGF-β_1-R, CCATGAGGAGCAGGAAGGG; TGF-β_1-P: TGGGCACCATCCATGACATGAACC; PDGF-F, TCAGAA-GCGGGCTACTATACCAT; PDGF-R, TTGAATGAGAGCTGGAC-CTGG; PDGF-P, CGGGCCTTCCATGCGGACG; AldSyn-F, TGT-GAGCTGAAGGGAGGAGG; AldSyn-R, GGTCTTGCCAGCCACA-CAT; AldSyn-P, TGGCAATGGCTCTCAGGGTGACAG; c-*fos*-F, CCATGATGTTCTCGGGTTTCA; c-*fos*-R, GCGCTACTGCAGC-GGG; and c-*fos*-P: CGCGGACTACGAGGCGTCATCC.

Each sample was tested twice. For quantification, the target sequence was normalized in relation to the GAPDH gene. Data are mean±SEM. ANOVA and the Scheffé test were used to test statistically significant differences in mean values.

Results

Nine of 20 vehicle-treated dTGR rats died before the end of week 7; the mortality rate was 45%. In contrast, 1 rat in the SPIRO group and no VAL-treated or SD rats died ($P<0.001$). The dTGR rats showed an increase in systolic blood pressure between weeks 5 to 7. Blood pressure in SPIRO-treated rats was slightly, but not significantly, lower compared with vehicle-treated dTGR rats (161±11 versus 182±8 mm Hg, $P=0.24$) at week 7 (Figure 1A). However, the blood pressure of SPIRO-treated rats was significantly higher than SD controls and VAL-treated dTGR rats (161±14 versus 109±2 versus 121±9 mm Hg, $P<0.01$, respectively; Figure 1A). Heart weight per body weight (Figure 1B) for the various groups were 5.7±0.2 for vehicle-treated dTGR rats, 4.2±0.1 for SPIRO-treated dTGR rats, 3.6±0.1 for VAL-treated dTGR rats, and 3.6±0.1 mg/g for SD rats. Thus, without affecting body weight, SPIRO treatment reduced heart weight ($P<0.001$), but not as well as did VAL treatment.

Plasma aldosterone levels were markedly elevated in untreated dTGR rats; the mean value was 15±5 nmol/L com-

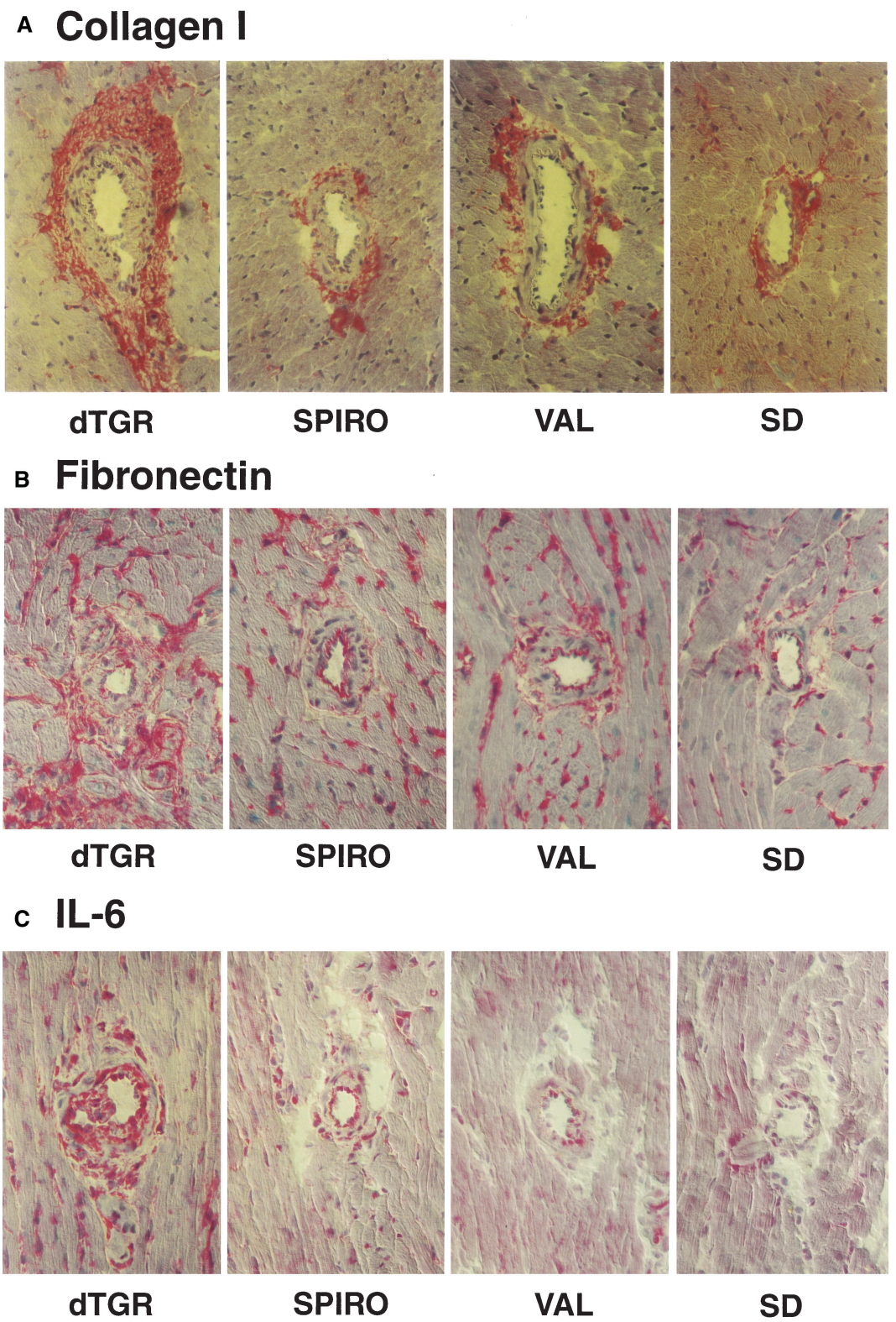

Figure 2. Matrix and cytokine protein immunohistochemistry of left ventricle from vehicle-treated dTGR rats, SPIRO-treated dTGR rats, VAL-treated dTGR rats, and SD rats. Collagen I (A), fibronectin (B), and IL-6 (C) were increased in dTGR rats and markedly decreased with both drug treatments.

pared with 0.7±0.2 nmol/L in the control group. In the treated groups, plasma aldosterone was significantly reduced. The VAL and SPIRO groups had values of 1.6±0.2 and 2.1±1.0 nmol/L, respectively (Figure 1C). No difference in the mRNA expression of aldosterone synthase, the key enzyme for aldosterone production, was detected after blocking the aldosterone receptor. However, blocking the AT_1 receptor suppressed gene expression for aldosterone synthase

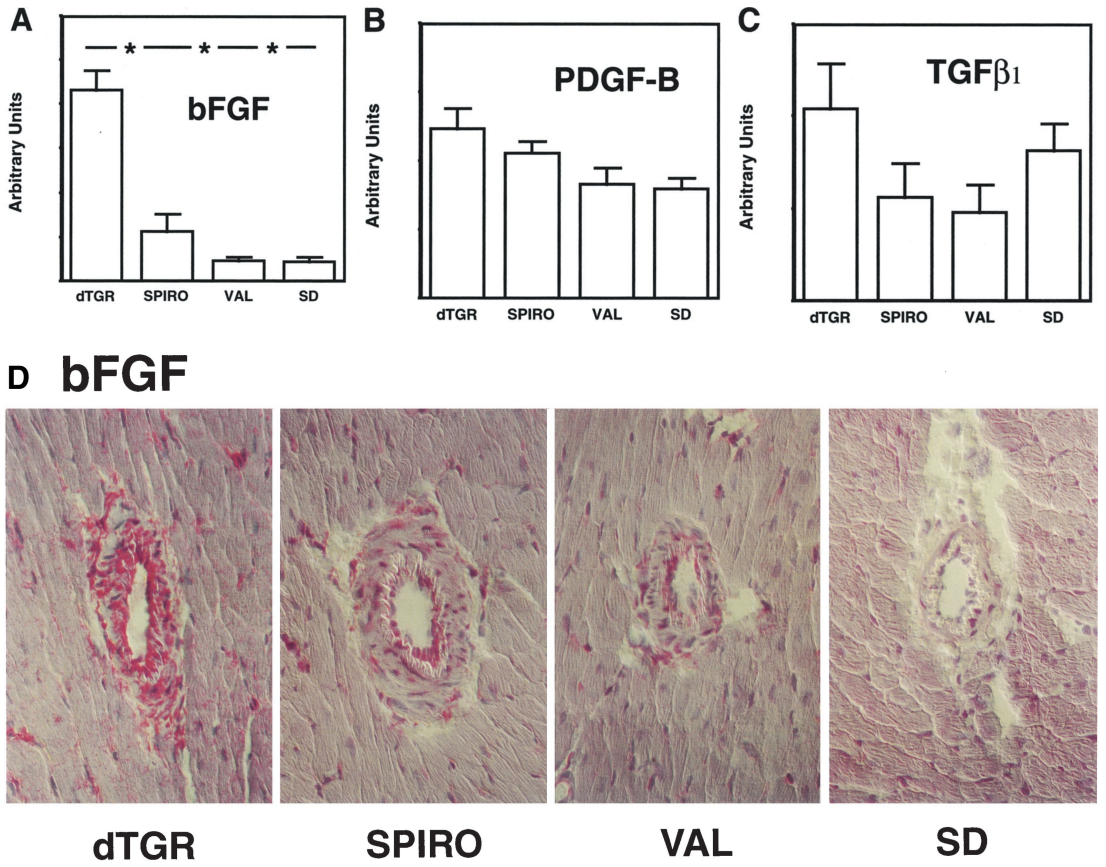

Figure 3. Quantitative RT-PCR for bFGF (A), PDGF-B (B), and TGFβ_1 (C) from the left ventricle. SPIRO and VAL treatment reduced bFGF mRNA. TGFβ_1 and PDGF-B were little influenced in this model. Immunohistochemistry for bFGF (D) showed that both SPIRO and VAL treatments reduced bFGF expression.

compared with all other groups. The expression values (arbitrary units) for dTGR, SPIRO, VAL, and SD rats were 12.5±5.5, 14.1±4.3, 0.5±0.2, and 8.0±3.4.

The vehicle-treated dTGR rats developed progressive inflammatory changes in the heart. Immunohistochemical analysis was made for the monocyte/macrophage marker ED-1 (Figure 1D). SPIRO treatment reduced the number of ED-1–positive cells by 34% ($P<0.01$). VAL treatment reduced the cells by 58% ($P<0.0001$) compared with vehicle-treated dTGR rats, which was a greater reduction than observed in SPIRO-treated dTGR rats ($P<0.05$). Interleukin (IL)-6 protein expression was upregulated in vehicle-treated dTGR rats. This upregulation was suppressed by VAL and SPIRO treatment (Figure 2C).

SPIRO treatment reduced extracellular matrix production. The hearts were stained for collagen I, fibronectin, and laminin. Collagen I (Figure 2A) and fibronectin (Figure 2B) were most prominently deposited around blood vessels, in the vascular adventitia, and focally around fibrotic areas of scarring. Fibronectin was also deposited in the neointima of remodeling vessels. Laminin was localized primarily between the cardiomyocytes (data not shown). All these interstitial deposits were substantially reduced in the SPIRO and VAL treatment groups.

To characterize the role of different growth factors in chronic ischemic remodeling, we analyzed mRNA expression of the growth factors bFGF, PDGF-B, and TGF-β_1 in the left ventricle. The bFGF expression was significantly increased in vehicle-treated dTGR rats compared with SD rats (Figure 3A). VAL and SPIRO both decreased bFGF expression. Block of the AT_1 receptor lowered bFGF gene expression to control levels; SPIRO reduced these levels by 75%. In contrast, PDGF-B (Figure 3B) and TGF-β_1 (Figure 3C) expression levels were only modestly, not significantly, increased. Immunohistochemistry for bFGF localized the protein to the neointima and media of arterial blood vessels, as well as to infiltrated cells perivascular and between cardiomyocytes (Figure 3D).

Further characterization of the DNA binding activity and transcription factor gene expression was performed. DNA binding activities for both NF-κB (Figure 4A) and AP-1 (Figure 4B) in response to SPIRO treatment were decreased, although activity was more pronounced for AP-1. Correspondingly, c-*fos* mRNA expression was upregulated in vehicle-treated dTGR rats compared with VAL- and SPIRO-treated animals. Binding specificity was demonstrated through competition of excess unlabeled oligonucleotides containing the κB site from the MHC enhancer (H2K) or the AP-1 site (Figure 4C).

Discussion

SPIRO reduced cardiac hypertrophy, inflammation, and matrix production independent of blood pressure and improved

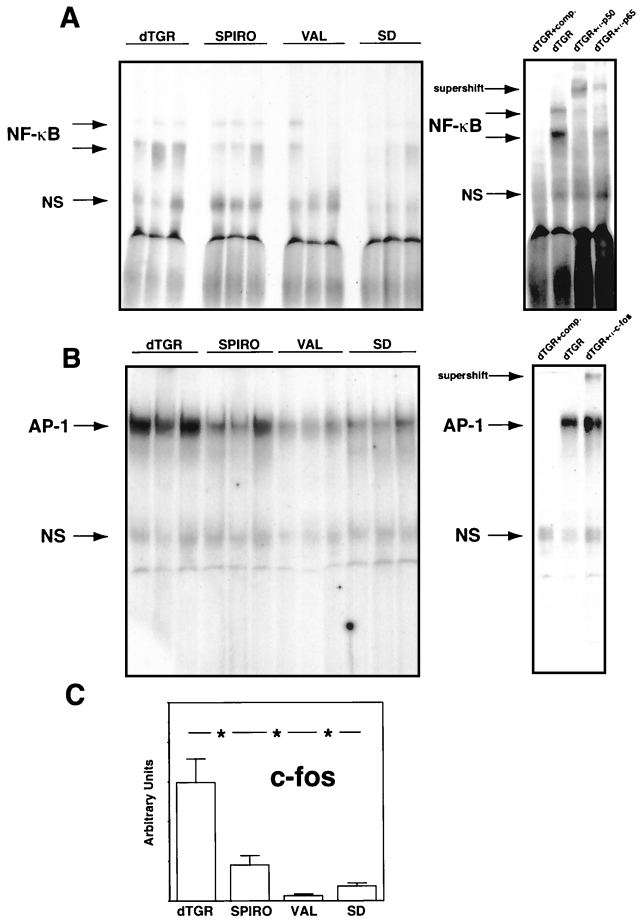

Figure 4. EMSA for NF-κB (A) and AP-1 (B) as well as quantitative RT-PCR for c-*fos* (C) from left ventricle. Both SPIRO and VAL reduced transcription factor activation. SPIRO was more effective in blocking AP-1, whereas VAL was more effective in blocking NF-κB. Binding specificity was demonstrated by competition of excess unlabeled oligonucleotides containing the κB site from the MHC enhancer (H2K) or the AP-1 site.

survival in dTGR rats compared with controls. Cardiac DNA-binding activities for AP-1 and NF-κB were lowered. Blocking the mineralocorticoid receptor resulted in effects similar to blocking the AT_1 receptor. dTGR rats had plasma aldosterone values >10-fold higher than those of SD rats. The adrenal gland was the likely source of the circulating aldosterone; degradation may also have been impaired because of hepatic malfunction. Both SPIRO and VAL lowered the values to normal levels. However, we do not believe that circulating aldosterone is the major mediator of injury nor a mirror of the degree of renin-angiotensin-aldosterone system tissue activation in this model. Silvestre et al[13] showed the control of plasma and cardiac aldosterone levels to be regulated independently and showed a 17-fold higher aldosterone concentration in myocardium than in plasma of rodents. We did not measure myocardial aldosterone concentrations. However, in the hearts of our dTGR rats, aldosterone synthase mRNA was upregulated, consistent with local production. SPIRO had no measurable effect on the gene expression of the enzyme. Instead, we observed a marked decrease in aldosterone synthase mRNA in VAL-treated dTGR rats. SPIRO-treated rats had lower aldosterone levels than dTGR rats. We believe that this effect was probably related to organ protection. SPIRO-treated animals had normal renal function and no hepatic damage.

Silvestre et al[3] found that after myocardial infarction, rats showed aldosterone synthase upregulation, aldosterone production, and collagen deposition. In their model, aldosterone synthase upregulation was abolished by AT_1 receptor blockade, whereas both mineralocorticoid receptor and AT_1 receptor blockade ameliorated fibrosis. Their findings, as well as our own, are consistent with earlier observations that aldosterone is largely responsible for cardiac matrix protein production via a direct effect on the mineralocorticoid receptor.[14] Robert et al[9] and Sun and Weber[15] recently showed that the cardiac AT_1 receptor was upregulated in DOCA-salt rats, an effect blocked by SPIRO treatment. We have observed a trend, although not significant, for AT_1 receptor downregulation in SPIRO-treated dTGR rats (data not shown). Thus, we do not believe that a downregulation of AT_1 receptor expression was the main mechanism of mediating SPIRO-related effects.

The effects of Ang II and aldosterone on cardiovascular remodeling are not the same. Campbell et al[7] found less cardiac inflammation and necrosis in a high aldosterone model compared with Ang II infusion, suggesting different mechanisms. Rocha et al[16] observed ACE inhibitor–mediated protection from fibrotic end-organ damage in salt-fed stroke-prone spontaneously hypertensive rats. Concomitant aldosterone infusion reversed this protective effect blood pressure independently. These results indicate a direct and distinct profibrotic effect of aldosterone. Benetos et al[17] investigated ACE inhibition and SPIRO treatment in spontaneously hypertensive rats. SPIRO primarily prevented collagen accumulation and, similar to our findings, did so independent of blood pressure reduction. A modest nonsignificant blood pressure reduction occurred that may have had some effect. However, such a reduction cannot account for the effects that we observed. Further evidence for a mineralocorticoid receptor–mediated role comes from the mineralocorticoid-resistant Wistar-Furth rat.[18] When subjected to 5/6 nephrectomy, these rats exhibited far less sclerosis than did Wistar rats. Together, these results underscore the role of the mineralocorticoid receptor in mediation of end-organ damage.

We focused on both AP-1 and NF-κB in our model. We speculate that AP-1 is activated via the mitogen-activated protein kinase/ERK cascade that we found to be activated in dTGR rats in an earlier study.[19] NF-κB, on the other hand, is probably activated by the Ang II–dependent generation of reactive oxygen species.[11] Tharaux et al[20] recently showed that the Ang II–related effect on the collagen I gene was mediated via AP-1 and not NF-κB. Their results suggest that these transcription factors are regulated by independent mechanisms. We observed earlier that Ang II activates both transcription factor pathways in this model via the AT_1 receptor. New is our observation that the mineralocorticoid receptor has an effect on the activation of both transcription factors. However, AP-1 activity was markedly reduced, whereas NF-κB activity was only moderately affected by SPIRO compared with VAL treatment. The effect on NF-κB

is in line with the fact that VAL reduced inflammatory response more effectively than did SPIRO. Our comments are based on comparisons of in vitro and in vivo experiments. Such experiments may not invariably lead to the same results. We believe that our in vivo studies may be more germane.

bFGF, with a 40-fold higher gene expression in untreated dTGR rats compared with controls, may be important to the inflammation we observed. IL-6 production is markedly increased in dTGR rats (data not shown), which may be related to induction by bFGF.[21] In cardiac myocytes, bFGF is a ligand for FGF-R2 and induces tyrosine phosphorylation and mitogen-activated protein kinase activation.[22] Mice that lack the bFGF gene exhibit thrombocytosis, decreased blood pressure, and decreased vascular smooth muscle cell tone.[23] Such mice also develop less aortic hypertrophy after aortic banding and had a reduced cardiomyocyte cross-sectional area compared with wild-type mice, suggesting a mediator role for bFGF.[24] Fibroblasts and infiltrating inflammatory cells can both produce bFGF. Klauber et al[25] demonstrated that SPIRO treatment inhibited angiogenesis in vivo through the suppression of bFGF, indicating a mineralocorticoid receptor–mediated effect.

PDGF-B and $TGFb_1$ signaling is involved in remodeling after ischemic injury. PDGF-B binds to PDGF-B receptor tyrosine kinase. The consensus sequences in the PDGF-B promoter contain AP-1 and NF-κB regulatory elements.[26] Ang II induces PDGF-B in vascular smooth muscle.[27] In vivo ligand and receptor are localized in the vascular neointima during vascular repair, which may explain the modestly increased PDGF-B expression we observed during the disease process in our model.[28] TGFβ_1 signaling is involved in remodeling after myocardial ischemia.[29] We were surprised to find no significant differences in the TGFβ_1 gene or protein expression pattern in our model. However, we did not characterize negative regulating effector molecules, such as decorin, which may have affected TGFβ_1 signaling in the hearts of our dTGR rats. Our model exhibited increased collagen, laminin, and fibronectin in the interstitium and perivascular areas. Both SPIRO and VAL were effective in minimizing fibrosis and production of extracellular matrix. The genes for these extracellular matrix proteins possess both AP-1– and NF-κB–binding sites.[30–32]

In summary, we demonstrated an important role for aldosterone in mediation of Ang II–induced cardiac damage. Mineralocorticoid receptor blockade with SPIRO ameliorated death, cardiac hypertrophy, inflammation, and extracellular matrix production. Inhibition of AP-1 was more pronounced than effects on NF-κB activation, which corresponded to more prominent effects on matrix deposition and less prominent effects on inflammation. These findings suggest mechanisms by which mineralocorticoid receptor blockade may improve clinical outcomes. Future studies must address how mineralocorticoid receptor signaling functions in vascular cells and which proteins are involved in early and late aldosterone response.

Acknowledgments

This work was supported by grants-in-aid from CAMMRAR, Hoffmann La Roche (Basel, Switzerland), Klinisch-Pharmakologischer Verbund (Berlin-Brandenburg, Germany), and Bundesministerium für Bildung und Forschung (Bonn, Germany). Karin Dressler, Mathilde Schmidt, and Christel Lipka provided expert technical assistance.

References

1. Pitt B, Zannad F, Remme WJ, Cody R, Castaigne A, Perez A, Palensky J, Wittes J. The effect of spironolactone on morbidity and mortality in patients with severe heart failure. Randomized Aldactone Evaluation Study Investigators. *N Engl J Med*. 1999;341:709–717.
2. Swedberg K, Eneroth P, Kjekshus J, Snapinn S. Effects of enalapril and neuroendocrine activation on prognosis in severe congestive heart failure (follow-up of the CONSENSUS trial). CONSENSUS Trial Study Group. *Am J Cardiol*. 1990;66:40D–44D.
3. Silvestre JS, Heymes C, Oubenaissa A, Robert V, Aupetit-Faisant B, Carayon A, Swynghedauw B, Delcayre C. Activation of cardiac aldosterone production in rat myocardial infarction: effect of angiotensin II receptor blockade and role in cardiac fibrosis. *Circulation*. 1999;99:2694–2701.
4. Delcayre C, Silvestre JS, Garnier A, Oubenaissa A, Cailmail S, Tatara E, Swynghedauw B, Robert V. Cardiac aldosterone production and ventricular remodeling. *Kidney Int*. 2000;57:1346–1351.
5. Ikeda U, Hyman R, Smith TW, Medford RM. Aldosterone-mediated regulation of Na^+,K^+-ATPase gene expression in adult and neonatal rat cardiocytes. *J Biol Chem*. 1991;266:12058–12066.
6. Brilla CG, Pick R, Tan LB, Janicki JS, Weber KT. Remodeling of the rat right and left ventricles in experimental hypertension. *Circ Res*. 1990;67:1355–1364.
7. Campbell SE, Janicki JS, Weber KT. Temporal differences in fibroblast proliferation and phenotype expression in response to chronic administration of angiotensin II or aldosterone. *J Mol Cell Cardiol*. 1995;27:1545–1560.
8. Verrey F, Pearce D, Pfeiffer R, Spindler B, Mastroberardino L, Summa V, Zecevic M. Pleiotropic action of aldosterone in epithelia mediated by transcription and post-transcription mechanisms. *Kidney Int*. 2000;57:1277–1282.
9. Robert V, Heymes C, Silvestre JS, Sabri A, Swynghedauw B, Delcayre C. Angiotensin AT_1 receptor subtype as a cardiac target of aldosterone: role in aldosterone-salt-induced fibrosis. *Hypertension*. 1999;33:981–986.
10. Luft FC, Mervaala E, Muller DN, Gross V, Schmidt F, Park JK, Schmitz C, Lippoldt A, Breu V, Dechend R, Dragun D, Schneider W, Ganten D, Haller H. Hypertension-induced end-organ damage: a new transgenic approach to an old problem. *Hypertension*. 1999;33:212–218.
11. Muller DN, Dechend R, Mervaala EM, Park JK, Schmidt F, Fiebeler A, Theuer J, Breu V, Ganten D, Haller H, Luft FC. NF-κB inhibition ameliorates angiotensin II–induced inflammatory damage in rats. *Hypertension*. 2000;35:193–201.
12. Muller DN, Mervaala EM, Dechend R, Fiebeler A, Park JK, Schmidt F, Theuer J, Breu V, Mackman N, Luther T, Schneider W, Gulba D, Ganten D, Haller H, Luft FC. Angiotensin II (AT_1) receptor blockade reduces vascular tissue factor in angiotensin II-induced cardiac vasculopathy. *Am J Pathol*. 2000;157:111–122.
13. Silvestre JS, Robert V, Heymes C, Aupetit-Faisant B, Mouas C, Moalic JM, Swynghedauw B, Delcayre C. Myocardial production of aldosterone and corticosterone in the rat: physiological regulation. *J Biol Chem*. 1998;273:4883–4891.
14. Brilla CG, Rupp H, Funck R, Maisch B. The renin-angiotensin-aldosterone system and myocardial collagen matrix remodelling in congestive heart failure. *Eur Heart J*. 1995;16(suppl O):107–109.
15. Sun Y, Weber KT. Angiotensin II and aldosterone receptor binding in rat heart and kidney: response to chronic angiotensin II or aldosterone administration. *J Lab Clin Med*. 1993;122:404–411.
16. Rocha R, Chander PN, Zuckerman A, Stier CT Jr. Role of aldosterone in renal vascular injury in stroke-prone hypertensive rats. *Hypertension*. 1999;33:232–237.
17. Benetos A, Lacolley P, Safar ME. Prevention of aortic fibrosis by spironolactone in spontaneously hypertensive rats. *Arterioscler Thromb Vasc Biol*. 1997;17:1152–1156.
18. Fitzgibbon WR, Greene EL, Grewal JS, Hutchison FN, Self SE, Latten SY, Ullian ME. Resistance to remnant nephropathy in the Wistar-Furth rat. *J Am Soc Nephrol*. 1999;10:814–821.
19. Park JK, Muller DN, Mervaala EM, Dechend R, Fiebeler A, Schmidt F, Bieringer M, Schafer O, Lindschau C, Schneider W, Ganten D, Luft FC, Haller H. Cerivastatin prevents angiotensin II-induced renal injury inde-

pendent of blood pressure- and cholesterol-lowering effects. *Kidney Int*. 2000;58:1420–1430.
20. Tharaux PL, Chatziantoniou C, Fakhouri F, Dussaule JC. Angiotensin II activates collagen I gene through a mechanism involving the MAP/ER kinase pathway. *Hypertension*. 2000;36:330–336.
21. Kozawa O, Suzuki A, Uematsu T. Basic fibroblast growth factor induces interleukin-6 synthesis in osteoblasts: autoregulation by protein kinase C. *Cell Signal*. 1997;9:463–468.
22. Bogoyevitch MA, Glennon PE, Andersson MB, Clerk A, Lazou A, Marshall CJ, Parker PJ, Sugden PH. Endothelin-1 and fibroblast growth factors stimulate the mitogen- activated protein kinase signaling cascade in cardiac myocytes: the potential role of the cascade in the integration of two signaling pathways leading to myocyte hypertrophy. *J Biol Chem*. 1994;269:1110–1119.
23. Zhou M, Sutliff RL, Paul RJ, Lorenz JN, Hoying JB, Haudenschild CC, Yin M, Coffin JD, Kong L, Kranias EG, Luo W, Boivin GP, Duffy JJ, Pawlowski SA, Doetschman T. Fibroblast growth factor 2 control of vascular tone. *Nat Med*. 1998;4:201–207.
24. Schultz JE, Witt SA, Nieman ML, Reiser PJ, Engle SJ, Zhou M, Pawlowski SA, Lorenz JN, Kimball TR, Doetschman T. Fibroblast growth factor-2 mediates pressure-induced hypertrophic response. *J Clin Invest*. 1999;104:709–719.
25. Klauber N, Browne F, Anand-Apte B, D'Amato RJ. New activity of spironolactone: inhibition of angiogenesis in vitro and in vivo. *Circulation*. 1996;94:2566–2571.
26. Khachigian LM, Resnick N, Gimbrone MA Jr, Collins T. Nuclear factor-kappa B interacts functionally with the platelet-derived growth factor B-chain shear-stress response element in vascular endothelial cells exposed to fluid shear stress. *J Clin Invest*. 1995;96:1169–1175.
27. Deguchi J, Makuuchi M, Nakaoka T, Collins T, Takuwa Y. Angiotensin II stimulates platelet-derived growth factor-B chain expression in newborn rat vascular smooth muscle cells and neointimal cells through Ras, extracellular signal-regulated protein kinase, and c-Jun N-terminal protein kinase mechanisms. *Circ Res*. 1999;85:565–574.
28. Majesky MW, Reidy MA, Bowen-Pope DF, Hart CE, Wilcox JN, Schwartz SM. PDGF ligand and receptor gene expression during repair of arterial injury. *J Cell Biol*. 1990;111:2149–2158.
29. Hao J, Ju H, Zhao S, Junaid A, Scammell-La Fleur T, Dixon IM. Elevation of expression of Smads 2, 3, and 4, decorin and TGF-beta in the chronic phase of myocardial infarct scar healing. *J Mol Cell Cardiol*. 1999;31:667–678.
30. Matsui T. Differential activation of the murine laminin B1 gene promoter by RAR alpha, ROR alpha, and AP-1. *Biochem Biophys Res Commun*. 1996;220:405–410.
31. Tamura K, Nyui N, Tamura N, Fujita T, Kihara M, Toya Y, Takasaki I, Takagi N, Ishii M, Oda K, Horiuchi M, Umemura S. Mechanism of angiotensin II-mediated regulation of fibronectin gene in rat vascular smooth muscle cells. *J Biol Chem*. 1998;273:26487–26496.
32. Chung KY, Agarwal A, Uitto J, Mauviel A. An AP-1 binding sequence is essential for regulation of the human alpha2(I) collagen (COL1A2) promoter activity by transforming growth factor-beta. *J Biol Chem*. 1996; 271:3272–3278.

3.2 Blockade der Aldosteronproduktion in einem Angiotensin II-abhängigen Tiermodell

3.2.1 Wirkungsweise des spezifischen Aldosteronsynthase-Inhibitors FAD286

Neben den Antagonisten des Aldosteron-Rezeptors wurde in den letzten Jahren eine neue Substanzklasse entwickelt, welche das Schlüsselenzym der Aldosteronproduktion, die Aldosteronsynthase (auch Cyp11B2 genannt), hemmt. FAD286 ist das Razemat von Fadrozole, welches als Aromataseinhibitor bei der Behandlung von Brustkrebs eingesetzt wird. FAD286 wirkt in nanomolarer Konzentration (IC50 = 37 ± 4 nM) als spezifischer Hemmer der Aldosteronsynthase, für die Aromatasehemmung sind Konzentrationen im mikromolaren Bereich notwendig. Die Strukturformel von FAD286 und die von der FAD286-Konzentration abhängige Hemmung der Aldosteronproduktion in adrenokortikalen Zellen finden sich in **Abbildung 8**.

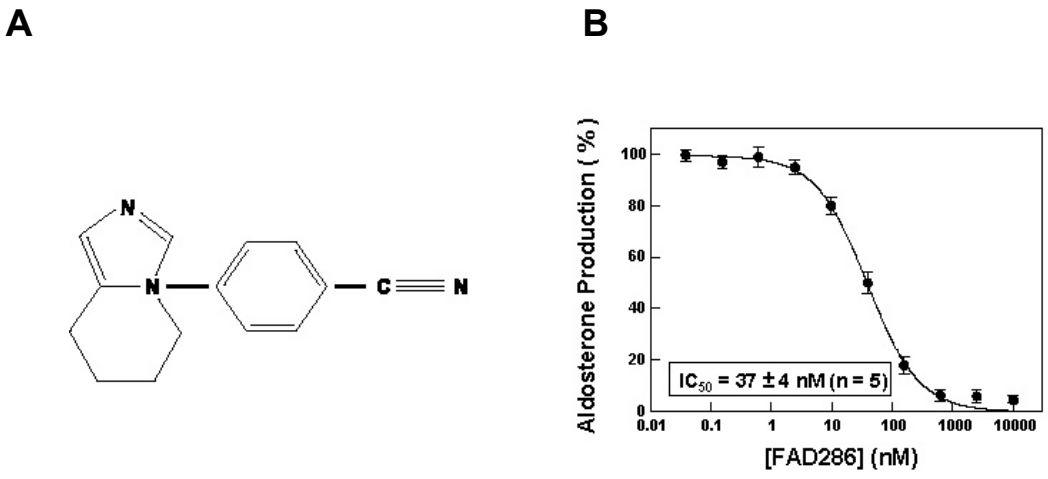

Abbildung 8 A: Strukturformel von FAD 286. FAD 286 ist ein Synonym für (+)-(5R)-4-(5,6,7,8-tetrahydroimidazo[1,5-a]pyridin-5-yl) benzonitrile hydrochloride; **B: Einfluss von FAD 286 auf die Aldosteronsynthese in vitro.** Hemmung der Aldosteronsynthese in adrenokortikalen Zellen (NCI-H295R).

Wir schlossen zunächst einen Einfluss von FAD286 auf die Aktivität von Plasmarenin *ex vivo* aus (**Abb. 9**).

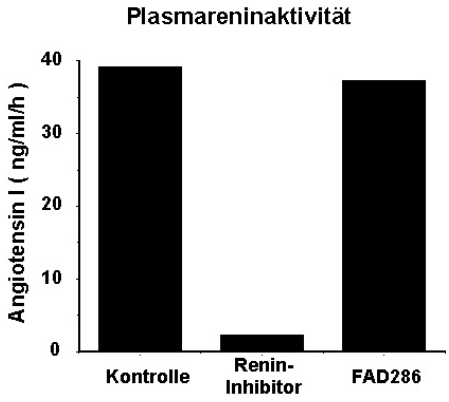

Abbildung 9: Plasmareninaktivität von einer unbehandelten dTGR. Der Renin-Inhibitor (2 µM) bzw. FAD286 (1 µM) wurde mit der Plasmaprobe inkubiert und die Menge von Angiotensin I nach 60 min bestimmt.

Es galt, den Effekt dieser neuen Substanz beim Angiotensin II-induzierten Endorganschaden zu testen. Wie bei den Untersuchungen zur Wirkung von Blockern des MR wurde auch für diese Experimente das dTGR-Modell untersucht (siehe oben, **Abb. 5**). Wir verglichen unbehandelte dTGR mit Tieren, die von der 4. bis zur 7. Lebenswoche mit FAD286 bzw. Losartan behandelt worden waren. Das Studienschema wird in **Abbildung 10** zusammengefasst.

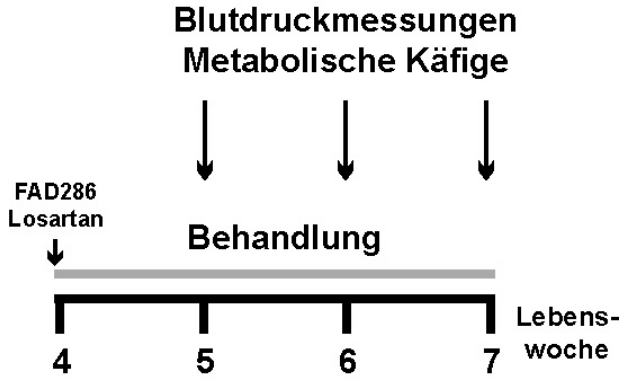

Abbildung 10: Design der FAD286-Studie

3.2.2 Einfluss auf Mortalität, Blutdruck, Herz- und Nierenfunktion

FAD286 reduzierte zur 7. Woche die Mortalität von 40 % auf 10 %. Unbehandelte und FAD286-behandelte dTGR hatten bis zur 6. Woche identische Blutdruckwerte. In der 7. Woche war der Blutdruck in der FAD286-behandelten Gruppe etwas niedriger, Losartan-behandelte Tiere hatten normale Blutdruckwerte. Die bei unbehandelten dTGR zur 7. Woche deutliche Herzhypertrophie war unter FAD286 signifikant geringer ausgeprägt, während sich unter Losartanbehandlung keine Herzhypertrophie ausbildete. Die FAD286-Behandlung schützte vor der Ausprägung der bei unbehandelten dTGR beobachteten Niereninsuffizienz partiell; Losartan verhinderte die Niereninsuffizienz.

3.2.3 Wirkmechanismen der Hemmung der Aldosteronsynthase

Wir untersuchten die Aldosteronspiegel im Plasma und im Herzen, die Histologie, die Zellinfiltration sowie die mRNA- und Proteinexpression in Herz und Nieren. Wie erwartet wurden sowohl die zirkulierenden als auch die lokalen Aldosteronspiegel am Herzen durch FAD286 vermindert. Die Kortikosteronspiegel unterschieden sich nicht zwischen den Gruppen.

Parallel zur Herzhypertrophie verhielt sich die mRNA-Expression verschiedener Hypertrophiemarker. So wurde die Überexpression von ANP (*atrial natriuretic peptid*) sowohl durch FAD286 als auch durch Losartan gesenkt, und beide Pharmaka beeinträchtigten die Verschiebung der mRNA-Expression von der adulten MHC (*myosin heavy chain*)- Isoform α-MHC zur fetalen β-MHC-Isoform. In den Nieren beobachteten wir in beiden Behandlungsgruppen weniger infiltrierende Zellen, und die Ablagerung von Kollagen Typ IV und Fibronektin war vermindert.

Schlussfolgerung: Der Aldosteronsynthase-Inhibitor FAD286 gehört zu einer neuen Substanzklasse, welche effektiv die Aldosteronkonzentration vermindert und im Tiermodell vor der vollen Ausprägung des Angiotensin II-induzierten Endorganschadens schützt. Mit FAD286 kann erstmalig selektiv in den Aldosteron-Signalweg ohne Beeinflussung der Glukokortikoide eingegriffen werden.

3.3 Entfernung des zirkulierenden Aldosterons durch Adrenalektomie

Durch Entfernung der Nebennieren konnten wir die Rolle des lokal produzierten Aldosterons für den Angiotensin II-induzierten Endorganschaden untersuchen (im Gegensatz zur Behandlung mit FAD286 wird die lokale Produktion von Aldosteron durch die Adrenalektomie nicht unmittelbar beeinflusst). Einer Tiergruppe wurden zur 4. Lebenswoche die Nebennieren entfernt. Die Tiere bekamen danach mehr Salz zugeführt, um den Salzverlust auszugleichen. Da bei der Adrenalektomie auch die Synthese des Kortikosterons unterbunden wird, mussten die Tiere mit Dexamethason substituiert werden. Zur besseren Vergleichbarkeit bekamen auch nicht adrenalektomierte dTGR Salz und Dexamethason. Der prinzipielle Versuchsaufbau und das verwendete Tiermodell waren den bereits dargestellten Untersuchungen ähnlich. Wir untersuchten dTGR und adrenalektomierte dTGR. Das Studienschema ist in **Abbildung 11** zusammengefasst.

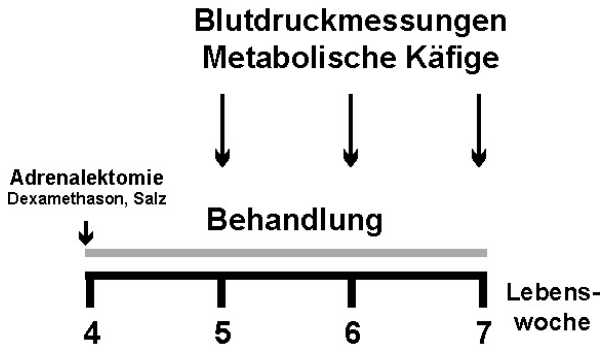

Abbildung 11: Design der Adrenalektomie-Studie

3.3.1 Einfluss auf Mortalität, Blutdruck, Herz- und Nierenfunktion

Die Mortalität von dTGR, welche zusätzlich mit Salz substituiert wurden, ist zur 7. Lebenswoche 73 %; die Adrenalektomie reduzierte diese auf 22 %. Die Entfernung des zirkulierenden Aldosterons durch Adrenalektomie hatte keinen Einfluss auf den Blutdruck. Die unter Salzbehandlung bei dTGR im Vergleich zu nicht Salz-substituierten Tieren noch ausgeprägtere Herzhypertrophie war in den adrenalektomierten Tieren deutlich reduziert. Auch die Entwicklung der Albuminurie war nach Adrenalektomie deutlich vermindert.

3.3.2 Wirkmechanismen der Adrenalektomie

Zum Verständnis zugrunde liegender Wirkmechanismen untersuchten wir auch in dieser Gruppe die Aldosteron- und Kortikosteronspiegel im Blut und im Herzen, sowie die Histologie, Zellinfiltration und Proteinexpression in Herz und Nieren. Drei Wochen nach Adrenalektomie waren sowohl im Plasma als auch im Herz die Aldosteronspiegel erniedrigt bis nicht mehr nachweisbar. Auch die Plasmaspiegel von Kortikosteron waren erwartungsgemäß niedrig (**Abb. 12**).

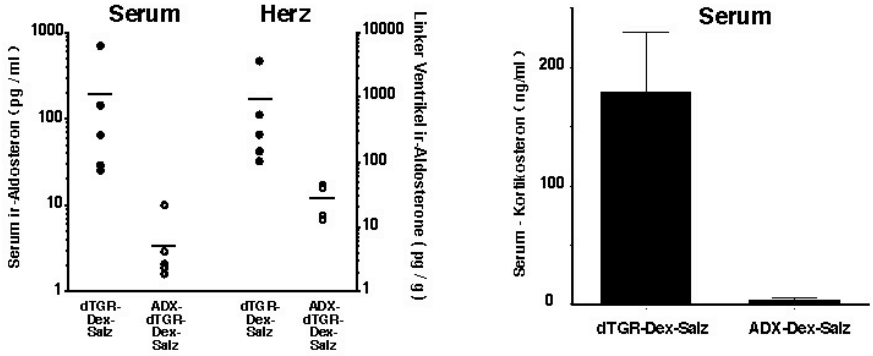

Abbildung 12: Aldosteron- und Kortikosteronspiegel im Serum und im Herz. Nach Adrenalektomie liegen die Aldosteron- und die Kortikosteronspiegel im Serum und im linken Ventrikel des Herzens nur gering oberhalb der Nachweisgrenze.

Die Infiltration von Entzündungszellen in den Endorganen war nach Adrenalektomie deutlich reduziert, ebenso die Ablagerung von Kollagen und Fibronektin.

3.3.3 Hemmung der Aldosteronsynthase nach Adrenalektomie

Zum Verständnis eines möglichen Beitrages der lokalen Aldosteronproduktion zum Angiotensin II-induzierten Endorganschaden verglichen wir adrenalektomierte dTGR mit FAD286-behandelten adrenalektomierten dTGR. In dieser Studie wurden die Tiere 9 Wochen beobachtet, da bis zur 7. Woche keine erkennbaren Unterschiede zwischen den Gruppen festzustellen waren. Obwohl auch eine nicht-adrenalektomierte Kontrollgruppe mitgeführt wurde, konnten zur 9. Woche keine Daten wegen der sehr hohen Mortalität bei Salz-behandelten dTGR erhoben werden. Bei den FAD286-behandelten adrenalektomierten dTGR kam es zu keiner signifikanten weiteren Reduktion der Mortalität im Vergleich zu unbehandelten adrenalektomierten dTGR. Es war kein Unterschied im Blutdruck, der Herzhypertrophie oder der Albuminurie zu beobachten. Die Aldosteronspiegel im

Plasma und in den Herzen blieben auch zur 9. Woche niedrig, und zwischen den Gruppen konnte kein signifikanter Unterschied gemessen werden. Lediglich die Infiltration von Monozyten/Makrophagen, T-Zellen und dendritischen Zellen im Herzen war in der FAD286-Gruppe signifikant niedriger. Die kardiale mRNA-Expression von bFGF war deutlich reduziert.

Schlussfolgerung: Das am kardialen und renalen Endorganschaden beteiligte Aldosteron wird größtenteils in den Nebennieren synthetisiert. Eine zusätzliche Blockade der lokalen Aldosteronproduktion in adrenalektomierten Tieren führt zu keinem Therapievorteil.

Reprint 2

Fiebeler A, Nussberger J, Shagdarsuren E, Rong S, Hilfenhaus G, Al-Saadi N, Dechend R, Wellner M, Meiners S, Maser-Gluth C, Jeng AY, Webb RC, Luft FC, Mueller DN. An Aldosterone Synthase Inhibitor Ameliorates Angiotensin II-induced Organ Damage.

***Circulation*. 2005;in press.**

balt2/zhc-ci/zhc-ci/zhc02305/zhc2296-05a | mortonk2 | S=4 | 5/19/05 | 7:39 | 4/Color Figure(s): 3,4 | Art: 165856

June 14, 2005

Aldosterone Synthase Inhibitor Ameliorates Angiotensin II–Induced Organ Damage

Anette Fiebeler, MD*; Jürg Nussberger, MD*; Erdenechimeg Shagdarsuren, MD; Song Rong; Georg Hilfenhaus; Nidal Al-Saadi, MD Ralf Dechend, MD; Maren Wellner, PhD; Silke Meiners, PhD; Christiane Maser-Gluth, PhD; Arco Y. Jeng, PhD; Randy L. Webb, PhD; Friedrich C. Luft, MD; Dominik N. Muller, PhD

Background—Aldosterone and angiotensin (Ang) II both may cause organ damage. Circulating aldosterone is produced in the adrenals; however, local cardiac synthesis has been reported. Aldosterone concentrations depend on the activity of aldosterone synthase (CYP11B2). We tested the hypothesis that reducing aldosterone by inhibiting CYP11B2 or by adrenalectomy (ADX) may ameliorate organ damage. Furthermore, we investigated how much local cardiac aldosterone originates from the adrenal gland.

Methods and Results—We investigated the effect of the CYP11B2 inhibitor FAD286, losartan, and the consequences of ADX in transgenic rats overexpressing both the human renin and angiotensinogen genes (dTGR). dTGR-ADX received dexamethasone and 1% salt. Dexamethasone-treated dTGR-salt served as a control group in the ADX protocol. Untreated dTGR developed hypertension and cardiac and renal damage and had a 40% mortality rate (5/13) at 7 weeks. FAD286 reduced mortality to 10% (1/10) and ameliorated cardiac hypertrophy, albuminuria, cell infiltration, and matrix deposition in the heart and kidney. FAD286 had no effect on blood pressure at weeks 5 and 6 but slightly reduced blood pressure at week7 (177±6 mm Hg in dTGR+FAD286 and 200±5 mm Hg in dTGR). Losartan normalized blood pressure during the entire study. Circulating and cardiac aldosterone levels were reduced in FAD286 or losartan-treated dTGR. ADX combined with dexamethasone and salt treatment decreased circulating and cardiac aldosterone to barely detectable levels. At week 7, ADX-dTGR-dexamethasone-salt had a 22% mortality rate compared with 73% in dTGR-dexamethasone-salt. Both groups were similarly hypertensive (190±9 and 187±4 mm Hg). In contrast, cardiac hypertrophy index, albuminuria, cell infiltration, and matrix deposition were significantly reduced after ADX ($P<0.05$).

Conclusions—Aldosterone plays a key role in the pathogenesis of Ang II–induced organ damage. Both FAD286 and ADX reduced circulating and cardiac aldosterone levels. The present results show that aldosterone produced in the adrenals is the main source of cardiac aldosterone. **(*Circulation*. 2005;111:&NA;-.)**

Key Words: aldosterone ■ angiotensin ■ heart failure ■ renin ■ inflammation

Since the publication of 2 clinical trials, RALES (Randomized Aldactone Evaluation Study) and EPHESUS, the role of aldosterone in cardiovascular remodeling has generated considerable attention.[1,2] The key enzyme in aldosterone production is aldosterone synthase (CYP11B2). CYP11B2 is predominantly expressed in the adrenal gland but is also expressed in the cardiovascular system.[3] Angiotensin (Ang) II is the main stimulus for CYP11B2-related aldosterone synthesis. Preclinical and clinical studies have shown that Ang II inhibition is pivotal to the treatment of heart failure and ischemic heart disease. The previous belief was that inhibition of Ang II should be sufficient to block aldosterone production; however, aldosterone levels can be elevated even though Ang II production is inhibited or its action is blocked.[4] This state of affairs is called the aldosterone breakthrough phenomenon; its mechanisms are unclear. Blocking the mineralocorticoid receptor (MR) reduces proteinuria in ACE inhibitor–treated patients with early diabetic nephropathy.[5] MR is directly involved in ischemia-induced cardiac remodeling. Hayashi et al[6] prevented postinfarct left ventricular remodeling with spironolactone added to an ACE inhibitor. However, whether aldosterone in the heart tissue is derived from the circulating blood or is produced locally, thereby contributing to remodeling, is unclear. We investigated FAD286, a novel CYP11B2 inhibitor, in an Ang II–dependent rat model of organ damage. The rats are transgenic for

Received November 15, 2004; revision received January 20, 2005; accepted February 18, 2005.

From the Medical Faculty of the Charité (A.F., E.S., G.H., N.A.-S., R.D., M.W., S.M., F.C.L., D.N.M.), HELIOS Klinikum-Berlin, Franz Volhard Clinic, Berlin, Germany; Max Delbrück Center for Molecular Medicine (F.C.L., D.N.M.), Berlin-Buch, Germany; Medical School of Hannover (S.R.), Hannover, Germany; Novartis Institutes for Biomedical Research (A.Y.J., R.L.W.), East Hanover, NJ; Centre Hospitalier Universitaire Vaudois (J.N.), Hypertension Division, Lausanne, Switzerland; and University of Heidelberg (C.M.-G.), Institute of Pharmacology, Heidelberg, Germany.

*Drs Fiebeler and Nussberger contributed equally to this article.

Correspondence to Anette Fiebeler, MD, Franz Volhard Clinic, Wiltberg Strasse 50, 13125 Berlin, Germany. E-mail fiebeler@fvk-berlin.de

Circulation **is available at http://www.circulationaha.org** **DOI: 10.1161/CIRCULATIONAHA.104.521625**

<ARTICLE DOCTOPIC="Original Articles" DOCSUBJ="Heart Failure" DATE="June 14, 2005" VID="111" ISS="23" PPF="&NA;" PPL="" DOI="10.1161/CIRCULATIONAHA.104.521625">

the human renin and angiotensinogen genes (dTGR). The animals develop hypertension and severe cardiac and renal damage. They die between 7 and 8 weeks of age.[7–10] In previous studies, we demonstrated that MR blockade with spironolactone or eplerenone prevented mortality and Ang II–induced organ damage.[9,10] The aim of the present study was to define the effect of FAD286 and the role of circulating or locally produced aldosterone in the pathogenesis of Ang II–induced renal and cardiac damage.

Methods

In Vitro Analysis of FAD286 in NCI-H295R Cells

Human adrenocortical carcinoma NCI-H295R cells (American Type Culture Collection, Manassas, Va) were seeded in NBS 96-well plates at a density of 25 000 cells/well in 100 μL of a growth medium containing DMEM/F12 (Gibco) supplemented with 10% FCS (Gibco), 2.5% Nu-serum (BD Biosciences), 1 μg ITS/mL (insulin/transferrin/selenium; Gibco), and 1x antibiotic/antimycotic (Gibco). The medium was changed after being cultured for 3 days at 37°C under an atmosphere of 5% CO_2/95% air. On the following day, cells were rinsed with 100 μL of DMEM/F12 and incubated with 100 μL of treatment medium containing 1 μmol/L Ang II (Sigma) and FAD286 at different concentrations in quadruplicate wells at 37°C for 24 hours. Immunoreactive aldosterone (ir-Ald) was measured in the supernatant by radioimmunoassay developed by Novartis Ltd.

Animal Studies

Experiments were conducted in 4-week-old male dTGR.[11] The rats were kept in rooms at 24±2°C and fed a standard rat diet containing sodium at 2 g/kg. They had free access to tap water or 1% saltwater depending on the protocols. All American Physiological Society guidelines for animal care were followed (permit No. G 408/97). Three different treatment protocols were performed. Systolic blood pressure was measured weekly by tail cuff. Urine was collected over 24 hours. Urinary albumin was measured by ELISA (CellTrend). Rats were killed at 7 or 9 weeks of age, and kidneys and hearts were excised, washed with ice-cold saline, blotted dry, weighed, and stored at −80°C. Serum was collected and stored at −20°C. Plasma renin concentration (PRC) and corticosterone and serum and cardiac ir-Ald levels were determined according to previously published methods.[12,13] Serum corticosterone was extracted from plasma with organic solvents and measured by specific radioimmunoassay with tritiated steroids (Amersham Biosciences) and specific antibodies, raised and characterized as described elsewhere.[14]

In protocol I, dTGR were treated with the aldosterone synthase inhibitor FAD286 (4 $mg \cdot kg^{-1} \cdot d^{-1}$ in the diet; n=10) or losartan (losartan, 30 $mg \cdot kg^{-1} \cdot d^{-1}$ in the diet; n=8) from week 4 to week 7. Untreated dTGR (n=13) were used as controls. At week 7, echocardiography (M-mode tracings in the short axis; n=5 to 6 per group) was performed with a commercially available system equipped with a 15-Mhz phased-array transducer under isoflurane anesthesia. Total wall thickness was calculated as the sum of the septum plus left ventricular posterior wall. Three measurements per heart were taken, averaged, and analyzed statistically. In protocol II, dTGR (n=12) were adrenalectomized (ADX) at week 4 and compared with non-ADX dTGR (n=9). Both groups were supplemented with dexamethasone (12 $\mu g \cdot kg^{-1} \cdot d^{-1}$ IP) to replace glucocorticoids and 1% salt in the drinking water. All rats were killed at week 7. Protocol III was identical to protocol II, but the rats were killed at week 9. An additional group of ADX-dTGR was treated with FAD286 (4 $mg \cdot kg^{-1} \cdot d^{-1}$; diet; n=12) to inhibit any extra-adrenal aldosterone synthase activity.

Immunohistochemistry

Ice-cold acetone-fixed cryosections (6 μm) of renal and cardiac tissue were stained by the alkaline phosphatase/anti–alkaline phosphatase technique and immunofluorescence as described previously.[7] To determine cell infiltration, sections were incubated with the following monoclonal antibodies: anti-CD4 (Pharmingen), anti-ED-1, anti-CD8 (Serotec), anti-major histocompatibility complex class II, anti-CD86, and anti-Ox6 (all BD Pharmingen). Polyclonal antibodies for anti-fibronectin (Paesel) and anti-collagen IV (Southern Biotechnology) were used to visualize fibrosis. Semiquantitative scoring of infiltrated cells, in 15 different cortical kidney and cardiac areas (n=5 per group), was done with samples examined in a blinded fashion. Collagen IV and fibronectin expression were presented in arbitrary units (0 to 5+) based on staining intensity.

RNA Expression With TaqMan

For reverse transcription–polymerase chain reaction (RT-PCR), RNA was isolated from left ventricular issue according to the TRIZOL protocol (Gibco Life Technology), and cDNA was transcribed with superscript II according to the protocol. Primers (18S, hypoxanthine phosphoribosyl transferase gene, α- and β-myosin heavy chain [MHC], atrial natriuretic peptide, MR, HSD, and CYP11B2; primer sequences available on request) were synthesized by Biotez. For CYP11B2, MR, and HSD, RT-PCR was performed with the TaqMan system (Prism 7700 Sequence Detection System, PE Biosystems). Forty-five cycles of PCR were performed according to the PCR TaqMan-Mastermix (Applied Biosystems) protocol instructions. For α-MHC, β-MHC, and atrial natriuretic peptide, quantitative RT-PCR amplification was performed in 25 μL of SYBRGreen PCR Master Mix (Applied Biosystems) containing 0.3 or 0.9 mol/L primer and 1 μL of the reverse-transcription reaction with a 5700 Sequence Detection System (Applied Biosystems). Thermal cycling conditions comprised an initial denaturation step at 95°C for 10 minutes, followed by 95°C for 15 seconds and 65°C for 1 minute for 40 cycles. mRNA expression was normalized relative to the housekeeping genes 18S and hypoxanthine phosphoribosyl transferase.

Statistical Analysis

Data are generally expressed as mean±SEM. Plasma renin serum and cardiac aldosterone concentrations are presented as median value (range). Statistically significant differences in mean values were tested by ANOVA, blood pressure by repeated-measures ANOVA followed by the Scheffé *t* test as indicated. Nonparametric testing was performed for differences between median values. Mortality is presented as Kaplan-Meier analysis. A value of $P<0.05$ was considered statistically significant. The data were analyzed with Statview statistical software.

Results

FAD286 and Its Effect on Ang II–Induced Aldosterone Production in NCI-H295R Cells

FAD286 [(+)-(5R)-4-(5,6,7,8-tetrahydroimidazo [1,5-a]pyridin-5-yl] benzonitrile hydrochloride] is shown in Figure 1A. FAD286 dose dependently inhibited the Ang II–induced generation of ir-Ald in NCI-H295R cells with an IC_{50} of 37 nmol/L (Figure 1B).

Effect of FAD286 and Losartan on Organ Damage

At week 7, untreated dTGR showed 40% mortality (5/13), whereas only 1 of 10 FAD286-treated and no losartan-treated dTGR died before the end of the study at week 7 (Figure 2A). Systolic blood pressure in untreated dTGR increased progressively from week 5 to week 7. FAD286-treated dTGR also showed elevated blood pressure at weeks 5 and 6 that was slightly reduced at week 7 compared with untreated dTGR (200±5 and 177±6 mm Hg, $P<0.05$; Figure 2B). In contrast, losartan normalized blood pressure (107±5 mm Hg, $P<0.05$; Figure 2B).

FAD286 and losartan both significantly reduced the cardiac hypertrophy index compared with untreated dTGR (4.4±0.1, 3.1±0.03, and 4.9±0.2 mg/g, respectively,

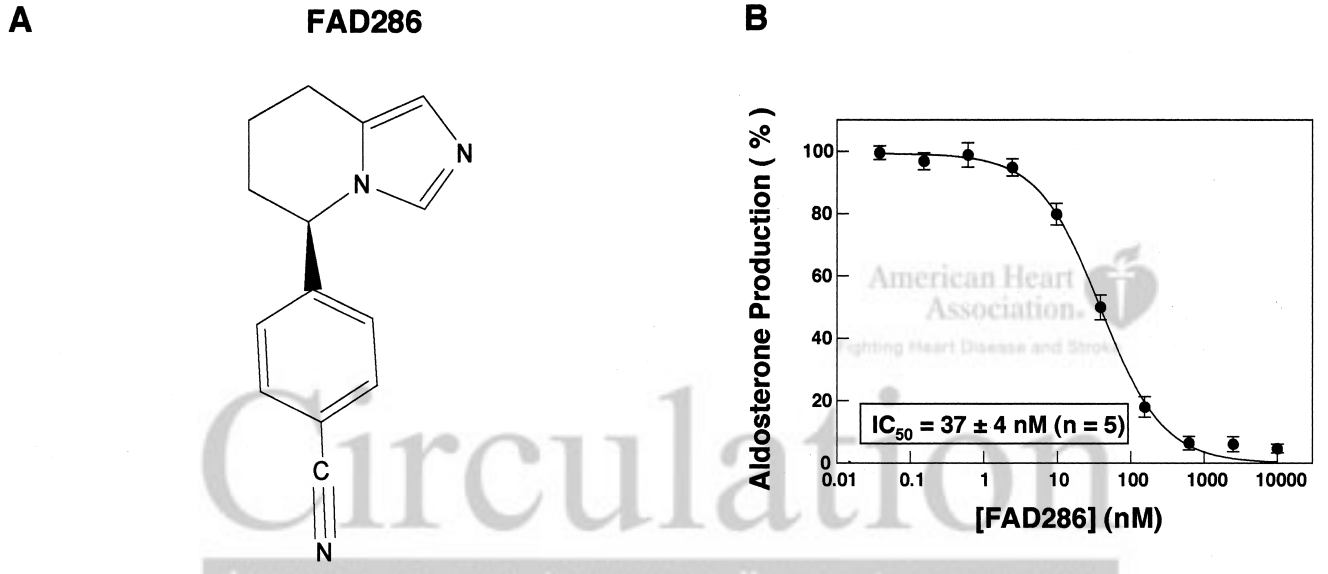

Figure 1. A, FAD286 structure. B, FAD286 dose dependently inhibits Ang II–stimulated ir-Ald production in NCI-H295R human adrenocortical carcinoma cells.

$P<0.05$; Figure 2C). Echocardiographic analysis demonstrated that untreated dTGR developed concentric cardiac hypertrophy that was reduced by FAD286 and normalized by losartan. Total wall thickness (expressed as the sum of the septum plus left ventricular posterior wall) of dTGR was 3.7 ± 0.01 mm with a normal left ventricular end-diastolic diameter. FAD286 and losartan significantly reduced wall thickness to 3.3 ± 0.004 and 2.5 ± 0.006 mm, respectively, $P<0.05$ (Figure 2D). Atrial natriuretic peptide mRNA was increased in untreated dTGR compared with both treatment groups (Figure 2E). Furthermore, untreated dTGR showed an α-MHC shift to the fetal β-MHC phenotype, which indicates cardiac hypertrophy. The MHC shift to the fetal β-isoform was slightly reduced by FAD286 and completely reversed by losartan (Figure 2E).

Aldosterone synthase and Ang II type 1 receptor inhibition improved renal function. Urinary albumin excretion at week 7 was significantly higher in untreated dTGR than in FAD286-treated or losartan-treated dTGR (20.3 ± 4.3, 9.6 ± 1.7, and 0.6 ± 0.14 mg/d, respectively, $P<0.05$; Figure 3A). Chronic FAD286 or losartan treatment reduced the infiltration of macrophages (Figure 3B), CD4 (Figure 3C) and CD8 T-cells, dendritic cells, major histocompatibility complex class II–positive cells, and CD86-positive cells (data not shown) in the kidney to a similar extent. FAD286 and losartan also reduced collagen IV (Figure 3D) and fibronectin (data not shown) deposition in the kidney. Fibronectin and collagen IV semiquantification demonstrated that losartan was slightly more effective (a score of 5+ for dTGR, 2+ for dTGR+FAD286, and 1+ for dTGR+losartan).

Effect of ADX on Organ Damage

To elucidate the role of aldosterone in the pathogenesis of Ang II–induced organ damage in more detail, we adrenalectomized dTGR at 4 weeks of age. The cumulative analysis from protocols II and III showed a 73% mortality rate of dTGR-dexamethasone-salt rats at week 7, whereas only 22% of ADX-dTGR-dexamethasone-salt rats died (Figure 4A). In protocol III at week 9, all dTGR-dexamethasone-salt rats were dead, whereas only 38% of ADX-dTGR-dexamethasone-salt rats had died (data not shown). ADX had no effect on systolic blood pressure (190 ± 9 and 187 ± 4 mm Hg at week 6, respectively; Figure 4B). Cardiac hypertrophy index was significantly more elevated in dTGR-dexamethasone-salt rats than in ADX-dTGR-dexamethasone-salt rats (5.7 ± 0.4 and 4.5 ± 0.1 mg/g, $P<0.05$; Figure 4C). Macrophage infiltration in hearts of ADX rats was significantly reduced compared with dTGR-dexamethasone-salt rats (not shown). At week 6, albuminuria was reduced in ADX-dTGR-dexamethasone-salt rats to almost normal levels, namely, 1.5 ± 0.7 mg/d compared with 47.8 ± 18.3 mg/d in dTGR-dexamethasone-salt rats ($P<0.05$; Figure 4D). Deposition of collagen IV in the kidney (a score of 4+ for dTGR-dexamethasone-salt and 1+ for ADX-dTGR-dexamethasone-salt; Figure 4E) and fibronectin in the heart (a score of 4+ for dTGR-dexamethasone-salt and 2+ for ADX-dTGR-dexamethasone-salt; Figure 4F) was significantly reduced after ADX. Renal CD4, CD8 T-cell, and macrophage infiltration, as well as dendritic cell and CD86-positive cell infiltration, were all significantly reduced in ADX rats (data not shown). These data document that ADX markedly improves renal and cardiac damage in salt-treated dTGR. In protocol III, the rats were followed up to week 9. FAD286 treatment of ADX-dTGR-dexamethasone-salt rats reduced mortality to 28% without affecting blood pressure. The treatment significantly reduced infiltration of macrophages and T cells in the heart (data not shown).

balt2/zhc-ci/zhc-ci/zhc02305/zhc2296-05a | mortonk2 | S=4 | 5/19/05 | 7:39 | 4/Color Figure(s): 3,4 | Art: 165856

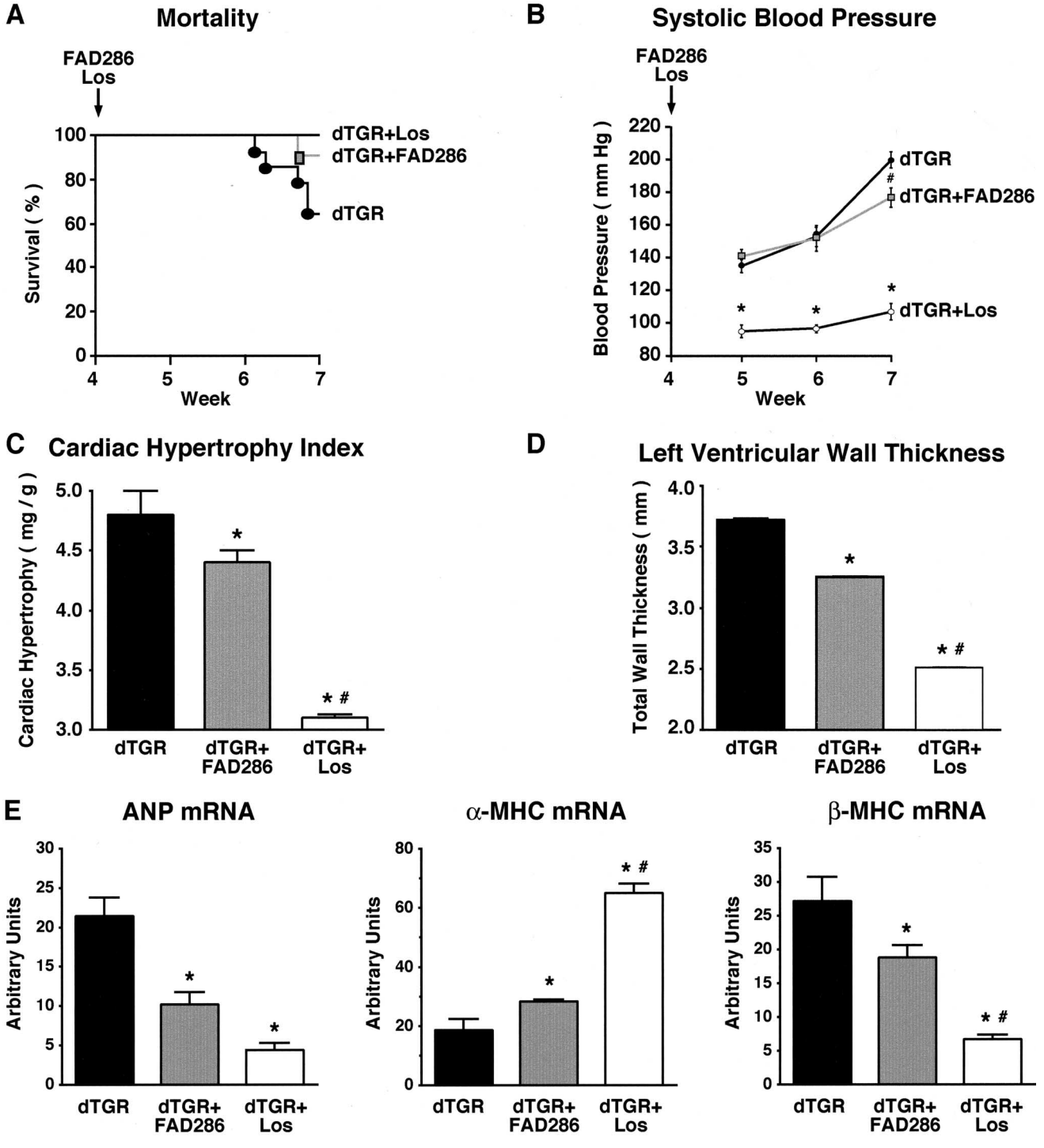

Figure 2. A, FAD286 and losartan reduced mortality. B, Losartan prevented hypertension. In contrast, FAD286 reduced blood pressure only slightly at week 7. C and D, FAD286 and losartan both reduced cardiac hypertrophy index and total wall thickness (expressed as septum+left ventricular wall diameter). E, FAD286 and losartan reduced atrial natriuretic peptide (ANP) expression and prevented MHC isotype switching from α- to β-form. Results are mean±SEM (*$P<0.05$ vs untreated dTGR, #$P<0.05$ vs dTGR+FAD286).

Effect of FAD286 on Plasma and Cardiac Aldosterone, Plasma Renin, and Corticosterone

FAD286 and losartan treatment both reduced circulating and cardiac levels of ir-Ald compared with untreated dTGR. Median values (ranges) were as follows: serum aldosterone 136 (81–454), 131 (8–296), and 408 (114–1410) pg/mL, respectively, and cardiac aldosterone 458 (274–827), 500 (173–3460), and 3826 (302–14286) pg/g wet weight, respectively (Figure 5A). The highest cardiac and plasma aldosterone levels were found in untreated dTGR with the most severe organ damage. Cardiac and plasma aldosterone concentrations were reduced in parallel by the treatments. Untreated dTGR showed very high total PRC with a median value at 53 (13–173) ng · mL^{-1} · h^{-1}. The highest PRC was

F5

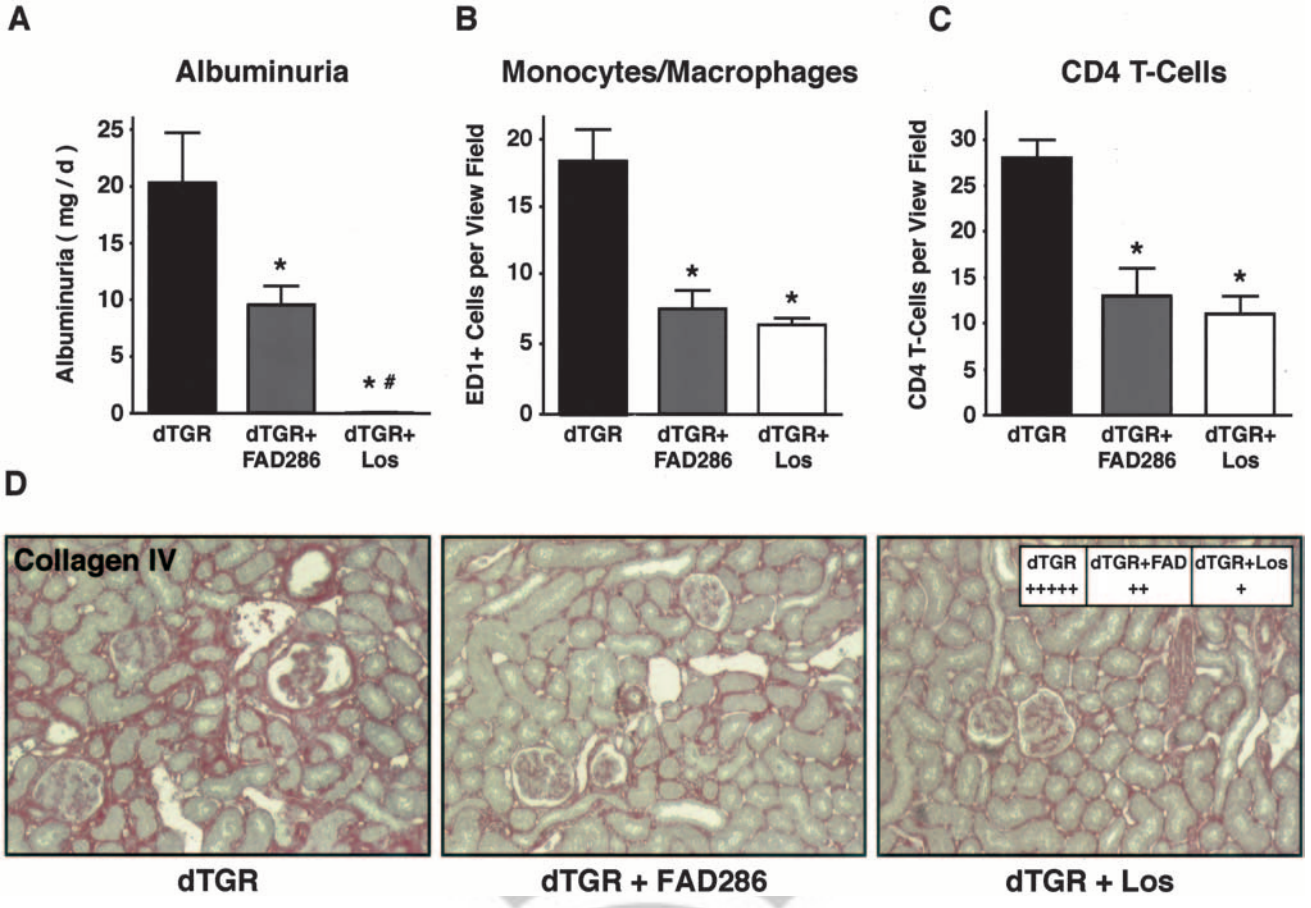

Figure 3. A, FAD286 and losartan both reduced albuminuria; losartan was more effective. Monocyte and macrophage infiltration (ED1-positive cells; B) and CD4 T cells (C) were reduced by both treatments. D, Renal collagen IV was reduced in FAD286- and losartan-treated animals. Results are mean±SEM (*$P<0.05$ vs untreated dTGR, #$P<0.05$ vs dTGR+FAD286).

again observed in untreated dTGR with the most severe organ damage. FAD286 treatment reduced serum aldosterone by 67%, from 408 to 136 pg/mL. Losartan treatment had an effect similar to that of FAD286 on serum aldosterone levels. FAD286 and losartan treatment did not affect PRC or serum corticosterone levels. Median PRC levels for FAD286- and losartan-treated dTGR were 8.0 (range 5.3 to 50) and 41 (range 13 to 57) ng · mL^{-1} · h^{-1}; corticosterone levels were 459 (range 103 to 524), 416 (range 187 to 563), and 395 (range 310 to 409) ng/mL, respectively.

Effect of ADX on Plasma and Cardiac Aldosterone, Plasma Renin, and Corticosterone

Dexamethasone-salt treatment (Figure 5B) of dTGR resulted in an 85% suppression of PRC, from a median value of 53 (13–173) ng · mL^{-1} · h^{-1} in untreated dTGR to low normal 8.0 (8.0 to 48) ng · mL^{-1} · h^{-1} (normal PRC in Sprague-Dawley rats is 23 (5.3 to 36) ng · mL^{-1} · h^{-1}). At the same time (week 7), dexamethasone-salt treatment reduced serum aldosterone by 84%, from 408 (114–1410) to 65 (25–699) pg/mL, and cardiac aldosterone by 95%, from a median of 3826 (302–14286) to 267 (102–3621) pg/g. Serum corticosterone decreased in a similar pattern, from 459 (103–524) ng/mL in untreated dTGR to 173 (57–317) ng/mL in dTGR-dexamethasone-salt rats (−62%). dTGR-dexamethasone-salt rats that underwent additional ADX showed a further reduction of serum and cardiac aldosterone to 2.0 (<1.6 to 10) pg/mL (−99.5%) and to 27 (13–45) pg/g (−99.3%), respectively, whereas PRC remained low at 16 (8–28) ng · mL^{-1} · h^{-1}. In parallel to the aldosterone vanishing after ADX, serum corticosterone also disappeared (assay detection limit <1 ng/mL).

By week 9, cardiac aldosterone had fallen below 20 pg/g in all rats (10 [<6.7 to 19] pg/g). Additional treatment of ADX-dTGR-dexamethasone-salt rats with FAD286 resulted in undetectable serum aldosterone (<1.6 pg/mL) in 7 of 8 rats and cardiac aldosterone values below 10 pg/g in all 5 hearts tested.

Discussion

We found that aldosterone production inhibition by FAD286 or ADX protected rats from Ang II–induced inflammatory and fibrotic organ damage. The present data also demonstrated that the main source of cardiac aldosterone in the dTGR model is the adrenal gland. These results show the first description of protection via aldosterone synthase inhibition in vivo. We found previously that MR blockade protects against Ang II–induced organ damage. The MR antagonists spironolactone and eplerenone also reduced mortality and ameliorated renal and cardiac damage in dTGR rats.[9,10]

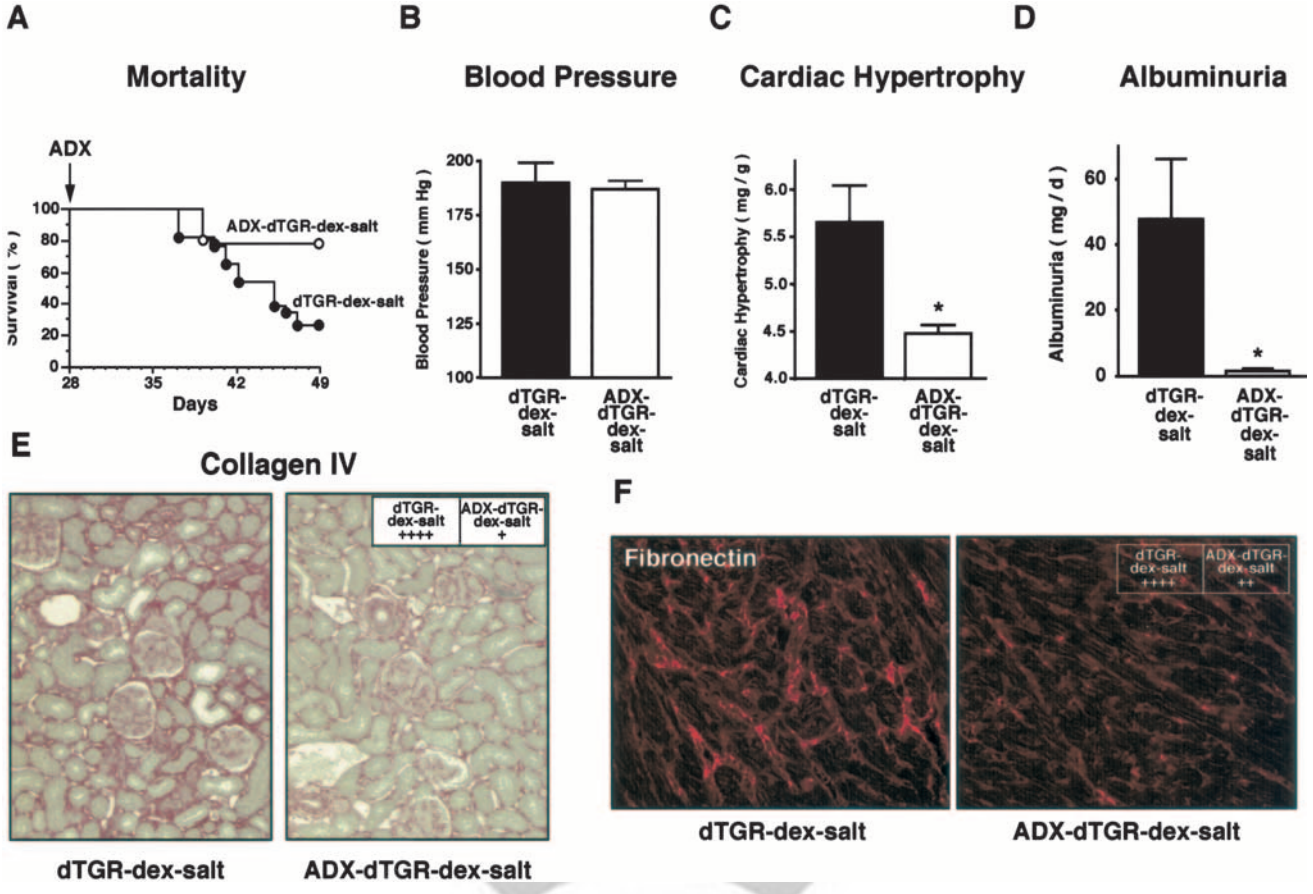

Figure 4. A, ADX reduced mortality in dTGR. B, Systolic blood pressure at week 6 was not different between 2 groups. C, ADX reduced cardiac hypertrophy. D, Albuminuria was reduced in ADX rats. E, Renal collagen IV immunoreactivity was reduced after ADX. F, ADX-dTGR-dexamethasone-salt showed less cardiac fibrosis (fibronectin immunoreactivity) than dTGR-dexamethasone-salt. Results are mean±SEM (*$P<0.05$ vs dTGR-dexamethasone-salt).

Rocha et al[15] showed that MR blockade prevents Ang II/salt-induced vascular inflammation in the rat heart. One explanation for this effect might be the interaction between the Ang II receptor and MR. Xiao et al[16] demonstrated the aldosterone-potentiated, Ang II–induced proliferation of vascular smooth muscle cells. We showed that aldosterone potentiated Ang II–induced extracellular signal-regulated kinase-1/2 (ERK1/2)mitogen-activated protein kinase signaling in vascular smooth muscle cells. In addition, Ang II–induced ERK1/2 phosphorylation depends on a functioning MR.[9] The effects are mediated in part via the generation of oxygen radicals. Keidar et al[17] demonstrated that the aldosterone antagonist eplerenone reduced oxidative stress in serum and peritoneal macrophages of apolipoprotein E knockout mice, which correlated with a significant reduction in atherosclerotic lesion area. Taken together, these findings fit well with observations made by Schiffrin et al[18] more than 20 years ago that demonstrated an interaction between the aldosterone and Ang II signaling pathways.

Besides the steroidogenic acute regulatory protein that moves cholesterol into the mitochondria (StAR), the key enzyme in the production of aldosterone is the aldosterone synthase or CYP11B2. CYP11B2 was isolated in 1992 by Kawamoto et al[19] and was mapped to human chromosome 8q24.3.[20] The enzyme is expressed in the adrenal gland zona glomerulosa and determines circulating aldosterone levels. CYP11B2 mRNA expression has also been found in blood vessels and brain.[21,22] However, the physiological relevance of these findings is currently not clear. In the present animal model, depletion of circulating aldosterone after ADX and reduction of aldosterone due to pharmacological intervention with the aldosterone synthase inhibitor FAD286 and the Ang II type 1 receptor blocker losartan ameliorated Ang II–induced renal and cardiac damage. Chander et al[23] showed similar results in saline-drinking, stroke-prone spontaneously hypertensive rats (SHRSP), in which ADX prevented the development of thrombotic microangiopathy. The authors suggested that aldosterone was the major pathogenic stimulus in this animal model, because only resubstitution with aldosterone, not Ang II, caused thrombotic microangiopathy in ADX-SHRSP.

Ang II and a high extracellular potassium concentration stimulate CYP11B2 activity. High salt suppresses circulating aldosterone levels.[24] In the present model, dexamethasone-salt treatment also led to 6-fold lower circulating aldosterone levels and 14-fold lower cardiac aldosterone levels. Takeda et al[21] observed a reduction in circulating aldosterone levels in sodium-loaded SHRSP; however, in contrast to the present results, they described an enhanced cardiac and vascular aldosterone synthesis in sodium-treated animals.[21,25] Very

balt2/zhc-ci/zhc-ci/zhc02305/zhc2296-05a | mortonk2 | S=4 | 5/19/05 | 7:39 | 4/Color Figure(s): 3,4 | Art: 165856

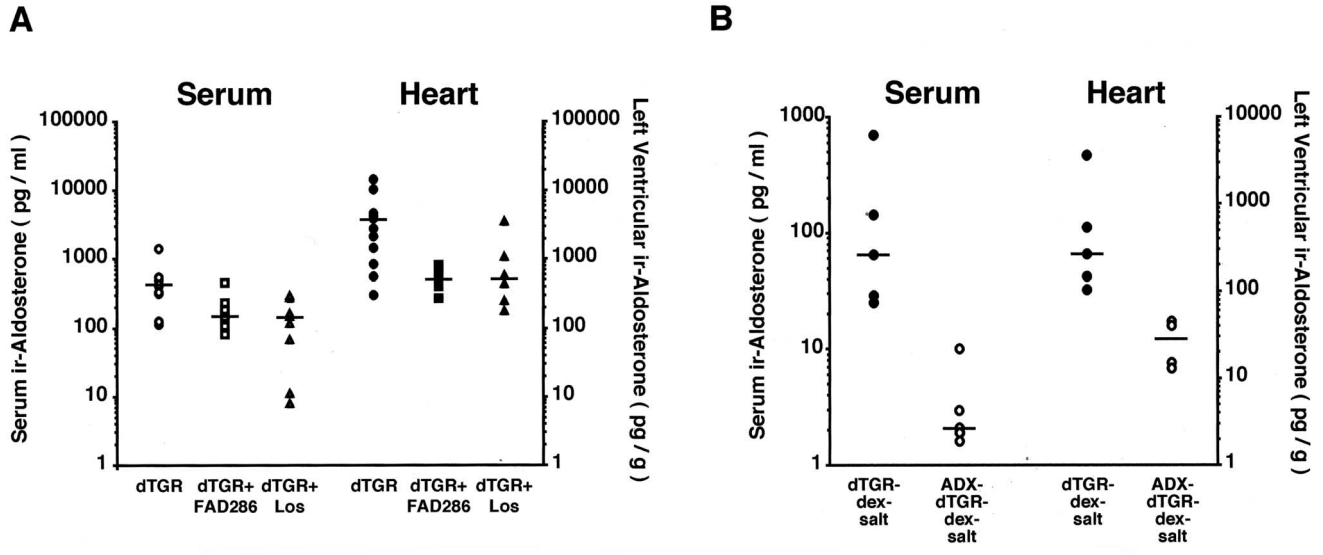

Figure 5. A and B, Serum and cardiac aldosterone concentrations (log scale). FAD286 and ADX decreased serum and cardiac aldosterone concentrations.

recently, Gomez-Sanchez et al[26] showed that in healthy rats, cardiac aldosterone levels were determined by aldosterone production in the adrenal gland. The present data in transgenic ADX rats confirm their findings and extend them to a pathophysiological situation. Three weeks after ADX, ADX-dTGR-dexamethasone-salt rats showed only a very small amount of ir-Ald in the heart, which equaled only 10% of cardiac aldosterone in dTGR-dexamethasone-salt rats with intact adrenals and 0.7% in untreated dTGR. At 5 weeks after ADX, cardiac ir-Ald was 3-fold lower than 3 weeks after ADX. These data suggest that in the present transgenic model, >99% of cardiac aldosterone is not produced locally, and the major source of aldosterone originates from the adrenal gland. The high cardiac aldosterone levels and the high cardiac/plasma ratio in untreated dTGR surprised us. In nontransgenic Sprague-Dawley controls, plasma aldosterone was 143 (range 79 to 226) pg/mL, and cardiac aldosterone was 140 (range 80 to 654) pg/g. These values correspond to those reported by Sanchez-Gomez et al.[26] However, when we compared these values with those found in the present dTGR model, we found only about a 3-fold increase in plasma levels but a 30-fold increase in cardiac levels. This suggests that substantial amounts of circulating aldosterone might be taken up into the heart. In support of this interpretation is the fact that we also found a strong correlation between plasma and cardiac aldosterone levels.

AQ: 11

The role of locally produced aldosterone and its pathophysiological significance are currently debated.[27,28] Sylvestre et al[29] found increased aldosterone concentrations after Ang II or adrenocorticotropic hormone administration in isolated perfused hearts of Wistar rats. Aldosterone production by the failing heart has been suggested on the basis of catheter-obtained aldosterone concentrations across the heart.[30] Studies of patients with acute myocardial infarction and with congestive heart failure have demonstrated that aldosterone is taken up from the circulation into the injured heart.[31,32] However, in patients with hypertrophic cardiomyopathy, a 7-fold upregulation of cardiac CYP11B2 mRNA was reported.[33] The latter finding suggests local production of aldosterone in addition to uptake of the hormone from the circulation. We also addressed the issue of CYP11B2 expression in failing hearts in the present model. We analyzed CYP11B2 mRNA expression in 2 dTGR subgroups, dTGR with cardiac hypertrophy and dTGR with terminal heart failure. Nevertheless, no CYP11B2 upregulation was observed (unpublished data). In addition, we found low levels of circulatory and cardiac aldosterone at 3 weeks after ADX. These values decreased further at 5 weeks after ADX and fell partly below the detection limit. Thus, the present data suggest that in the dTGR model, most, if not all, cardiac aldosterone was generated in the adrenal glands, released into the bloodstream, and taken up by the heart. The amount of aldosterone necessary to regulate salt balance is 100 to 1000 times less than the cortisol concentration needed to influence carbohydrate metabolism. Therefore, even small changes in aldosterone concentration might change the fate of cells and tissues locally. This state of affairs has been shown in vitro, where nanomolar concentrations of aldosterone potentiated epidermal growth factor–induced early signaling in Chinese hamster ovary cells[34] or Ang II–induced signaling in vascular smooth muscle cells.[9,16]

In conclusion, the present results document the potential therapeutic utility of the novel aldosterone synthase inhibitor FAD286 in an Ang II–dependent hypertensive animal model. Depletion of aldosterone due to ADX prevented organ damage, although we cannot completely rule out a modest contribution by corticosterone. The present data demonstrate that in this model, cardiac aldosterone levels depend on aldosterone synthesis in the adrenal glands. Whether or not a local aldosterone production contributes to other forms of heart disease (ischemia, for example) deserves further study.[35]

Acknowledgments

The present studies were supported by grants-in-aid from the NGFN (Nationales Genom Netzwerk) and by Novartis Institutes for Bio-

Medical Research USA. Dr Muller holds a Helmholtz fellowship. The Deutsche Forschungsgemeinschaft (DFG) supported Drs Muller and Luft. We thank M. Köhler, G. Ńdiaye, M. Schmidt, A. Schiche, J. Meisel, A. Weller, F. Nicoud, I. Keller, S. Novelli, and J. Czychi for their excellent technical assistance.

References

1. Pitt B, Zannad F, Remme WJ, Cody R, Castaigne A, Perez A, Palensky J, Wittes J, for the Randomized Aldactone Evaluation Study Investigators. The effect of spironolactone on morbidity and mortality in patients with severe heart failure. *N Engl J Med*. 1999;341:709–717.
2. Pitt B, Remme W, Zannad F, Neaton J, Martinez F, Roniker B, Bittman R, Hurley S, Kleiman J, Gatlin M. Eplerenone, a selective aldosterone blocker, in patients with left ventricular dysfunction after myocardial infarction. *N Engl J Med*. 2003;348:1309–1321.
3. Takeda Y. Vascular synthesis of aldosterone: role in hypertension. *Mol Cell Endocrinol*. 2004;217:75–79.
4. Sato A, Saruta T. Aldosterone escape during angiotensin-converting enzyme inhibitor therapy in essential hypertensive patients with left ventricular hypertrophy. *J Int Med Res*. 2001;29:13–21.
5. Sato A, Hayashi K, Naruse M, Saruta T. Effectiveness of aldosterone blockade in patients with diabetic nephropathy. *Hypertension*. 2003;41:64–68.
6. Hayashi M, Tsutamoto T, Wada A, Tsutsui T, Ishii C, Ohno K, Fujii M, Taniguchi A, Hamatani T, Nozato Y, Kataoka K, Morigami N, Ohnishi M, Kinoshita M, Horie M. Immediate administration of mineralocorticoid receptor antagonist spironolactone prevents post-infarct left ventricular remodeling associated with suppression of a marker of myocardial collagen synthesis in patients with first anterior acute myocardial infarction. *Circulation*. 2003;107:2559–2565.
7. Muller DN, Shagdarsuren E, Park JK, Dechend R, Mervaala E, Hampich F, Fiebeler A, Ju X, Finckenberg P, Theuer J, Viedt C, Kreuzer J, Heidecke H, Haller H, Zenke M, Luft FC. Immunosuppressive treatment protects against angiotensin II–induced renal damage. *Am J Pathol*. 2002;161:1679–1693.
8. Luft FC, Mervaala E, Muller DN, Gross V, Schmidt F, Park JK, Schmitz C, Lippoldt A, Breu V, Dechend R, Dragun D, Schneider W, Ganten D, Haller H. Hypertension-induced end-organ damage: a new transgenic approach to an old problem. *Hypertension*. 1999;33:212–218.
9. Mazak I, Fiebeler A, Muller DN, Park JK, Shagdarsuren E, Lindschau C, Dechend R, Viedt C, Pilz B, Haller H, Luft FC. Aldosterone potentiates angiotensin II–induced signaling in vascular smooth muscle cells. *Circulation*. 2004;109:2792–2800.
10. Fiebeler A, Schmidt F, Muller DN, Park JK, Dechend R, Bieringer M, Shagdarsuren E, Breu V, Haller H, Luft FC. Mineralocorticoid receptor affects AP-1 and nuclear factor-kappaB activation in angiotensin II–induced cardiac injury. *Hypertension*. 2001;37:787–793.
11. Ganten D, Wagner J, Zeh K, Bader M, Michel JB, Paul M, Zimmermann F, Ruf P, Hilgenfeldt U, Ganten U, Kaling M, Bachmann S, Fukamizu A, Mullins JJ, Murakami K. Species specificity of renin kinetics in transgenic rats harboring the human renin and angiotensinogen genes. *Proc Natl Acad Sci U S A*. 1992;89:7806–7810.
12. Nussberger J, Waeber B, Brunner HR, Burris JF, Vetter W. Highly sensitive microassay for aldosterone in unextracted plasma: comparison with two other methods. *J Lab Clin Med*. 1984;104:789–796.
13. Poulsen K, Jorgensen J. An easy radioimmunological microassay of renin activity, concentration and substrate in human and animal plasma and tissues based on angiotensin I trapping by antibody. *J Clin Endocrinol Metab*. 1974;39:816–825.
14. Vecsei P. Glucocorticoids: cortisol, corticosterone, compound S and their metabolites. In: Jaffe BM, Behrmann HR, eds. *Methods of Hormone Radioimmunoassays.* New York, NY: Academic Press; 1979:767–796.
15. Rocha R, Martin-Berger CL, Yang P, Scherrer R, Delyani J, McMahon E. Selective aldosterone blockade prevents angiotensin II/salt-induced vascular inflammation in the rat heart. *Endocrinology*. 2002;143:4828–4836.
16. Xiao F, Puddefoot JR, Barker S, Vinson GP. Mechanism for aldosterone potentiation of angiotensin II-stimulated rat arterial smooth muscle cell proliferation. *Hypertension*. 2004;44:340–345.
17. Keidar S, Hayek T, Kaplan M, Pavlotzky E, Hamoud S, Coleman R, Aviram M. Effect of eplerenone, a selective aldosterone blocker, on blood pressure, serum and macrophage oxidative stress, and atherosclerosis in apolipoprotein E-deficient mice. *J Cardiovasc Pharmacol*. 2003;41:955–963.
18. Schiffrin EL, Thome FS, Genest J. Vascular angiotensin II receptors in renal and DOCA-salt hypertensive rats. *Hypertension*. 1983;5:V16–V21.
19. Kawamoto T, Mitsuuchi Y, Toda K, Yokoyama Y, Miyahara K, Miura S, Ohnishi T, Ichikawa Y, Nakao K, Imura H, et al. Role of steroid 11 beta-hydroxylase and steroid 18-hydroxylase in the biosynthesis of glucocorticoids and mineralocorticoids in humans. *Proc Natl Acad Sci U S A*. 1992;89:1458–1462. AQ: 12
20. Taymans SE, Pack S, Pak E, Torpy DJ, Zhuang Z, Stratakis CA. Human CYP11B2 (aldosterone synthase) maps to chromosome 8q24.3. *J Clin Endocrinol Metab*. 1998;83:1033–1036.
21. Takeda Y, Yoneda T, Demura M, Miyamori I, Mabuchi H. Sodium-induced cardiac aldosterone synthesis causes cardiac hypertrophy. *Endocrinology*. 2000;141:1901–1904.
22. Gomez-Sanchez CE, Zhou MY, Cozza EN, Morita H, Foecking MF, Gomez-Sanchez EP. Aldosterone biosynthesis in the rat brain. *Endocrinology*. 1997;138:3369–3373.
23. Chander PN, Rocha R, Ranaudo J, Singh G, Zuckerman A, Stier CT Jr. Aldosterone plays a pivotal role in the pathogenesis of thrombotic microangiopathy in SHRSP. *J Am Soc Nephrol*. 2003;14:1990–1997.
24. Volpe M, Rubattu S, Ganten D, Enea I, Russo R, Lembo G, Mirante A, Condorelli G, Trimarco B. Dietary salt excess unmasks blunted aldosterone suppression and sodium retention in the stroke-prone phenotype of the spontaneously hypertensive rat. *J Hypertens*. 1993;11:793–798.
25. Takeda Y, Miyamori I, Inaba S, Furukawa K, Hatakeyama H, Yoneda T, Mabuchi H, Takeda R. Vascular aldosterone in genetically hypertensive rats. *Hypertension*. 1997;29:45–48.
26. Gomez-Sanchez EP, Ahmad N, Romero DG, Gomez-Sanchez CE. Origin of aldosterone in the rat heart. *Endocrinology*. 2004;145:4796–4802.
27. Davies E, MacKenzie SM. Extra-adrenal production of corticosteroids. *Clin Exp Pharmacol Physiol*. 2003;30:437–445.
28. Funder JW. Cardiac synthesis of aldosterone: going, going, gone? *Endocrinology*. 2004;145:4793–4795.
29. Silvestre JS, Robert V, Heymes C, Aupetit-Faisant B, Mouas C, Moalic JM, Swynghedauw B, Delcayre C. Myocardial production of aldosterone and corticosterone in the rat; physiological regulation. *J Biol Chem*. 1998;273:4883–4891.
30. Mizuno Y, Yoshimura M, Yasue H, Sakamoto T, Ogawa H, Kugiyama K, Harada E, Nakayama M, Nakamura S, Ito T, Shimasaki Y, Saito Y, Nakao K. Aldosterone production is activated in failing ventricle in humans. *Circulation*. 2001;103:72–77.
31. Tsutamoto T, Wada A, Maeda K, Hayashi M, Tsutsui T, Ohnishi M, Fujii M, Matsumoto T, Yamamoto T, Takayama T, Ishii C. Transcardiac gradient of aldosterone before and after spironolactone in patients with congestive heart failure. *J Cardiovasc Pharmacol*. 2003;41(suppl 1):S19–S22.
32. Hayashi M, Tsutamoto T, Wada A, Maeda K, Mabuchi N, Tsutsui T, Matsui T, Fujii M, Matsumoto T, Yamamoto T, Horie H, Ohnishi M, Kinoshita M. Relationship between transcardiac extraction of aldosterone and left ventricular remodeling in patients with first acute myocardial infarction: extracting aldosterone through the heart promotes ventricular remodeling after acute myocardial infarction. *J Am Coll Cardiol*. 2001;38:1375–1382.
33. Tsybouleva N, Zhang L, Chen S, Patel R, Lutucuta S, Nemoto S, DeFreitas G, Entman M, Carabello BA, Roberts R, Marian AJ. Aldosterone, through novel signaling proteins, is a fundamental molecular bridge between the genetic defect and the cardiac phenotype of hypertrophic cardiomyopathy. *Circulation*. 2004;109:1284–1291.
34. Krug AW, Schuster C, Gassner B, Freudinger R, Mildenberger S, Troppmair J, Gekle M. Human epidermal growth factor receptor-1 expression renders Chinese hamster ovary cells sensitive to alternative aldosterone signaling. *J Biol Chem*. 2002;277:45892–45897.
35. Silvestre JS, Heymes C, Oubenaissa A, Robert V, Aupetit-Faisant B, Carayon A, Swynghedauw B, Delcayre C. Activation of cardiac aldosterone production in rat myocardial infarction: effect of angiotensin II receptor blockade and role in cardiac fibrosis. *Circulation*. 1999;99:2694–2701.

3.4 Untersuchung zum Einfluss von Aldosteron auf die Angiotensin II-vermittelte Signaltransduktion in glatten Muskelzellen

Die von uns und anderen erhobenen tierexperimentellen Daten veranlassten uns zu *in-vitro*-Studien, welche die frühe Signaltransduktion von Angiotensin II und Aldosteron verglichen und ihre Interaktion prüften.

3.4.1 Stimulierung einer frühen Signaltransduktion durch Aldosteron

Wir untersuchten in glatten Muskelzellen der Ratte in Primärkultur die Phosphorylierung von MAP-Kinasen (*mitogen activated protein kinases*), die Produktion von Sauerstoffradikalen und die Abhängigkeit der Signaltransduktion vom EGFR (*epidermal growth factor receptor*). Aldosteron verursacht in glatten Muskelzellen sowohl die Phosphorylierung von ERK 1/2 (*extracellular signal-regulated kinase 1/2*) als auch von JNK (*c-Jun N-terminal kinase*) nach 10 bis 15 min. In dieser kurzen Zeitspanne ist eine Neusynthese von Proteinen unwahrscheinlich, sodass hier von nicht-transkriptionellen Effekten ausgegangen werden kann. Die beobachtete Phosphorylierung von MAP-Kinasen ist durch den MR vermittelt und benötigt Sauerstoffradikale und einen funktionierenden EGFR (gezeigt durch Vorinkubation mit Spironolakton, Glutathion, Tiron bzw. dem selektiven EGFR-Blocker AG1478).

3.4.2 Potenzierung der Angiotensin II-induzierten nicht-transkriptionellen Signaltransduktion durch Aldosteron

Während die Aldosteron-induzierte ERK1/2-Phosphorylierung nach 10 min zu beobachten ist, bewirkt Angiotensin II bereits eine Phosphorylierung nach etwa 2

min. Stimuliert man glatte Muskelzellen simultan mit Aldosteron und Angiotensin II, ist bereits nach 2 min eine Verstärkung der ERK1/2- und JNK-Phosphorylierung im Vergleich zu Einzelstimulationen festzustellen.

3.4.3 Wirkung von Mineralokortikoid-Rezeptor-Blockern bei der Aldosteron und Angiotensin II-induzierten Signaltransduktion

Zur genaueren Beschreibung der Interaktion zwischen Aldosteron und Angiotensin II auf den Aldosteronrezeptor untersuchten wir die Rolle des Aldosteronrezeptors (MR) bei der Aldosteron- und Angiotensin II-induzierten Signaltransduktion. Eine Vorinkubation der glatten Muskelzellen mit Spironolakton oder Eplerenon verhinderte die Aldosteron-induzierte Phosphorylierung von MAP-Kinasen. Die frühen Effekte des Aldosterons werden also durch den MR vermittelt. Die Blockade am MR beeinträchtigte aber auch die Angiotensin II-induzierte Phosphorylierung von ERK1/2 und JNK. Die EGF-induzierte Phosphorylierung von ERK 1/2 wurde durch Spironolakton nicht beeinflusst. Daher ist es wahrscheinlich, dass die Interaktion zwischen Aldosteron und Angiotensin II proximal des EGF-Rezeptors stattfindet.

Schlussfolgerung: Aldosteron stimuliert über nicht-transkriptionelle Signalwege die Phosphorylierung von MAP-Kinasen und die Produktion von Sauerstoffradikalen. Diese Effekte werden über den MR vermittelt. Aldosteron potenziert die durch Angiotensin II-induzierte frühe Signaltransduktion. Diese Ergebnisse deuten auf eine enge Interaktion zwischen Angiotensin II und Aldosteron auf die Aktivierung der nicht-transkriptionellen Signaltransduktion hin.

Reprint 3

Fiebeler A*, Mazak I*, Muller DN, Park JK, Shagdarsuren E, Lindschau C, Dechend R, Viedt C, Pilz B, Haller H, Luft FC. Aldosterone potentiates angiotensin II-induced signaling in vascular smooth muscle cells. *Circulation*. 2004;109:2792-800.

Aldosterone Potentiates Angiotensin II–Induced Signaling in Vascular Smooth Muscle Cells

Istvan Mazak, MD*; Anette Fiebeler, MD*; Dominik N. Muller, PhD; Joon-Keun Park, PhD; Erdenechimeg Shagdarsuren, PhD; Carsten Lindschau, MSc; Ralf Dechend, MD; Christiane Viedt, MD; Bernhard Pilz, MD; Hermann Haller, MD; Friedrich C. Luft, MD

Background—In a double-transgenic human renin and human angiotensinogen rat model, we found that mineralocorticoid receptor (MR) blockade ameliorated angiotensin II (Ang II)–induced renal and cardiac damage. How Ang II and aldosterone (Ald) might interact is ill defined.

Methods and Results—We investigated the effects of Ang II (10^{-7} mol/L) and Ald (10^{-7} mol/L) on extracellular signal–regulated kinase (ERK) and c-Jun N-terminal kinase (JNK) signaling in vascular smooth muscle cells (VSMCs) with Western blotting and confocal microscopy. Ang II induced ERK 1/2 and JNK phosphorylation by 2 minutes. Ald achieved the same at 10 minutes. Ang II+Ald had a potentiating effect by 2 minutes. Two oxygen radical scavengers and the epidermal growth factor receptor (EGFR) antagonist AG1478 reduced Ang II–, Ald-, and combination-induced ERK1/2 phosphorylation. Preincubating the cells with the MR blocker spironolactone (10^{-6} mol/L) abolished Ang II–induced ROS generation, EGFR transactivation, and ERK1/2 phosphorylation.

Conclusions—Ald potentiates Ang II–induced ERK-1/2 and JNK phosphorylation. Oxygen radicals, the MR, and the EGFR play a role in early signaling induced by Ang II and Ald in VSMCs. These in vitro data may help explain the effects of MR blockade on Ang II–induced end-organ damage in vivo. **(*Circulation*. 2004;109:2792-2800.)**

Key Words: angiotensin ■ aldosterone ■ receptors ■ kinases ■ reactive oxygen species

The Randomized Aldactone Evaluation Study (RALES) showed that adding spironolactone (Spi) to an ACE inhibitor and furosemide-based heart failure treatment reduced mortality by 30%.[1] The beneficial effects of Spi were correlated with decreased plasma levels of N-terminal procollagen III propeptide, a marker of cardiac fibrosis.[2] Recently, a selective aldosterone (Ald) blocker, eplerenone (Epl), was introduced, which has fewer side effects but achieved similarly impressive results in patients with decreased ventricular function after acute myocardial infarction.[3] These data rekindled interest in mineralocorticoid receptor (MR) blockade in the treatment of heart failure and drew attention to a body of evidence supporting the notion that Ald has direct effects on the cardiovascular system independent of renal salt and water regulation. Angiotensin (Ang) II and Ald have very different receptors. Ang II uses G protein–coupled surface receptors, whereas Ald relies on the cytosolic MR, which, when activated, serves as a transcription factor.[4,5] Nevertheless, Ald signaling is not solely a genomic event, and nongenomic signaling is known to occur.[6] Recently, Gekle et al[7] and Krug et al[8] showed in renal tubular epithelial and Chinese hamster ovary (CHO) cells that the epidermal growth factor receptor (EGFR) mediates Ald signaling. The EGFR has been described as a crucial molecule in Ang II–induced signaling as well.[9] We examined the effects of MR blockade on cardiac and renal end-organ damage in a double transgenic rat model. To explore the potential interactions of Ang II and Ald in vascular smooth muscle cells (VSMCs) further, we relied on in vitro experiments.

Methods

Animal Groups and Physiological Measurements

Rats overexpressing the human renin and angiotensinogen genes (dTGR) have been described in detail earlier.[10,11] Rats were purchased from RCC Ltd (Fuellinsdorf, Switzerland). Experiments were conducted in 4-week-old male dTGR (n=28) and nontransgenic, age-matched Sprague-Dawley (SD; Tierzucht Schoenwalde, Germany; n=7) rats after due approval (permit No. G 408/97). The Ald blockade dTGR group (n=14) received Epl (provided by Pharmacia USA) for 3 weeks (100 mg · kg^{-1} · d^{-1} in the diet). Systolic blood pressure was measured by tail-cuff under light ether anesthesia. Urine samples were collected over 24 hours. Urinary albumin was measured by ELISA (CellTrend). Echocardiography with M-mode and pulse-wave Doppler was performed with a commercially available system equipped with a 7-MHz phased-array transducer under

Received February 10, 2003; de novo received October 14, 2003; revision received February 10, 2004; accepted February 24, 2004.

From Medical Faculty of the Charité, Franz Volhard Clinic, HELIOS Klinikum-Berlin and Max Delbrück Center for Molecular Medicine, Berlin, Germany (I.M., A.F., D.N.M., E.S., R.D., B.P., F.C.L.); the Department of Internal Medicine and Nephrology, Hannover University Medical School, Hannover, Germany (J.-K.P., C.L., H.H.); and the Department of Internal Medicine III, University of Heidelberg, Heidelberg, Germany (C.V.).

*The first 2 authors contributed equally to this work.

Correspondence to Friedrich C. Luft, Wiltberg Strasse 50, 13125 Berlin, Germany. E-mail luft@fvk-berlin.de

Circulation **is available at http://www.circulationaha.org** **DOI: 10.1161/01.CIR.0000131860.80444.AB**

light ether anesthesia. Three measurements per heart were averaged. Rats were killed at the age of 7 weeks.

Cell Culture

Aortic VSMCs were isolated from SD rats.[12] Passages 2 to 4 were used for immunohistochemistry and passage 4 to 10 for Western blotting. VSMCs were phenotyped by staining for muscle-specific α-actin (Dako) and desmin (Boehringer-Mannheim). VSMCs were also analyzed for MR expression. TaqMan polymerase chain reaction (PCR) demonstrated RNA expression of the receptor (primer sequences as follows: MR-F, GCACTCACACCATCCCCG; MR-R, TCGTAGCCTGCATACACGGTC; MR-P, FAM-CCATGATCCT-GGAGAACATCGAGCCT-TAMRA; data not shown). Cells were treated with Ang II (Sigma), Ald (Clinalfa), glutathione (GSH) (Sigma), or Tiron (4,5-dihydroxy-1,3-benzene-disulfonic acid; Sigma). The following blockers were used as indicated: AG 1478 (Calbiochem) and Spi (Sigma). All experiments were performed under 18-hour serum-free conditions.

Immunohistochemistry

Confocal microscopy was performed as described.[12] At least 50 to 80 cells from each experiment were examined under each condition by 2 different investigators without knowledge of the origin of the specimens. Quantification was performed with histogram function in the MRC Laser Sharp software. The subcellular regions were outlined manually, and the calculated mean fluorescence intensity was obtained for the delineated regions. Data are presented as the mean fluorescence intensity in the respective cell area. Immunohistochemistry for collagen IV and phospho-ERK was performed.[10,11] For collagen IV detection, we used an antibody from Southern Biotech (1:500), and for phospho-ERK, from Santa Cruz (1:100). Ten different areas per organ (n=5 per group) were analyzed semiquantitatively. The data are expressed in arbitrary units (0 to 5), based on the staining intensity.

Western Blot

The following primary antibodies were used: polyclonal ERK1/2 (NEB; 1:1000), phospho-ERK1/2 (NEB; 1:1000), phospho-Elk-1 (NEB; 1:1000), phospho-JNK (Dianova; 1:1000), and p-EGFR (NEB; 1:1000). Peroxidase-conjugated secondary antibodies were from Sigma (1:5000). Blots were developed with the chemiluminescence substrate and visualized on Kodak films. Three to 5 cell stimulation experiments of each protocol were performed and quantified. For semiquantification, the most intense band was defined as 100%. All other bands of the experiment were calculated as percentage of the maximum.

p42/44 MAP Kinase Assay

The kinase assay for ERK 1/2 (p42/44 kinase assay) was performed with a kit from New England BioLabs. Briefly, after stimulation, active mitogen-activated protein (MAP) kinase was selectively immunoprecipitated. The precipitate was incubated with ATP and Elk-1 fusion protein in a kinase buffer. This allows active MAP kinase to phosphorylate Elk-1. Elk-1 phosphorylation was measured by Western blotting and quantified as described above.

Dichlorofluorescein to Measure Intracellular Reactive Oxygen Species

Intracellular reactive oxygen species (ROS) production was measured in rat VSMCs by the method of Ohba et al.[13] Briefly, cells were kept in serum-free conditions for 24 hours (0.1% BSA). Cells were preincubated with Spi 10^{-6} mol/L for 30 minutes or DMSO 10 μmol/L for 30 minutes. H2DCF-DA (2′7′-dichlorofluorescein-diacetate, Sigma, 5 μmol/L) was added, and cells were stimulated with Ang II 10^{-7} mol/L.

Statistics

Data are presented as mean±SEM. Statistical significance was tested by ANOVA, blood pressure and albuminuria by repeated-measures ANOVA and the Scheffé test, and ROS generation by SPSS. We used a general linear model with repeated measurements and post hoc by paired *t* test with the Bonferroni correction. A value of $P<0.05$ was considered statistically significant. The data were analyzed by use of StatView statistical software.

Results

MR Blockade Prevents Ang II–Induced End-Organ Damage In Vivo

Untreated dTGR (n=14) showed increased systolic blood pressure compared with Epl-treated dTGR (n=14) and nontransgenic (n=7) rats (204±5 versus 180±5 versus 119±6 mm Hg, $P<0.05$, respectively). Systolic blood pressure at week 7 was 61 mm Hg higher in Epl-treated dTGR compared with SD rats ($P<0.05$; Figure 1A). Urinary albumin excretion was markedly higher in dTGR than in SD rats: 17.8±2.1 versus 0.2±0.02 mg/d ($P<0.001$). Epl treatment reduced albuminuria (9.2±1.3 mg/d; $P<0.05$; Figure 1B). Epl also reduced collagen IV matrix deposition in the kidney (n=5 each; Figure 1C) and heart (data not shown). Untreated dTGR show ERK1/2 phosphorylation in the media of renal dTGR vessels, which was reduced by Epl (n=5 each; Figure 1D). Epl also reduced cardiac hypertrophy index (4.5±0.1 versus 5.4±0.2 mg/g; $P<0.05$; Figure 1E) and improved left ventricular diastolic function (normalized E/A ratio; Figure 1F) compared with untreated dTGR. Nevertheless, cardiac hypertrophy index remained increased in Epl-treated dTGR compared with nontransgenic SD rats (3.6±0.1 mg/g; $P<0.05$). These data document marked amelioration of renal and cardiac damage by MR blockade.

Ald Potentiates Ang II–Induced ERK Phosphorylation

Ang II (10^{-7} mol/L) induced ERK phosphorylation in VSMCs with a maximal intensity after 2 minutes (Figure 2A). After Ald (10^{-7} mol/L), the maximal intensity of ERK phosphorylation was observed at 10 minutes (Figure 2B). The combination of Ang II and Ald resulted in a stronger ERK phosphorylation at 1 and 2 minutes than with Ang II or Ald alone (Figure 2, C and E). Western blot and confocal microscopy experiments showed that Ang II and Ald at a lower concentration (both 10^{-8} mol/L) still caused a similar potentiation (data not shown). Using the ERK1/2 MAP kinase assay, kinase activity was increased after Ang II and Ald alone as well as after the combination. However, the combination resulted in a higher MAP kinase activity, resulting in enhanced Elk-1 phosphorylation compared with the single compounds (Figure 2D). We also investigated Ang II– and/or Ald-induced ERK phosphorylation in the presence of the protein synthesis inhibitors actinomycin D and cycloheximide. Neither inhibitor affected short-term ERK phosphorylation, supporting a nongenomic Ang II/Ald effect (data not shown).

Ald Potentiates Ang II–Induced JNK Phosphorylation

Ang II (10^{-7} mol/L) also induced JNK phosphorylation with a maximal intensity after 2 minutes, whereas the maximal intensity of JNK phosphorylation after Ald (10^{-7} mol/L) stimulation was observed at 10 minutes. When the cells were

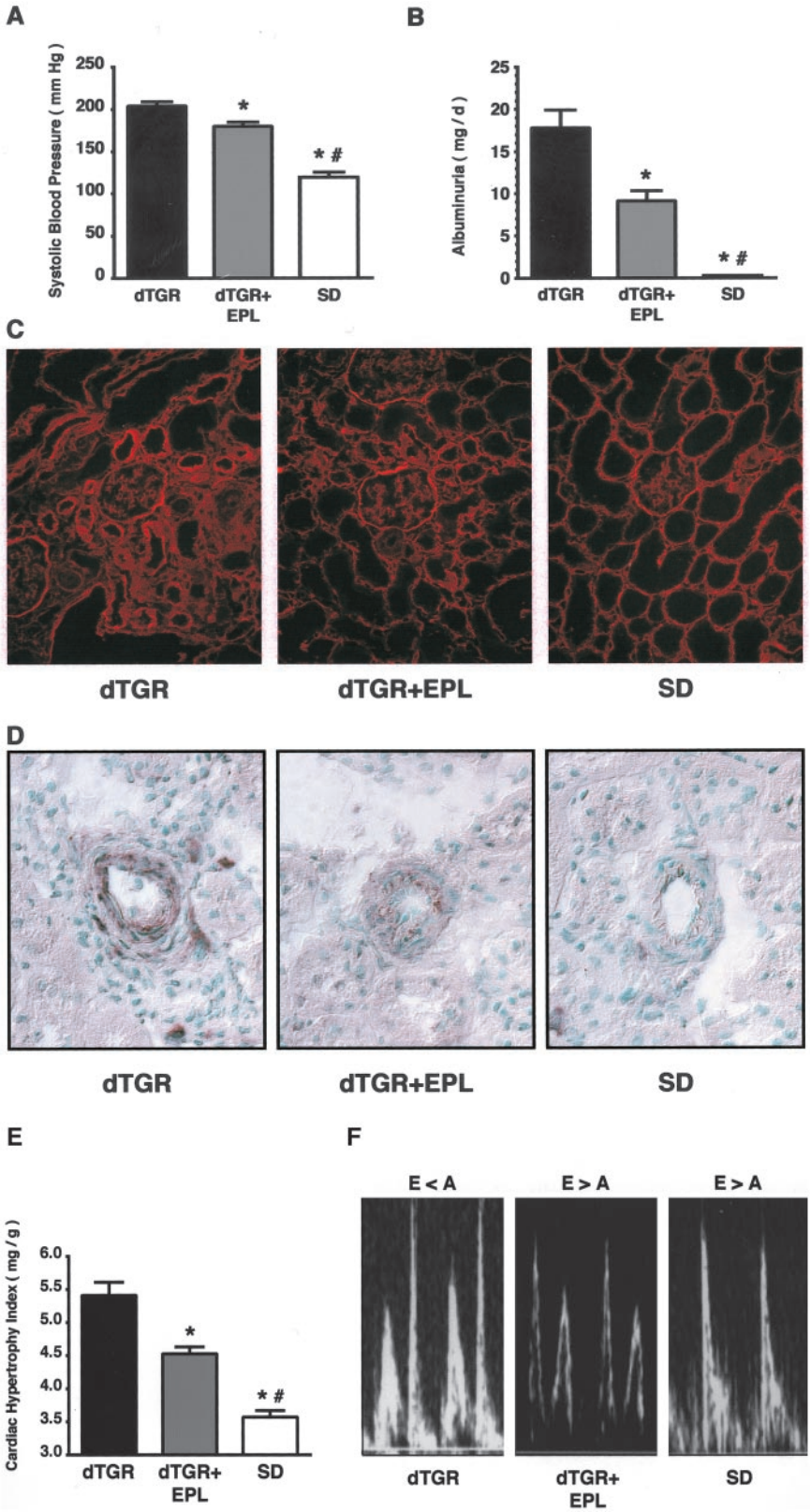

Figure 1. A, Systolic blood pressure was lowered by Epl treatment ($P<0.05$) but not to Sprague-Dawley (SD) levels (mean±SEM). *$P<0.05$ dTGR vs dTGR+EPL; #$P<0.05$ dTGR+EPL and SD. B, Epl reduced albuminuria ($P<0.001$). C, Epl markedly reduced collagen IV deposition in glomerulus, basement membrane, and peritubular capillaries. D, Untreated dTGRs show p-ERK 1/2 immunoreaction in renal vessel media. Epl reduced p-ERK toward SD levels. E, Epl reduced cardiac hypertrophy. F, Epl restored E>A diastolic filling.

stimulated with the combination of both Ang II and Ald, a significantly stronger JNK phosphorylation was observed at 1 minute than with the single compounds alone (data not shown).

Ang II and Ald Signaling Is Mediated Through Oxygen Radicals

VSMCs were preincubated with GSH for 90 minutes before stimulation. GSH (2 mmol/L) preincubation suppressed both

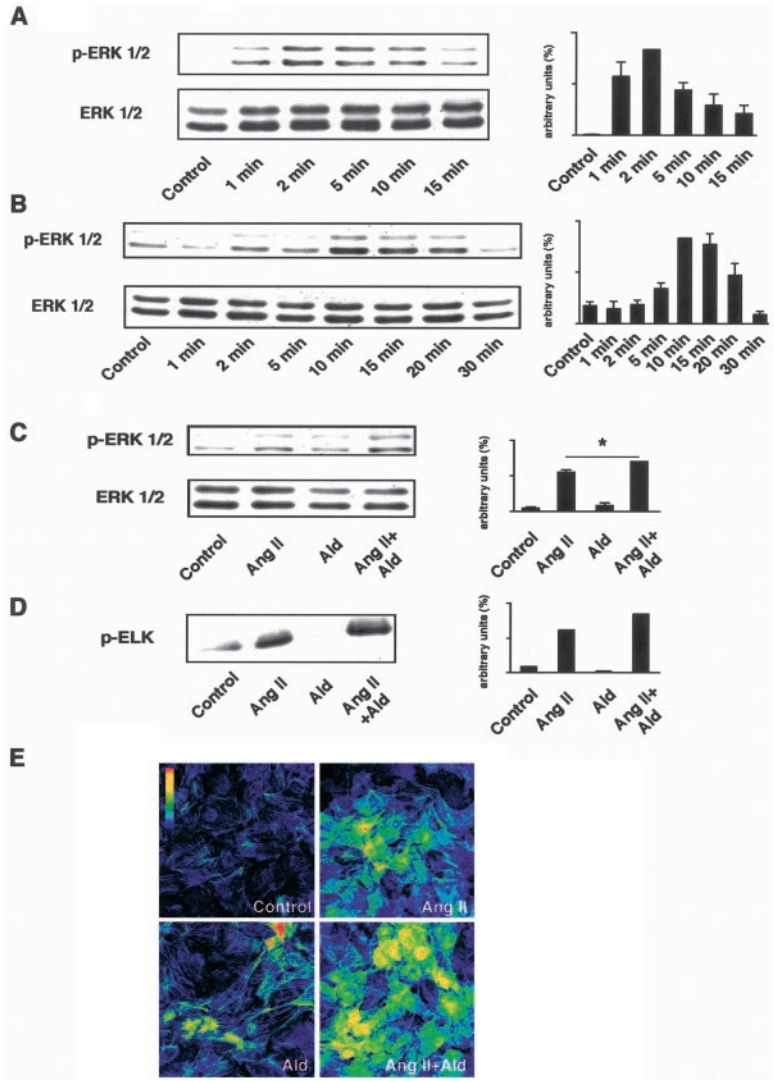

Figure 2. A, Ang II (10^{-7} mol/L) stimulated ERK 1/2 phosphorylation in VSMCs at 2 minutes (n=4). B, Ald (10^{-7} mol/L) stimulated ERK 1/2 phosphorylation at 10 minutes (n=4). C, At 2 minutes, effects of Ang II and Ald were potentiated ($P<0.01$; n=6). *$P<0.05$ Ang II vs Ang II+Ald. D, MAP kinase–induced Elk-1 phosphorylation was enhanced in VSMCs treated with Ang II and Ald after 2 minutes. E, Immunofluorescence and confocal microscopy confirmed potentiating effect of Ald on Ang II–induced ERK 1/2 phosphorylation.

ERK (Figure 3, A through C) and JNK (Figure 3, D through F) phosphorylation after stimulation with Ang II (10^{-7} mol/L), Ald (10^{-7} mol/L), and the combination of Ang II and Ald. To verify the effect, we preincubated the cells with a distinct oxygen radical scavenger, Tiron. Tiron preincubation (10 μmol/L) caused a similar suppression of ERK phosphorylation induced by Ang II (10^{-7} mol/L), Ald (10^{-7} mol/L), and the combination of Ang II and Ald (data not shown).

Effect of Spi on Ang II Signaling

Next, we preincubated VSMCs for 30 minutes with Spi. Thereafter, the cells were stimulated with Ang II (10^{-7} mol/L) for 10 minutes. Spi decreased Ang II–induced ERK phosphorylation at 10 minutes but not at 2 minutes, as shown by Western blot (Figure 4A) and by confocal microscopy (Figure 4B). Consistent with this result, Ang II–induced EGFR phosphorylation was reduced by Spi at 10 minutes (Figure 4B; $P=0.01$); no effect was observed at 2 minutes. Furthermore, we measured the effect of Spi on ROS production induced by Ang II (10^{-7} mol/L) and Ald (10^{-7} mol/L). Spi reduced Ang II–induced ROS generation from 5 minutes onward (Figure 4C, $P=0.05$ at 5 minutes, 0.01 at 10 minutes). The Ald (10^{-7} mol/L)–induced ERK phosphorylation was abolished with MR blockade (Figure 4D), whereas EGF (10 ng/mL)–induced ERK phosphorylation was not influenced by Spi (Figure 4E). Spi did not inhibit EGF-induced ROS production (data not shown).

Ang II and Ald Signaling Is Mediated Through the EGFR

We preincubated VSMCs with increasing concentrations (10, 100, and 300 nmol/L) of AG 1478, a specific EGFR blocker. We then stimulated the cells with Ang II (10^{-7} mol/L), Ald (10^{-7} mol/L), and a combination of both compounds. ERK phosphorylation was diminished dose-dependently by blocking the EGFR in all protocols (Figure 5, A through C).

Discussion

We found that Ang II and Ald both induced ERK 1/2 and JNK phosphorylation in VSMCs and that the agonists were additive. The stimulation was dependent on ROS generation, because GSH and Tiron strongly attenuated the phosphorylation. Spi did not inhibit early NADPH oxidase–dependent ROS generation. Instead, Spi affected the later phase of ROS

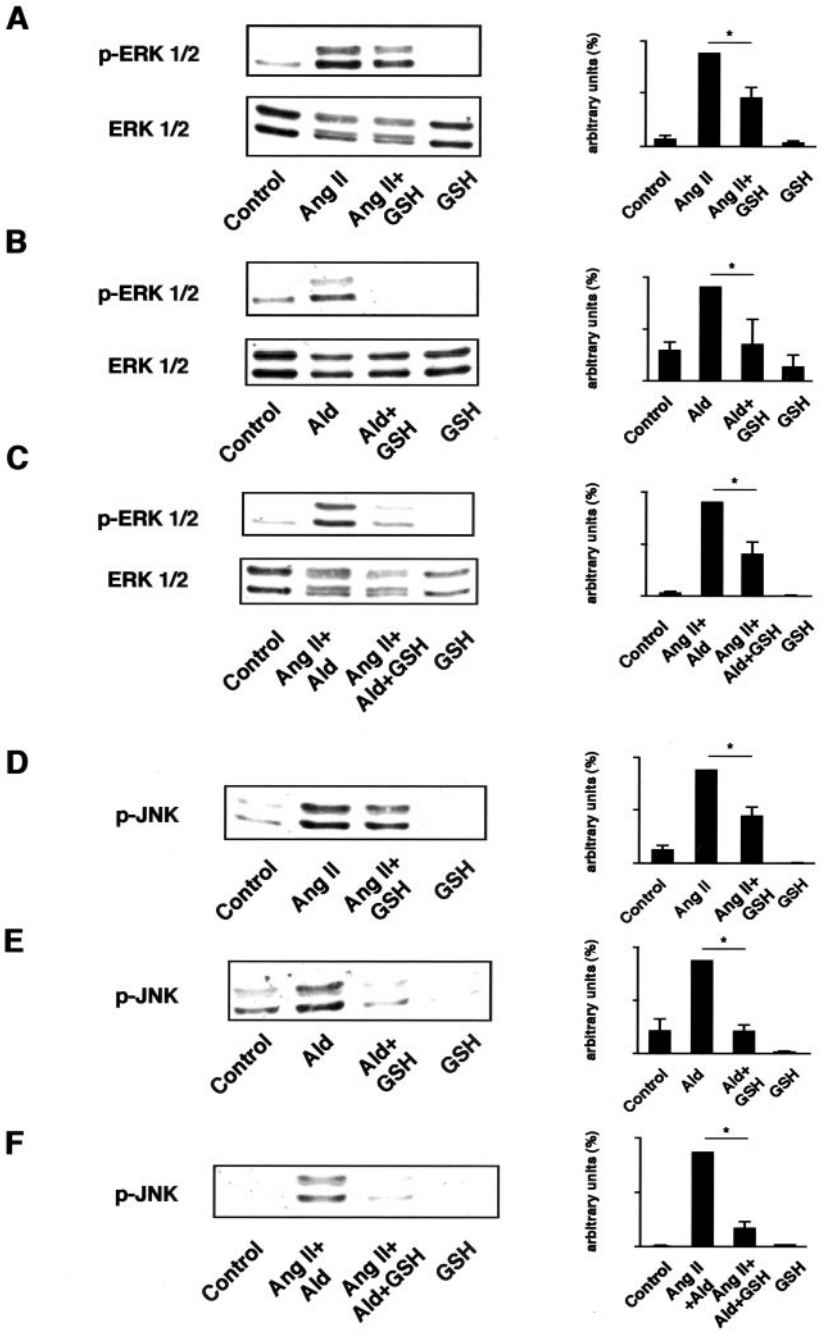

Figure 3. A through C, GSH (preincubation for 90 minutes) reduced Ang II–, Ald-, and Ang II+Ald–induced ERK 1/2 phosphorylation ($P<0.01$; n=4 each). D through F, GSH reduced Ang II–, Ald-, and Ang II+Ald—induced JNK phosphorylation ($P<0.01$; n=4 each).

generation, phosphorylation of the EGFR, and ERK 1/2 after Ang II stimulation. We then tested the notion that Ang II– and Ald-induced phosphorylation of ERK 1/2 was dependent on the EGFR. A specific EGFR blocker inhibited both the Ang II– and Ald-induced signaling events. We believe that these data are relevant to our in vivo findings that MR blockade with Epl reduced ERK 1/2 phosphorylation in dTGR vessels and greatly ameliorated Ang II–induced end-organ damage.

The MR is expressed not only in the cortical collecting duct but also in many other tissues, including the heart.[14] Northern blotting, RNAse protection assay, RT-PCR, in situ hybridization, immunohistochemistry, and Ald binding studies have been performed in cardiac tissue. However, precise cellular localization studies have not been entirely satisfactory. Endothelial cells, cardiac fibroblasts, VSMCs, and cardiomyocytes have all been implicated in terms of MR expression. The MR can be occupied not only by Ald but also by glucocorticoids. As a matter of fact, the MR may dimerize with the glucocorticoid receptor.[15]

Brilla et al[16] and Young et al[17] used different rat models and found that increased circulating Ald levels resulted in cardiac fibrosis. The DOCA-salt model results led to the suggestion that mineralocorticoid-mediated sodium entry into cardiac cells might be responsible.[18] Further support came from the finding that Spi ameliorated the effects. Ang II regulates cardiac Ald production. Several studies were conducted to address the possibility that Ang II was responsible for cardiac fibrosis rather than Ald. Rocha et al[18,19] showed

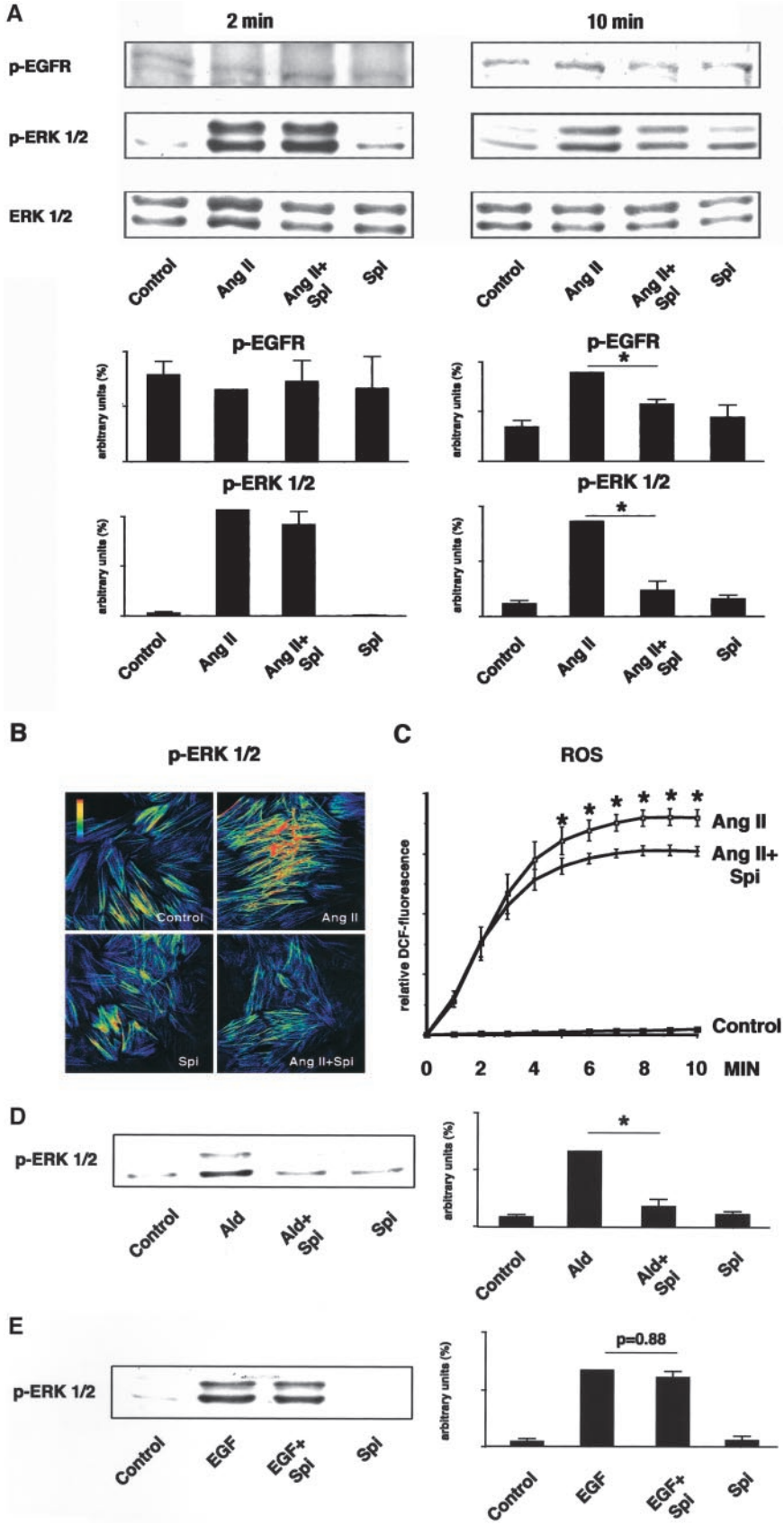

Figure 4. A, Spi (preincubation for 30 minutes) reduced Ang II–induced ERK 1/2 phosphorylation and EGFR phosphorylation at 10 minutes ($P<0.01$; n=4 each) but not at 2 minutes. B, Same effects were documented with immunofluorescence and confocal microscopy. C, Spi (preincubation for 30 minutes) reduces Ang II–induced generation of ROS ($P<0.05$ from 5 minutes; n=5 each). D, Spi (preincubation for 30 minutes) abolished Ald-induced ERK 1/2 phosphorylation ($P<0.01$; n=7 each). E, Spi (preincubation for 30 minutes) did not influence EGF-induced ERK 1/2 phosphorylation ($P=0.88$; n=3 each).

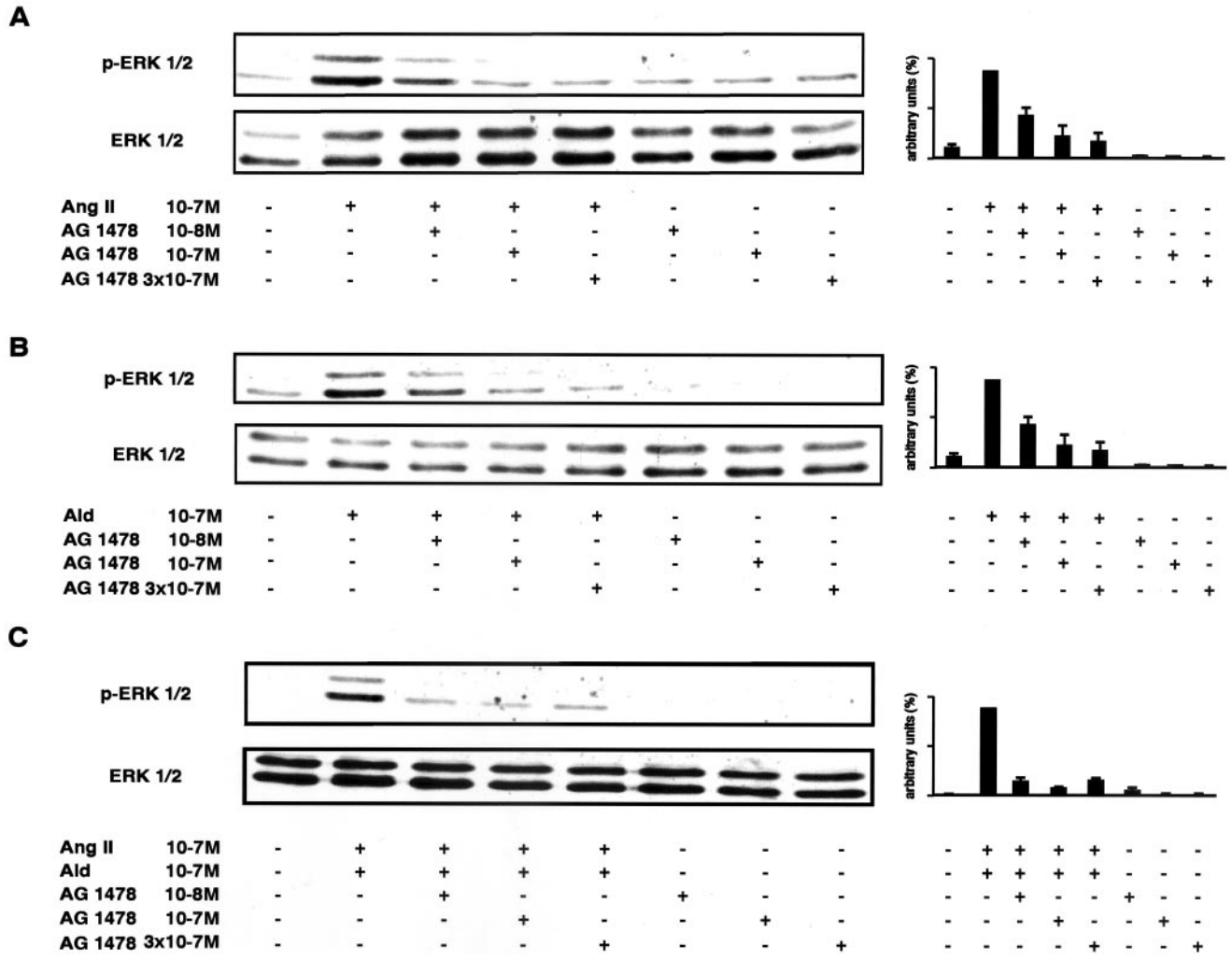

Figure 5. A and B, Ang II and Ald-induced ERK 1/2 phosphorylation was reduced by EGFR blocker AG 1478 dose-dependently (preincubation for 30 minutes). C, A similar inhibitory effect of AG1478 was obtained on Ang II+Ald–induced ERK 1/2 phosphorylation, indicating that combination was also EGFR-dependent (n=4 each).

that Ald infusion stimulates cardiac fibrosis in the rat. They suppressed Ang II production simultaneously with an ACE inhibitor. Benetos et al[20] used a combined infusion of Spi and an ACE inhibitor in spontaneously hypertensive rats. They found that Spi reversed cardiac fibrosis. Earlier, we studied a similar rat model using Spi.[21] In that study, we also found that Spi ameliorated cardiac hypertrophy and fibrosis, largely independently of blood pressure. Taken together, these studies support the notion that Ald induces cardiac fibrosis independently of other renin-angiotensin system components.

Ullian et al[22] first suggested that Ald increases Ang II receptor number, increases Ang II–stimulated inositol phosphate responses, and prevents the Ang II–induced downregulation of Ang II receptors. This group also showed enhanced phospholipase Cγ–dependent signaling when VSMCs were preincubated with Ald for 24 hours before Ang II stimulation.[23] In contrast to our findings, transcriptional regulation was involved in the studies by Ullian et al. We cannot exclude the possibility that genomic and nongenomic effects might have contributed to our in vivo observations. Nevertheless, the short duration of our in vitro experiments, as well as our results obtained with actinomycin D and cycloheximide, support a nongenomic effect.

Nongenomic effects have been reported for other steroids. Limbourg et al[24] described a rapid and nontranscriptional activation of eNOS by corticosteroids that is transmitted via phosphatidylinositol 3-kinase and Akt. Nongenomic Ald-related effects have also been described in humans.[6] For instance, Schmidt et al[25] found that Ald, via nongenomic mechanisms, has diverse effects on the cardiovascular system that depend on the preexisting adrenergic state. Data from the rat remnant kidney model also support the idea that chronic Ald-related effects may include a nongenomic component. Greene et al[26] studied 5/6 nephrectomy remnant kidney rats given AT_1 receptor blockers with ACE inhibitors and compared them with remnant kidney rats given these drugs along with Ald. In the former group, Ang II–related effects were blocked, and the rats were protected. In the latter group, given Ald, the effects were not ameliorated. This group resembled the no-treatment remnant kidney group. In their study, MR blockade did not reverse the effects of Ald, suggesting that MR-independent effects were present. The effects that we

observed appeared to be MR dependent, because Spi was capable of blocking the effects. In the case of the estrogen receptor, considerable evidence suggests that the receptor mediates both nuclear genomic and nonnuclear nongenomic effects.[27,28] Exactly how nongenomic steroid-receptor signaling occurs is unclear.

Our data suggest that the MR interacts with Ang II–induced signaling, influencing ROS production, EGFR transactivation, and ERK phosphorylation. Ang II signals primarily via the AT_1 receptor. The AT_1 receptor is coupled to heterotrimeric G proteins, and stimulation results in the release of oxygen free radicals, phosphorylation of MAP kinases and receptor tyrosine kinases, protein kinase C activation, and activation of the transcription factors AP-1 and NF-κB.[29] Ang II–induced ROS release has been suggested to function as a feed-forward mechanism.[30] The early release depends on protein kinase C activation (H_2O_2; first peak at 30 seconds). The H_2O_2 activates src, which leads to EGFR activation. The activated EGFR mediates stimulation of PI3-K and the G-protein Rac. The latter binds to NADPH oxidase to activate generation of more O_2^- and H_2O_2, resulting in a sustained ROS generation that lasts up to 6 hours.[30] Ald caused generation of ROS in VSMCs in vitro; however, this effect began later (6 to 8 minutes) than Ang II–induced ROS generation. This result suggests that Ald does not influence the early generation of Ang II–induced ROS production. The relevance of Ald-induced ROS production has also been shown in animal models. In aortic segments of Ald-infused rats, ROS levels were increased because of enhanced NADPH oxidase activity.[31] Furthermore, rats receiving chronic Ald/salt treatment exhibited NADPH oxidase and NF-κB activation in their endothelial and inflammatory cells. The effect was ameliorated with MR blockade and antioxidants.[32] In our study, both GSH and Tiron significantly inhibited Ang II/Ald signaling in VSMCs.

The EGFR also holds a key position in Ang II–induced signaling and is required for sustained Ang II–induced NADPH oxidase activation and ROS generation.[30,33] Ald also mediated its effects via the EGFR. Ald enhanced EGF signaling, resulting in potentiated ERK 1/2 phosphorylation and Ca^{2+} homeostasis in MDCK cells.[7] Further evidence about the role of the EGFR in Ald signaling comes from studies with CHO cells that lack the EGFR and do not respond to EGF or Ald. In EGFR-transfected CHO cells, EGF caused ERK 1/2 and src phosphorylation. Ald potentiated this signaling.[8] From our results, we conclude that VSMCs require a functioning EGFR for Ang II– and Ald-induced tyrosine kinase signaling. The cytosolic tyrosine kinase c-src regulates trafficking of the EGFR out of the caveolae. This trafficking might be needed for EGFR internalization and transactivation.[34] We did not investigate src-kinase phosphorylation. However, Ald potentiates Ang II–induced tyrosine phosphorylation in VSMCs (A. Fiebeler, unpublished data, 2003), and c-src may be one of these tyrosine kinases. Altogether, the feed-forward model,[30] as well as our findings, suggests that the interaction between Ang II and Ald is downstream of the first Ang II–induced ROS production but upstream of the EGFR. Kinases such as src and their regulating phosphatases may well be an interconnection between the 2 signaling pathways.[35]

Our earlier studies in dTGR indicated that the NADPH oxidase is strongly activated in this model.[11] Both NF-κB and AP-1 are activated, and both control the inducible expression of genes whose products are part of the inflammatory response. The JNK and ERK pathways are 2 members of the MAP kinase family that are also activated by ROS. The ERK pathway also modulates the expression of genes via phosphorylation of the transcription factor Elk-1, which controls the production of the c-Fos transcription factor. Nevertheless, not all Ang II–induced MAP kinase activation is under control of the EGFR.[36] Our data show that not only Ang II but also Ald participate in both JNK and ERK signaling. They suggest that blockade of both the AT_1 and the MR receptor may be necessary to accrue maximal effects in terms of vascular protection.

Acknowledgments

These studies were supported by grants-in-aid from the Klinisch-Pharmakologischer Verbund Berlin-Brandenburg, the Deutsche Forschungsgemeinschaft (to Dr Muller), the Nationales Genomnetzwerk (NGNF), and Pharmacia Inc, USA. We thank A. Busjahn for help with the statistical analysis and M. Kamimura, M. Köhler, C. Lipka, G. N'diaye, P. Quass, and M. Schmidt for their excellent technical assistance.

References

1. Pitt B, Zannad F, Remme WJ, et al. The effect of spironolactone on morbidity and mortality in patients with severe heart failure. Randomized Aldactone Evaluation Study Investigators. *N Engl J Med*. 1999;341:709–717.
2. Zannad F, Alla F, Dousset B, et al. Limitation of excessive extracellular matrix turnover may contribute to survival benefit of spironolactone therapy in patients with congestive heart failure: insights from the Randomized Aldactone Evaluation Study (RALES). Rales Investigators. *Circulation*. 2000;102:2700–2706.
3. Pitt B, Remme W, Zannad F, et al. Eplerenone, a selective aldosterone blocker, in patients with left ventricular dysfunction after myocardial infarction. *N Engl J Med*. 2003;348:1309–1321.
4. Okuda M, Kawahara Y, Yokoyama M. Angiotensin II type 1 receptor–mediated activation of Ras in cultured rat vascular smooth muscle cells. *Am J Physiol*. 1996;271:H595–H601.
5. Arriza JL, Weinberger C, Cerelli G, et al. Cloning of human mineralocorticoid receptor complementary DNA: structural and functional kinship with the glucocorticoid receptor. *Science*. 1987;237:268–275.
6. Losel RM, Feuring M, Falkenstein E, et al. Nongenomic effects of aldosterone: cellular aspects and clinical implications. *Steroids*. 2002;67:493–498.
7. Gekle M, Freudinger R, Mildenberger S, et al. Aldosterone interaction with epidermal growth factor receptor signaling in MDCK cells. *Am J Physiol*. 2002;282:F669–F679.
8. Krug AW, Schuster C, Gassner B, et al. Human epidermal growth factor receptor-1 expression renders chinese hamster ovary cells sensitive to alternative aldosterone signaling. *J Biol Chem*. 2002;277:45892–45897.
9. Eguchi S, Iwasaki H, Ueno H, et al. Intracellular signaling of angiotensin II–induced p70 S6 kinase phosphorylation at Ser(411) in vascular smooth muscle cells: possible requirement of epidermal growth factor receptor, Ras, extracellular signal–regulated kinase, and Akt. *J Biol Chem*. 1999;274:36843–36851.
10. Park JK, Muller DN, Mervaala EM, et al. Cerivastatin prevents angiotensin II–induced renal injury independent of blood pressure– and cholesterol-lowering effects. *Kidney Int*. 2000;58:1420–1430.
11. Muller DN, Shagdarsuren E, Park JK, et al. Immunosuppressive treatment protects against angiotensin II–induced renal damage. *Am J Pathol*. 2002;161:1679–1693.
12. Haller H, Quass P, Lindschau C, et al. Platelet-derived growth factor and angiotensin II induce different spatial distribution of protein kinase C-α and -β in vascular smooth muscle cells. *Hypertension*. 1994;23:848–852.

13. Ohba M, Shibanuma M, Kuroki T, et al. Production of hydrogen peroxide by transforming growth factor-beta 1 and its involvement in induction of egr-1 in mouse osteoblastic cells. *J Cell Biol*. 1994;126:1079–1088.
14. Lombes M, Oblin ME, Gasc JM, et al. Immunohistochemical and biochemical evidence for a cardiovascular mineralocorticoid receptor. *Circ Res*. 1992;71:503–510.
15. Trapp T, Holsboer F. Heterodimerization between mineralocorticoid and glucocorticoid receptors increases the functional diversity of corticosteroid action. *Trends Pharmacol Sci*. 1996;17:145–149.
16. Brilla CG, Matsubara LS, Weber KT. Anti-aldosterone treatment and the prevention of myocardial fibrosis in primary and secondary hyperaldosteronism. *J Mol Cell Cardiol*. 1993;25:563–575.
17. Young M, Fullerton M, Dilley R, et al. Mineralocorticoids, hypertension, and cardiac fibrosis. *J Clin Invest*. 1994;93:2578–2583.
18. Rocha R, Martin-Berger CL, Yang P, et al. Selective aldosterone blockade prevents angiotensin II/salt–induced vascular inflammation in the rat heart. *Endocrinology*. 2002;143:4828–4836.
19. Rocha R, Chander PN, Khanna K, et al. Mineralocorticoid blockade reduces vascular injury in stroke-prone hypertensive rats. *Hypertension*. 1998;31:451–458.
20. Benetos A, Levy BI, Lacolley P, et al. Role of angiotensin II and bradykinin on aortic collagen following converting enzyme inhibition in spontaneously hypertensive rats. *Arterioscler Thromb Vasc Biol*. 1997; 17:3196–3201.
21. Fiebeler A, Schmidt F, Muller DN, et al. Mineralocorticoid receptor affects AP-1 and nuclear factor-κB activation in angiotensin II–induced cardiac injury. *Hypertension*. 2001;37:787–793.
22. Ullian ME, Schelling JR, Linas SL. Aldosterone enhances angiotensin II receptor binding and inositol phosphate responses. *Hypertension*. 1992; 20:67–73.
23. Ullian ME, Fine JJ. Mechanisms of enhanced angiotensin II–stimulated signal transduction in vascular smooth muscle by aldosterone. *J Cell Physiol*. 1994;161:201–208.
24. Limbourg FP, Huang Z, Plumier JC, et al. Rapid nontranscriptional activation of endothelial nitric oxide synthase mediates increased cerebral blood flow and stroke protection by corticosteroids. *J Clin Invest*. 2002; 110:1729–1738.
25. Schmidt BM, Georgens AC, Martin N, et al. Interaction of rapid nongenomic cardiovascular aldosterone effects with the adrenergic system. *J Clin Endocrinol Metab*. 2001;86:761–767.
26. Greene EL, Kren S, Hostetter TH. Role of aldosterone in the remnant kidney model in the rat. *J Clin Invest*. 1996;98:1063–1068.
27. Simoncini T, Genazzani AR, Liao JK. Nongenomic mechanisms of endothelial nitric oxide synthase activation by the selective estrogen receptor modulator raloxifene. *Circulation*. 2002;105:1368–1373.
28. Ho KJ, Liao JK. Nonnuclear actions of estrogen. *Arterioscler Thromb Vasc Biol*. 2002;22:1952–1961.
29. Wolf G, Butzmann U, Wenzel UO. The renin-angiotensin system and progression of renal disease: from hemodynamics to cell biology. *Nephron*. 2003;93:P3–P13.
30. Seshiah PN, Weber DS, Rocic P, et al. Angiotensin II stimulation of NAD(P)H oxidase activity: upstream mediators. *Circ Res*. 2002;91: 406–413.
31. Virdis A, Neves MF, Amiri F, et al. Spironolactone improves angiotensin-induced vascular changes and oxidative stress. *Hypertension*. 2002; 40:504–510.
32. Sun Y, Zhang J, Lu L, et al. Aldosterone-induced inflammation in the rat heart: role of oxidative stress. *Am J Pathol*. 2002;161:1773–1781.
33. Kagiyama S, Eguchi S, Frank GD, et al. Angiotensin II–induced cardiac hypertrophy and hypertension are attenuated by epidermal growth factor receptor antisense. *Circulation*. 2002;106:909–912.
34. Carpenter G. The EGF receptor: a nexus for trafficking and signaling. *Bioessays*. 2000;22:697–707.
35. Griendling KK, Harrison DG. Dual role of reactive oxygen species in vascular growth. *Circ Res*. 1999;85:562–563.
36. Eguchi S, Dempsey PJ, Frank GD, et al. Activation of MAPKs by angiotensin II in vascular smooth muscle cells: metalloprotease-dependent EGF receptor activation is required for activation of ERK and p38 MAPK but not for JNK. *J Biol Chem*. 2001;276:7957–7962.

3.5 Bedeutung der G-Proteine und Kalziumkanäle für das Renin-Angiotensin-Aldosteron-System

Eine Reihe weiterer Signalwege sind eng mit dem RAAS verknüpft. Im oben beschriebenen Tiermodell (dTGR; siehe oben: **Abb. 5**) mit Angiotensin II- und Aldosteron-induzierten Endorganschäden untersuchten wir u.a. Statine als Inhibitoren der Aktivierung von G-Proteinen (Statine hemmen die 3-Hydroxy-3-Methyl-Glytaryl-CoenzymA-Reduktase) und einen Kalzium-Kanal-Blocker.

3.5.1 Reduktion des Angiotensin II- und Aldosteron-induzierten Endorganschadens durch Cerivastatin

Die von Statinen gehemmte 3-Hydroxy-3-Methyl-Glytaryl-CoenzymA-Reduktase bedingt die Farnesylierung und Geranylierung und somit den Aktivitätsgrad von G-Proteinen. Statine sind bei Patienten mit kardiovaskulären Erkrankungen protektiv, wofür nicht nur der cholesterinsenkende Effekt verantwortlich zu sein scheint [27,28]. dTGR wurden von der 4. bis zur 7. Lebenswoche täglich mit 0,5 mg/kg/KG Cerivastatin behandelt. Während die Statintherapie keinen Einfluss auf die Cholesterinspiegel der Tiere hatte, schützte die Behandlung vor der Ausprägung des Endorganschadens in Herz und Nieren. Zur 7. Woche reduzierte Cerivastatin die Mortalität und die Herzhypertrophie. Der Blutdruck wurde durch Statine signifikant – wenn auch nicht auf Kontrollniveau – gesenkt. Diese Blutdrucksenkung könnte sekundär durch die Nephroprotektion bedingt und kein primärer Effekt der Statine auf den Blutdruck sein. Dafür sprechen auch die Ergebnisse der angeschlossenen *in-vitro*-Experimente, in denen eine Vorinkubation

der Zellen mit Statin die Angiotensin II-induzierte frühe Signaltransduktion hemmt. In den Herzen der Tiere fanden wir nach Statintherapie weniger Entzündungszellen, eine geringere Ablagerung von Bindegewebe und eine reduzierte Expression von Entzündungsmediatoren und Wachstumsfaktoren im Vergleich zu unbehandelten dTGR. Cerivastatin verhinderte die zur 7. Woche ausgeprägte Albuminurie. Immunhistologisch beobachteten wir nach Statinbehandlung weniger Arteriolosklerose und fokale Nekrose. Die Expression von iNOS war deutlich reduziert.

Schlussfolgerung: Die alleinige Behandlung mit Statinen schützt im Tiermodell unabhängig von der Lipidsenkung vor den Folgen eines aktivierten RAAS.

Reprint 4

Fiebeler A*, Dechend R*, Park JK, Muller DN, Theuer J, Mervaala E, Bieringer M, Gulba D, Dietz R, Luft FC, Haller H. Amelioration of angiotensin II-induced cardiac injury by a 3-hydroxy-3-methylglutaryl coenzyme a reductase inhibitor. *Circulation*. 2001;104:576-81.

Amelioration of Angiotensin II–Induced Cardiac Injury by a 3-Hydroxy-3-Methylglutaryl Coenzyme A Reductase Inhibitor

Ralf Dechend, MD; Anette Fiebeler, MD; Joon-Keun Park, PhD; Dominik N. Muller, PhD; Juergen Theuer, MD; Eero Mervaala, MD; Markus Bieringer, MS; Dietrich Gulba, MD; Rainer Dietz, MD; Friedrich C. Luft, MD, FRCP (Edin); Hermann Haller, MD

Background—3-Hydroxy-3-methylglutaryl coenzyme A (HMG-CoA) reductase inhibitors (statins) have effects that extend beyond cholesterol reduction. We used an angiotensin (Ang) II–dependent model to test the hypothesis that cerivastatin ameliorates cardiac injury.

Methods and Results—We treated rats transgenic for human renin and angiotensinogen (dTGR) chronically from weeks 4 to 7 with cerivastatin (0.5 mg/kg by gavage). We used immunohistochemistry, electrophoretic mobility shift assays, and reverse transcription–polymerase chain reaction techniques. Compared with control dTGR, dTGR treated with cerivastatin had reduced mortality, blood pressure, cardiac hypertrophy, macrophage infiltration, and collagen I, laminin, and fibronectin deposition. Basic fibroblast growth factor mRNA and protein expression were markedly reduced, as was interleukin-6 expression. The transcription factors NF-κB and AP-1 were substantially less activated, although plasma cholesterol was not decreased.

Conclusions—These results suggest that statins ameliorate Ang II–induced hypertension, cardiac hypertrophy, fibrosis, and remodeling independently of cholesterol reduction. Although the clinical significance remains uncertain, the results suggest that statins interfere with Ang II–induced signaling and transcription factor activation, thereby ameliorating end-organ damage. **(*Circulation*. 2001;104:576-581.)**

Key Words: statins ■ angiotensin ■ remodeling ■ cholesterol

Statins (3-hydroxy-3-methylglutaryl coenzyme A [HMG-CoA] reductase inhibitors) are effective in preventing acute coronary events; however, careful analysis suggests that the benefits of statins cannot be fully explained on the basis of cholesterol reduction alone. Clinical and laboratory observations have shown an inhibition of vascular smooth muscle cell (VSMC) proliferation by statins that is independent of LDL cholesterol levels. Such an effect might be expected, because inhibition of isoprenoid formation, precursors of sterol synthesis, is important in altering the processing of signaling proteins that require lipidation, such as Ras.[1] In a patient study, Nickenig et al[2] recently showed that statin treatment effectively reduced angiotensin (Ang) II type 1 (AT1) receptor density and decreased the blood pressure-elevating effects of Ang II. They suggested that this effect might explain some of the cholesterol-independent statin effects. We have studied a double transgenic rat (dTGR) model of Ang II–induced end-organ damage.[3] The rats harbor the human renin and angiotensinogen genes. dTGR display severe cardiac and renal inflammatory injury and die at ≈7 weeks of age if untreated. We used this model to test the hypothesis that HMG Co-A reductase inhibition might exert cholesterol-independent protective effects on the heart.

Methods

Study Design

Experiments were conducted in 4-week-old male dTGR and age-matched Sprague-Dawley (SD) rats. The dTGR line and characteristics were described elsewhere.[4] All procedures were done according to guidelines from the American Physiological Society and were approved by local authorities. The statin dTGR group (n=15) received cerivastatin for 3 weeks by gavage once a day (0.5 mg/kg). Control dTGR (n=20) and SD rats (n=15) received vehicle. This dose, on a weight basis, is much higher than the human dose, although the pharmacokinetic area under the curve and peak plasma levels are similar in both species.[5] Statins do not lower serum cholesterol in rats because of compensatory increases in hepatic enzyme production. Nevertheless, the enzyme is effectively inhibited in the liver and elsewhere.[6] Cholesterol was measured in plasma by an automated method. Systolic blood pressure was measured at

Received December 1, 2000; revision received March 30, 2001; accepted April 5, 2001.

From the Franz Volhard Clinic and Max Delbrück Center for Molecular Medicine, Medical Faculty of the Charité, Humboldt University of Berlin (R.D., D.N.M., J.T., E.M., M.B., D.G., R.D., F.C.L.), Berlin, Germany, and Nephrology Division, Department of Medicine, Hannover Medical School (A.F., J.-K.P., H.H.), Hannover, Germany.

The first 3 authors contributed equally to this work.

Correspondence to Friedrich C. Luft, MD, Charité Campus-Buch, Franz Volhard Clinic, Wiltberg Str 50, 13125 Berlin, Germany. E-mail luft@fvk-berlin.de

Circulation **is available at http://www.circulationaha.org**

weeks 5, 6, and 7 by the tail-cuff method under light ether anesthesia. Rats were killed at 7 weeks of age. The hearts were washed with ice-cold saline, blotted dry, and weighed. For Western blot and nuclear factor-κB (NF-κB) analysis, the tissues were snap-frozen in liquid nitrogen for immunohistochemistry in isopentane (−35°C) and stored at −80°C.

Immunohistochemistry

Immunohistochemistry (APAAP technique) was performed as described previously.[3,4] Antibodies were purchased against monocytes/macrophages (ED1, Serotec), lymphocytes (CD4 and CD8, PharMingen), NF-κB subunit p65 (Roche Boehringer), interleukin (IL)-6 (R&D Systems), c-fos, and basic fibroblast growth factor (bFGF, Santa Cruz Biotechnology, Inc). For immunofluorescence, ice-cold acetone-fixed cryosections (6 μm) were air-dried and immersed in TBS (0.05 mol/L Tris buffer, 0.15 mol/L NaCl, pH 7.6). All incubations were performed in a humid chamber at room temperature. At first, the sections were incubated in 10% normal donkey serum (Diavova) for 30 minutes to block any nonspecific binding. The sections were incubated for 60 minutes with the primary antibodies. After being washed with TBS, the sections were incubated with Cy3-conjugated secondary antibodies (donkey anti-mouse IgG-Cy3, donkey anti-rabbit IgG-Cy3, or donkey anti-goat IgG-Cy3, Dianova) for 60 minutes. After a final washing with TBS, slides were mounted in Vectashield mounting medium (Vector Laboratories). In controls, in which a primary antibody was substituted for by isotype control antibody CBL 600 mouse IgG1-negative control (Cymbus Biotechnology) at the same final concentration, no specific immunolabeling was observed. The nonspecific binding of secondary antibodies was excluded by omission of the primary antibody. Preparations were examined under a Zeiss Axioplan-2 microscope and photographed with a color reversal film Agfa CTX 100. Semiquantitative scoring of ED1-, CD4-, and CD8-positive cells in the heart was performed with a computerized cell count program (KS 300 3.0, Zeiss). Fifteen different areas of each heart sample (n=5 in all groups) were analyzed. The hearts were examined without knowledge of the rats' identity. Collagen, fibronectin, laminin, c-fos, and p65 were assessed semiquantitatively by 2 different observers without knowledge of the rats' identity. The data are expressed in arbitrary units (0 to 5) based on the staining intensity.

Electrophoretic Mobility Shift Assay and TaqMan Analyses

Tissue extracts and electrophoretic mobility shift assay (EMSA) for NF-κB and AP-1 were performed thrice. Densitometry quantification values (NIH Image Program, version 1.61) are given in percent of untreated dTGR. Nuclear extracts of the left ventricle (10 μg) were incubated in binding reaction medium with 0.5 ng of ^{32}P-dATP end-labeled oligonucleotide containing the NF-κB binding site from the major histocompatibility complex enhancer (H2K, 5′-GATCCAGGGCTGGGGATTCCCCATCTCCACAGG). For AP-1, double-stranded oligonucleotides containing the consensus sequence for AP-1 (Santa Cruz Biotechnology, 5′-GAT CGA ACT GAC CGC CCG CCG CCC GT-3′) were radiolabeled with γ-^{32}P with the use of T4 polynucleotide kinase by standard methods and purified over a column. The DNA-protein complexes were analyzed on a 5% polyacrylamide gel 0.5% Tris buffer, dried, and autoradiographed. In competition assays, 50 ng of unlabeled H2K or AP-1 oligonucleotides was used.[4]

Primers were synthesized by Biotez (Berlin-Buch) with sequences described previously.[4] Real-time quantitative reverse transcription–polymerase chain reaction (RT-PCR) was performed with the TaqMan system (Prism 7700 Sequence Detection System, PE Biosystems). For quantification of gene expression, the target sequence was normalized in relation to the expressed housekeeping gene *GAPDH*.

Statistical Analysis

Data are presented as mean±SEM. Statistically significant differences in mean values were tested by ANOVA, except for differences in blood pressure, which were tested by repeated-measures ANOVA and the Scheffé test. A value of $P<0.05$ was considered statistically significant. Data were analyzed with StatView statistical software.

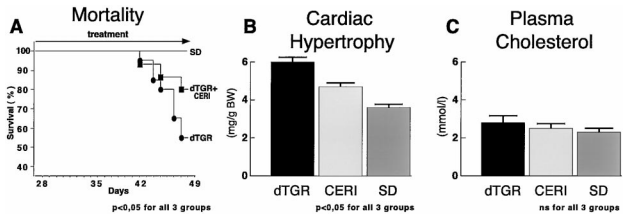

Figure 1. A, Kaplan-Meier survival analysis in dTGR, dTGR receiving cerivastatin (CERI), and SD rats. By week 7, half of untreated dTGR were dead. In contrast, cerivastatin reduced mortality. No controls died before end of study. B, Cerivastatin also significantly reduced cardiac hypertrophy, expressed as ratio of heart weight to body weight, compared with untreated dTGR. However, cardiac hypertrophy of cerivastatin-treated dTGR was higher than in SD rats. C, Plasma cholesterol levels did not differ significantly between groups. Cerivastatin treatment did not lower plasma cholesterol levels ($P=0.7$).

Results

Nine of 20 dTGR died before the end of week 7; the mortality rate was 45%. In contrast, mortality in the cerivastatin group was 20%, and no SD rats died ($P<0.001$; Figure 1A). Cerivastatin treatment reduced the heart weight ($P<0.05$; Figure 1B). In contrast, body weight of the 3 groups was not different. Heart weights corrected for body weight were 5.9±0.23 versus 5.0±0.11 versus 3.6±0.05 mg/g for dTGR, dTGR treated with cerivastatin, and SD rats, respectively. Plasma cholesterol levels in untreated dTGR were 2.84±0.21 mmol/L compared with 2.52±0.32 mmol/L in cerivastatin-treated dTGR (Figure 1C). However, nontransgenic rats tended to lower levels (2.34±0.12 mmol/L). Differences between the 3 groups were not statistically significant ($P=0.7$). Systolic blood pressure of cerivastatin-treated rats was significantly decreased (54 mm Hg) compared with untreated dTGR (147±14 versus 201±06 mm Hg, $P<0.001$) at week 7. The dTGR showed a progressive increase in systolic blood pressure from 5 to 7 weeks. However, the blood pressure of cerivastatin-treated rats was significantly elevated compared with SD rats (147±14 versus 109±02 mm Hg, $P<0.001$). dTGR small vessels showed increased intimal and medial thickness. dTGR myocardial sections showed hemorrhage, patchy areas of necrosis, and interstitial fibrosis, whereas cerivastatin ameliorated the cardiac damage (data not shown).

Cerivastatin treatment reduced extracellular matrix. The hearts were stained for collagen I (Figure 2), fibronectin, and laminin (data not shown). Collagen I and fibronectin were most prominently deposited around blood vessels, in the vascular adventitia, and focally around fibrotic scarred areas. Fibronectin was also deposited in the neointima of remodeled vessels. Laminin was localized primarily between cardiomyocytes (data not shown). All 3 interstitial deposits were substantially reduced in the cerivastatin group.

EMSA from 3 animals in each group showed increased NF-κB (Figure 3A) and AP-1 (Figure 4A) activation in dTGR, which was reduced by cerivastatin to SD levels. Competition with unlabeled oligonucleotide and supershift

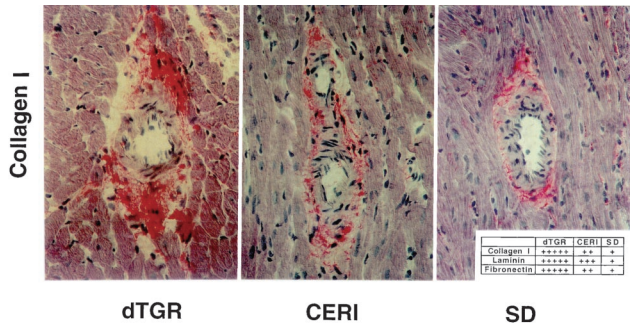

Figure 2. Immunohistochemistry of cardiac tissue for collagen I from dTGR, cerivastatin-treated dTGR (CERI), and SD rats. Collagen I was increased in dTGR but was markedly decreased with cerivastatin treatment (inset shows quantification).

experiments revealed specificity of the increased DNA binding activity for NF-κB and AP-1 (Figures 3B, 3C, 4B, and 4C, respectively). A single-base-pair mutant oligonucleotide for NF-κB and AP-1 showed no binding differences, indicating the specificity of the assay (Figures 3D and 4D, respectively). Quantification of NF-κB and AP-1 binding activity and mutants showed that cerivastatin reduced binding by 65% and 75%, respectively (Figures 3E and 4E). mRNA expression of c-fos (Figure 4F), an important member of the AP-1 complex that was increased in dTGR, was reduced by cerivastatin. Reduced DNA binding activity for AP-1 and NF-κB in response to cerivastatin treatment was confirmed by immunohistochemical expression of activated p65 (Figure 3F), the member of the NF-κB family with the strongest transactivation potential, and c-fos (Figure 4G). Both transcription factors showed weak staining in SD animals; however, in dTGR, intense red staining of the vessel and perivascular region was visible. Cerivastatin reduced p65 expression and c-fos toward SD levels.

Untreated dTGR showed markedly increased expression of IL-6 (Figure 5A) and bFGF (Figure 5B) in the media of cardiac vessels, which was reduced by cerivastatin treatment. bFGF and IL-6 were also present in the perivascular space and between myofibrils. With cerivastatin treatment, staining for both substances was reduced (data not shown). Immunofluorescence data were confirmed by semiquantitative RT-PCR TaqMan RNA analyses for IL-6 and bFGF. bFGF and IL-6 were markedly increased in the hearts of dTGR. Cerivastatin reduced both factors close to control SD levels.

We then investigated the effect of cerivastatin on cell infiltration. Staining for the macrophage marker ED1 in dTGR hearts was substantially increased around the small vessel and between cardiac muscle fibers (Figure 6A). Staining was performed in at least 5 hearts from each group, and a semiquantitative assessment for ED1 and the lymphocyte markers CD4 and CD8 was done for statistical analysis (Figure 6B). Semiquantitative analysis showed that cerivastatin reduced ED1-, CD4-, and CD8-positive cells significantly compared with untreated controls, although not to levels observed in SD rats. Cerivastatin had a more pronounced effect on reduction of ED1-positive and CD8-positive cells. The effect on CD4-positive cells was weaker;

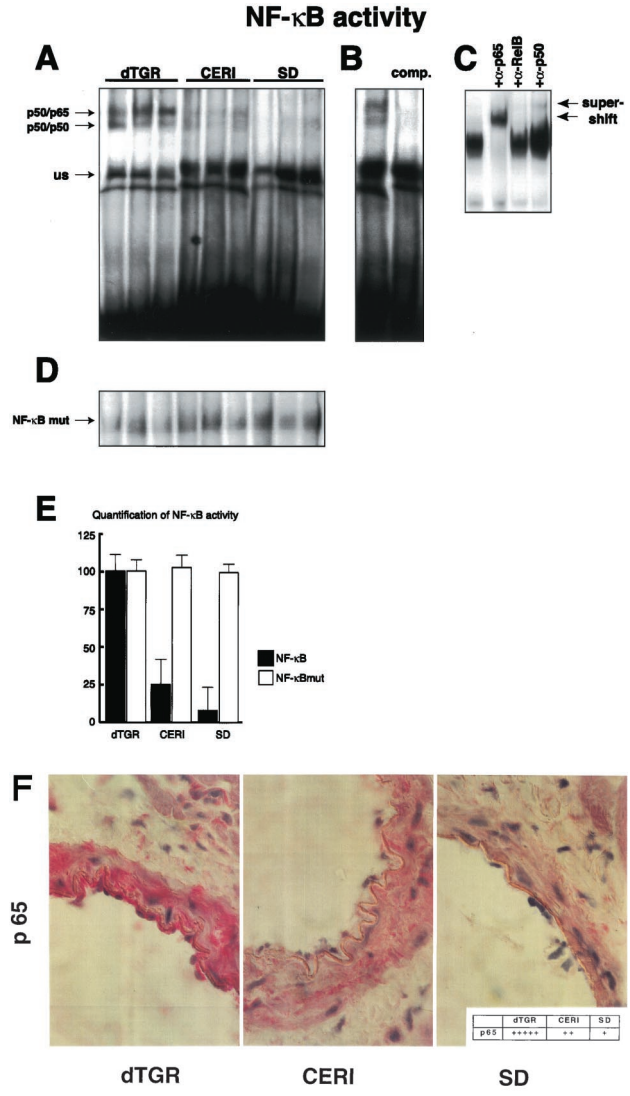

Figure 3. A, EMSA showing NF-κB DNA binding activity. DNA binding was induced in dTGR and reduced with cerivastatin (CERI). Specific bands and nonspecific bands (us) are indicated. B, With unlabeled NF-κB oligonucleotides, specific bands disappeared (competition). Specific antibodies to p50 and p65 resulted in supershifts. C, Addition of control antibodies to c-rel showed no supershift. Also shown are results of mutated NF-κB (mut) oligonucleotides that gave similar NF-κB activity for all 3 groups (D) and quantification of DNA binding activity (E). Immunohistochemistry shows expression of activated p65 (F). Nuclear red staining of activated p65 NF-κB subunit in dTGR was reduced by cerivastatin.

however, the reduction was significant for all 3 parameters ($P<0.05$).

Discussion

We relied on a dTGR model of high Ang II–induced hypertension and end-organ damage to show that cerivastatin treatment reduces mortality, blood pressure, left ventricular hypertrophy, fibrosis (collagen I, fibronectin, and laminin deposition), and macrophage infiltration. Furthermore, bFGF expression was markedly reduced by cerivastatin, as was expression of IL-6. These results were accompanied by a marked reduction in NF-κB and AP-1 activation compared

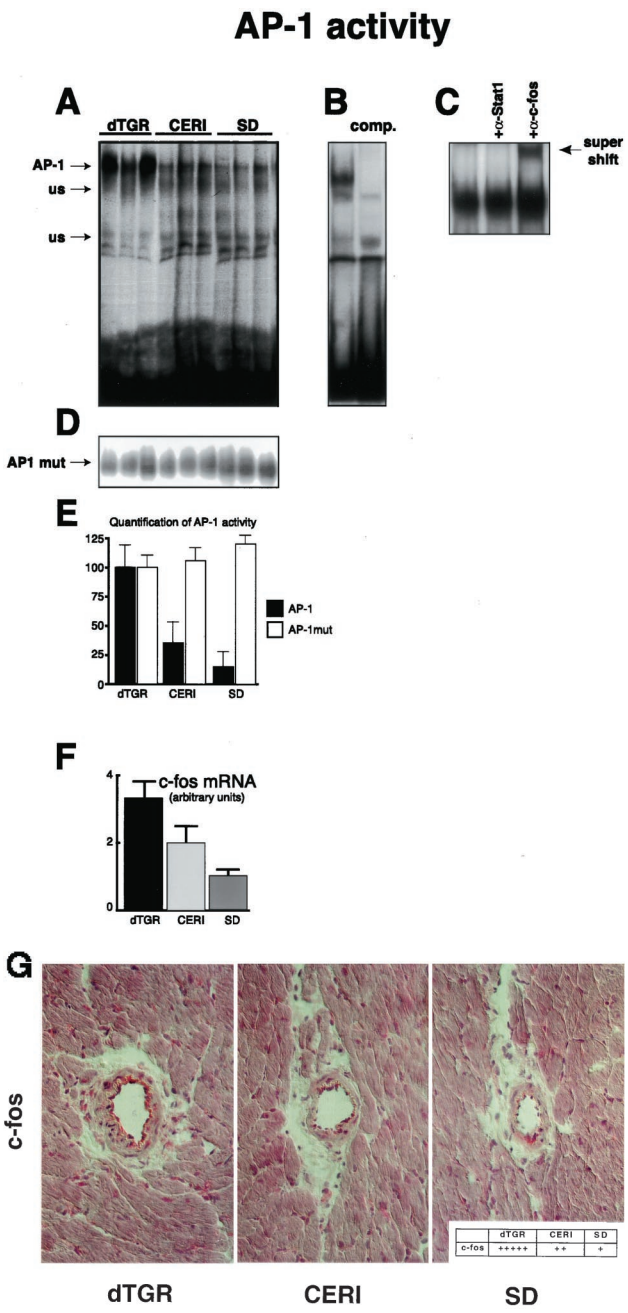

Figure 4. A, EMSA showing AP-1 DNA binding activity. DNA binding was increased in dTGR and reduced with cerivastatin (CERI). Specific bands and nonspecific bands (us) are indicated. B, Competition with unlabeled AP-1 oligonucleotides resulted in disappearance of specific bands. C, Specific antibodies to c-fos resulted in supershift, but addition of control antibodies to Stat-1 did not. Also shown are results of single-base-pair mutation (mut) in AP-1 oligonucleotides, which resulted in similar binding activity for all 3 groups (D). E, Quantification of AP-1 and mutated AP-1 DNA binding activity. F, c-fos mRNA expression substantiated AP-1 results. Immunohistochemistry shows increased expression of c-fos in dTGR that was markedly reduced by cerivastatin (G). c-fos staining was prominent in vessel wall, perivascular area, and between myofibrils.

with dTGR controls. We do not believe that our results were related primarily to a cerivastatin-induced reduction of blood pressure, although we cannot rule out blood pressure–related effects. Statins regularly lower blood pressure in rodent

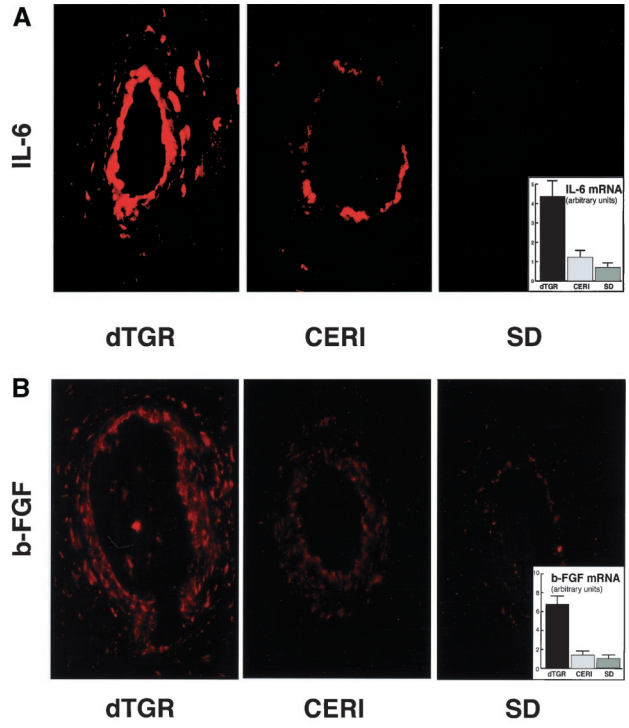

Figure 5. Immunofluorescent expression of IL-6 (A) and bFGF (B) is shown in media from cardiac vessel, as well as RNA analysis. Both factors were upregulated in dTGR and reduced by cerivastatin (CERI) on mRNA and protein levels toward control values.

hypertension models and have been shown to be effective in a randomized, double-blind crossover trial in humans.[7]

In a previous study,[3] we compared blood pressure reduction with a human renin inhibitor to hydralazine, reserpine, and hydrochlorothiazide and found that triple therapy–treated dTGR nevertheless developed severe heart and kidney damage in the face of blood pressure reduction. Although cerivastatin treatment reduced inflammation, cytokine expression, AP-1 and NF-κB activity, and blood pressure, the reduction in cardiac hypertrophy was significant but incomplete. In a previous aortic banding study,[8] a statin reduced cardiac hypertrophy in a manner similar to the effects reported here; however, an ACE inhibitor was more effective. Similar results were observed in an in vitro study of cardiomyocytes.[9] The cerivastatin-related effects, as in the present study, were independent of cholesterol reduction. We have also made similar observations in this same model in terms of nephroprotection from Ang II–related injury.[10] In that study, we found that cerivastatin inhibited extracellular-regulated kinase activation in the kidney.

We observed increased collagen I, fibronectin, and laminin deposition in dTGR hearts that was ameliorated by statin treatment. Collagen I is regulated by Ras and AP-1.[11] Ang II has been shown to activate the collagen I gene in transgenic mice, an effect that was blocked by losartan, raising the possibility that Ang II might directly initiate the process of organ fibrosis.[12] Previous work has demonstrated that Ang II stimulates collagen protein synthesis in cardiac myofibroblasts in vitro and increases collagen I mRNA expression in rat hearts in vivo.[13]

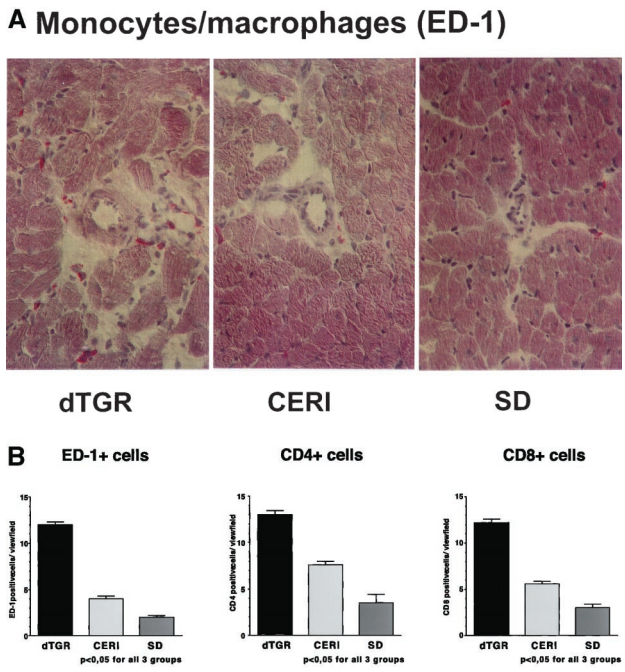

Figure 6. A, Immunohistochemistry for macrophages. B, Semiquantification revealed that cerivastatin (CERI) reduced ED1-, CD4-, and CD8-positive cells in heart. Fifteen different areas of each heart were analyzed. Results are mean±SEM of 5 animals per group.

Cardiac hypertrophy and heart failure both feature hypertrophy of cardiomyocytes, hyperplasia of nonmyocyte cells, extracellular matrix deposition, fibrosis, vessel remodeling, cytokine activation, and inflammation. bFGF has been implicated in the pathogenesis of hypertrophy. Schultz et al[14] studied a mouse with a disrupted bFGF gene. These mice developed less hypertrophy after aortic banding than wild-type mice. Paced cardiomyocytes exposed to antibodies directed at bFGF showed less hypertrophy than control cells in an in vitro study.[15] bFGF was found to mediate VSMC hypertrophy, leading to vessel wall remodeling in response to Ang II treatment.[16] IL-6 is important in heart failure and arteriosclerosis. In the present study, bFGF and IL-6 expression were both markedly increased in the hearts of dTGR but were reduced by cerivastatin. Interestingly, the genes for both contain NF-κB and AP-1 transcription factor regulatory elements. bFGF may have been responsible in part for the increased IL-6 production. Kozawa et al[17] demonstrated that bFGF induces IL-6 synthesis in osteoblasts and that this process is autoregulated by protein kinase C. On the other hand, IL-6 can also upregulate bFGF. The reciprocal interaction between these components is regulated by AP-1.[18] dTGR featured both inflammation and fibrosis in the heart. The presence of inflammatory cells in hypertrophied hearts is well recognized. Nicoletti and Michel[19] showed that bFGF is released by inflammatory cells, thereby mediating hypertrophy and fibrosis.

The mechanisms of the statin-related protection are unknown but may involve G proteins involved in receptor-coupled signal transduction, particularly Rho.[19] The Rho proteins belong to the Ras superfamily. The Ras proteins alternate between an inactivated GDP-bound form and an activated GTP-bound form, allowing them to act as molecular switches for growth and differentiation signals. Prenylation is a process involving the binding of hydrophobic isoprenoid groups consisting of farnesyl or geranylgeranyl residues to the carboxy-terminal region of the Ras protein superfamily. Farnesyl pyrophosphate and geranylgeranyl pyrophosphate are metabolic products of mevalonate that are able to supply prenyl groups. The prenylation is conducted by prenyl transferases. The hydrophobic prenyl groups are necessary to anchor the Ras superfamily proteins to intracellular membranes so that they can be translocated to the plasma membrane.[20] The final cell membrane fixation is necessary for Ras proteins to participate in their specific interactions. Several groups have presented evidence supporting such a statin-induced mechanism. For instance, Bourcier and Libby[21] recently showed that a statin reduced plasminogen activator inhibitor-1 expression by VSMC and endothelial cells. Their study also implicated geranylgeranyl-modified intermediates and exonerated farnesyl pyrophosphate. Furthermore, Laufs and Liao[22] demonstrated that Rho negatively regulates endothelial nitric oxide synthase expression and that statins upregulate endothelial nitric oxide synthase expression by blocking Rho geranylgeranylation, which is necessary for its membrane-associated activity.

Statins decrease the production of mevalonate, geranyl pyrophosphate, farnesyl pyrophosphate, and subsequent products on the way to construction of the cholesterol molecule. Thus, statins could act independently of circulating LDL by intracellularly interfering with Ras superfamily protein function. Ikeda et al[23] recently showed that statins decrease matrix metalloproteinase-1 expression through inhibition of Rho. In cultured VSMCs, HMG-CoA reductase inhibition diminished collagen I, thrombospondin, and fibronectin synthesis.[24] Similarly, HMG-CoA reductase inhibitors interfered with surface adhesion molecule expression by macrophages, leading to monocyte-endothelium adhesion inhibition.[25] Conceivably, the effects could also be related to a cholesterol-independent decreased AT1 receptor expression in response to statin treatment.[2]

Kureishi et al[26] recently showed that statins are capable of activating the Akt kinase and promote angiogenesis in normocholesterolemic rats. They found that simvastatin enhanced phosphorylation of the endogenous Akt substrate endothelial nitric oxide synthase, inhibited apoptosis, and accelerated blood vessel formation. Their observations suggest that Akt may represent a mechanism by which non–cholesterol-related effects of statins may occur. Akt also activates NF-κB, in addition to a host of other transcription factors, to brake apoptosis.[27] We would speculate that in our Ang II–related model, Akt would be activated by Ang II to participate in NF-κB activation. However, that hypothesis remains to be tested. We conclude that the statins exhibit actions independent of cholesterol lowering that appear to exert vasculoprotective and anti-inflammatory effects. Finally, cerivastatin is a vascular cell–permeable statin; however, whether that feature provides any clinical advantage remains to be seen. A vascular cell–impermeable statin was found to preserve interstitial plaque collagen content in a

recent animal study, whereas a vascular cell–permeable statin reduced the number of VSMCs within plaques.[28] Clearly, additional investigations are necessary to establish any clinical relevance of our findings.

Acknowledgments

This study was supported by grants-in-aid from Hoffmann LaRoche, Basel, Switzerland; Bayer AG, Leverkusen, Germany; Klinisch-Pharmakologischer Verbund, Berlin-Brandenburg; and the Bundesministerium für Bildung und Forschung, Bonn, Germany.

References

1. Khwaja A, Connolly JO, Hendry BM. Prenylation inhibitors in renal disease. *Lancet*. 2000;355:741–744.
2. Nickenig G, Bäumer AT, Temur Y, et al. Statin-sensitive dysregulated AT1 receptor function and density in hypercholesterolemic men. *Circulation*. 1999;100:2131–2134.
3. Mervaala E, Müller DN, Schmidt F, et al. Blood pressure-independent effects in rats with human renin and angiotensinogen genes. *Hypertension*. 2000;35:587–594.
4. Müller DN, Dechend R, Mervaala EMA, et al. NF-κB inhibition ameliorates Ang II-induced inflammatory damage in rats. *Hypertension*. 2000;35:193–201.
5. Bischoff H, Angerbauer R, Boberg M, et al. Preclinical review of cerivastatin sodium: a step forward in HMG-CoA reductase inhibition. *Atherosclerosis*. 1998;139(suppl 1):S7–S13.
6. Fears R, Richards DH, Ferres H. The effect of compactin, a potent inhibitor of 3-hydroxy-3-methylglutaryl coenzyme-A reductase activity, on cholesterogenesis and serum cholesterol levels in rats and chicks. *Atherosclerosis*. 1980;35:439–449.
7. Glorioso N, Troffa C, Filigheddu F, et al. Effect of the HMG-CoA reductase inhibitors on blood pressure in patients with essential hypertension and primary hypercholesterolemia. *Hypertension*. 1999;34:1281–1286.
8. Luo JD, Zhang WW, Zhang GP, et al. Simvastatin inhibits cardiac hypertrophy and angiotensin-converting enzyme activity in rats with aortic stenosis. *Clin Exp Pharmacol Physiol*. 1999;26:903–908.
9. Oi S, Haneda T, Osaki J, et al. Lovastatin prevents angiotensin II-induced cardiac hypertrophy in cultured neonatal rat heart cells. *Eur J Pharmacol*. 1999;376:139–148.
10. Park J-K, Müller DN, Mervaala EMA, et al. Cerivastatin prevents leukocyte infiltration and iNOS induction by inhibition of ERK phosphorylation and NF-κB activation in angiotensin II-induced end-organ damage. *Kidney Int*. 2000;58:1420–1430.
11. Slack JL, Parker MI, Roginson VR, et al. Regulation of collagen I gene expression by ras. *Mol Cell Biol*. 1992;10:4714–4723.
12. Boffa J-J, Tharaux P-L, Placier S, et al. Angiotensin II activates collagen type I gene in the renal vasculature of transgenic mice during inhibition of nitric oxide synthesis. *Circulation*. 1999;100:1901–1908.
13. Brilla CG, Zhou G, Matsubara L, et al. Collagen metabolism in cultured adult rat cardiac fibroblasts: response to angiotensin II and aldosterone. *J Mol Cell Cardiol*. 1994;26:809–820.
14. Schultz JJ, Witt SA, Nieman ML, et al. bFGF mediates pressure-induced hypertrophic response. *J Clin Invest*. 1999;104:709–719.
15. Kaye D, Pimental D, Prasad S, et al. Role of transiently altered sarcolemmal membrane permeability and basic fibroblast growth factor release in the hypertrophic response of adult rat ventricular myocytes to increased mechanical activity in vitro. *J Clin Invest*. 1996;97:281–291.
16. Su E, Lombardi D, Wiener J, et al. Mitogenic effect of angiotensin II on rat carotid arteries and type II or III mesenteric microvessels but not type I mesenteric microvessels is mediated by endogenous bFGF. *Circ Res*. 1998;82:321–327.
17. Kozawa O, Suzuki A, Uematsu T. Basic FGF induces interleukin-6 synthesis in osteoblasts: autoregulation by protein kinase C. *Cell Signal*. 1997;9:463–468.
18. Faris M, Ensoli B, Kokot N, et al. Inflammatory cytokines induce the expression of basic fibroblast growth factor (b-FGF) isoforms required for the growth of Kaposi's sarcoma and endothelial cells through the activation of AP-1 response elements in the bFGF promoter. *AIDS*. 1998;12:19–27.
19. Nicoletti A, Michel JB. Cardiac fibrosis and inflammation: interaction with hemodynamic and hormonal factors. *Cardiovasc Res*. 1999;41:532–543.
20. Magee T, Marshall C. New insights into the interaction of Ras with the plasma membrane. *Cell*. 1999;98:9–12.
21. Bourcier T, Libby P. HMG CoA reductase inhibitors reduce plasminogen activator-1 expression by human vascular smooth muscle and endothelial cells. *Arterioscler Thromb Vasc Biol*. 2000;20:556–562.
22. Laufs U, Liao JK. Post-transcriptional regulation of endothelial nitric oxide synthase mRNA stability by Rho GTPase. *J Biol Chem*. 1998;273:24266–24271.
23. Ikeda U, Shimpo M, Ohki R, et al. Fluvastatin inhibits matrix metalloproteinase-1 expression in human vascular endothelial cells. *Hypertension*. 2000;36:325–329.
24. Riessen R, Axel DI, Fenchel M, et al. Effect of HMG-CoA reductase inhibitors on extracellular matrix expression in human vascular smooth muscle cells. *Basic Res Cardiol*. 1999;94:322–332.
25. Weber C, Erl W, Weber KS, et al. HMG-CoA reductase inhibitors decrease CD11b expression and CD11b-dependent adhesion of monocytes to endothelium and reduce increased adhesiveness of monocytes isolated from patients with hypercholesterolemia. *J Am Coll Cardiol*. 1997;30:1212–1217.
26. Kureishi Y, Luo Z, Shiojima I, et al. The HMG-CoA reductase inhibitor simvastatin activates the protein kinase Akt and promotes angiogenesis in normocholesterolemic animals. *Nat Med*. 2000;9:1004–1010.
27. Datta SR, Brunet A, Greenberg ME. Cellular survival: a play in three Akts. *Genes Dev*. 1999;13:2905–2927.
28. Fukumoto Y, Libby P, Rabkin E, et al. Statins alter smooth muscle cell accumulation and collagen content in established atheroma of Watanabe heritable hyperlipidemic rabbits. *Circulation*. 2001;103:993–999.

Reprint 5

Park JK, Muller DN, Mervaala EM, Dechend R, Fiebeler A, Schmidt F, Bieringer M, Schafer O, Lindschau C, Schneider W, Ganten D, Luft FC, Haller H. Cerivastatin prevents angiotensin II-induced renal injury independent of blood pressure- and cholesterol-lowering effects.

***Kidney Int*. 2000;58:1420-30.**

Kidney International, Vol. 58 (2000), pp. 1420–1430

Cerivastatin prevents angiotensin II-induced renal injury independent of blood pressure- and cholesterol-lowering effects

JOON-KEUN PARK, DOMINIK N. MÜLLER, EERO M.A. MERVAALA, RALF DECHEND, ANETTE FIEBELER, FOLKE SCHMIDT, MARKUS BIERINGER, OLAF SCHÄFER, CARSTEN LINDSCHAU, WOLFGANG SCHNEIDER, DETLEV GANTEN, FRIEDRICH C. LUFT, and HERMANN HALLER

Franz Volhard Clinic, Medical Faculty of the Charité, Humboldt University of Berlin, Berlin, Germany; Max Delbrück Center for Molecular Medicine, Institute of Biomedicine, University of Helsinki, Helsinki, Finland; and Department of Nephrology, Hannover Medical School, Hannover, Germany

Cerivastatin prevents angiotensin II-induced renal injury independent of blood pressure- and cholesterol-lowering effects.

Background. Statins are effective in prevention of end-organ damage; however, the benefits cannot be fully explained on the basis of cholesterol reduction. We used an angiotensin II (Ang II)-dependent model to test the hypothesis that cerivastatin prevents leukocyte adhesion and infiltration, induction of inducible nitric oxide synthase (iNOS), and ameliorates end-organ damage.

Methods. We analyzed intracellular targets, such as mitogen-activated protein kinase and transcription factor (nuclear factor-κB and activator protein-1) activation. We used immunohistochemistry, immunocytochemistry, electrophoretic mobility shift assays, and enzyme-linked immunosorbent assay techniques. We treated rats transgenic for human renin and angiotensinogen (dTGR) chronically from week 4 to 7 with cerivastatin (0.5 mg/kg by gavage).

Results. Untreated dTGR developed hypertension, cardiac hypertrophy, and renal damage, with a 100-fold increased albuminuria and focal cortical necrosis. dTGR mortality at the age of seven weeks was 45%. Immunohistochemistry showed increased iNOS expression in the endothelium and media of small vessels, infiltrating cells, afferent arterioles, and glomeruli of dTGR, which was greater in cortex than medulla. Phosphorylated extracellular signal regulated kinase (p-ERK) was increased in dTGR; nuclear factor-κB and activator protein-1 were both activated. Cerivastatin decreased systolic blood pressure compared with untreated dTGR (147 ± 14 vs. 201 ± 6 mm Hg, $P < 0.001$). Albuminuria was reduced by 60% ($P = 0.001$), and creatinine was lowered (0.45 ± 0.01 vs. 0.68 ± 0.05 mg/dL, $P = 0.003$); however, cholesterol was not reduced. Intercellular adhesion molecule-1 and vascular cell adhesion molecule-1 expression was diminished, while neutrophil and monocyte infiltration in the kidney was markedly reduced. ERK phosphorylation and transcription factor activation were reduced. In addition, in vitro incubation of vascular smooth muscle cells with cerivastatin (0.5 μmol/L) almost completely prevented the Ang II-induced ERK phosphorylation.

Conclusion. Cerivastatin reduced inflammation, cell proliferation, and iNOS induction, which led to a reduction in cellular damage. Our findings suggest that 3-hydroxy-3-methylglutaryl coenzyme (HMG-CoA) reductase inhibition ameliorates Ang II-induced end-organ damage. We suggest that these effects were independent of cholesterol.

Key words: statins, inducible nitric oxide synthase, MAP kinase, nuclear factor-κB, cell adhesion.

Received for publication August 31, 1999
and in revised form April 17, 2000
Accepted for publication April 22, 2000

3-Hydroxy-3-methylglutaryl coenzyme (HMG-CoA) reductase inhibitors (statins) ameliorate glomerular injury and preserve renal function in several models, including 5/6 nephrectomy and the diabetic nephropathy of Zucker rats [1–4]. The drugs are also effective in a model of the nephrotic syndrome [5]. Since lipid disturbances are not a salient feature in most rat models of disease, the beneficial effects of statins may involve mechanisms independent of their cholesterol-lowering effect [6, 7]. In human disease, alternative modes of action have also been postulated. Support for cellular mechanisms has accrued involving effects on chemokines, surface adhesion molecules, endothelin expression, and nitric oxide synthase (NOS) activity [8–13]. Data from several laboratories have shown that statins can directly interfere with intracellular signaling pathways. Statins inhibit the activation of the transcription factor nuclear factor-κB (NF-κB) in vitro [14]. The exact mechanisms whereby statins exert these intracellular effects are not yet clear; however, the geranolgeranyl pathway may be involved. Statins interfere with farnesylation by farnesol depletion and could thereby modify the activation of *ras*. We recently demonstrated that statins may influence ion channel regulation via a decrease in farnesol production [15]. Statins could conceivably influence

cellular mechanisms of renal damage via the ras-dependent signaling pathway and thereby reduce the activity of downstream signaling components such as raf, mitogen-activated protein (MAP) kinases, and the transcription factors NF-κB and activator protein-1 (AP-1) [16–19]. To test this hypothesis, we used an angiotensin II (Ang II)-dependent transgenic rat model. The rats carry both human renin and angiotensinogen genes, develop hypertension, and die of renal and cardiac damage by the age seven to eight weeks. The tissue damage features inflammation, microthrombosis, fibrinoid necrosis, fibrosis, and matrix production [20]. We have shown that NF-κB and AP-1 activation, chemokine production, adhesion molecule expression, plasminogen activator-1, and tissue factor expression are prominent features in this model [21, 22].

METHODS

Study design

Experiments were conducted in four-week-old male dTGR and age-matched Sprague-Dawley (SD) rats. The dTGR line and characteristics are described elsewhere [21, 22]. The rats were purchased from RCC Ltd. (Füllinsdorf, CH), kept in rooms at 24 ± 2°C, fed a standard rat diet containing 0.2% sodium by weight, and allowed free access to tap water. All procedures were done according to guidelines from the American Physiological Society and were approved by local authorities. The statin dTGR group ($N = 15$) received cerivastatin for three weeks by gavage once a day (0.5 mg/kg). Control dTGR ($N = 20$) and SD rats ($N = 15$) received vehicle (1% sodium carboxymethylcellulose).

Systolic blood pressure was measured weekly by the tail-cuff method under light ether anesthesia 20 hours after the last drug dose. Urine samples were collected over a 24-hour period. Rats were killed at the age of seven weeks. The kidneys and hearts were washed with ice-cold saline, blotted dry, and weighed. For electrophoretic mobility shift assay (EMSA) of NF-κB and AP-1, the tissues were snap frozen in liquid nitrogen for immunohistochemistry in isopentane (−35°C) and were stored at −80°C.

Immunohistochemistry

Frozen kidneys and hearts were cryosectioned at 6 μm thickness and were air dried as described earlier [23–25]. The sections were fixed with cold acetone and were air dried and washed with Tris-buffered saline (TBS; 0.05 mol/L Tris buffer, 0.15 mol/L NaCl, pH 7.6). The sections were incubated for 60 minutes in a humid chamber at room temperature with primary monoclonal antibodies against rat monocytes/macrophages (ED1; Serotec, Oxford, UK), NF-κB subunit p65 (Roche Boehringer, Mannheim, Germany), intercellular adhesion molecule-1 (ICAM-1; 1A29; R&D Systems, Abingdon, UK), neutrophils (HIS48; PharMingen, Heidelburg, Germany), the Ki-67, a nuclear cell proliferation-associated antigen expressed in all active stages of the cell cycle (MIB-5; Dianova, Hamburg, Germany), and polyclonal inducible NOS (iNOS) and endothelial NOS (ABR, Golden, CO, USA), phosphorylated extracellular signal regulated kinase (p-ERK; Santa Cruz, Heidelberg, Germany). After washing with TBS, the sections were incubated with a bridging antibody (rabbit-anti-mouse IgG; Dako, Hamburg, Germany) for 30 minutes at room temperature and washed again with TBS. The APAAP-complex (Dako) was applied, and the sections were incubated for 30 minutes at room temperature. The immunoreactivity was visualized by development in a mixture of naphthol-AS-BI-phosphate (Sigma) with neufuchsin (Merck, Darmstadt, Germany). Endogenous alkaline phosphatase was blocked by addition of 10 mmol/L levamisole (Sigma) to the substrate solution. The sections were slightly counterstained in Mayer's hemalaun (Merck) blued in a tap water and mounted with GelTol (Coulter-Immunotech, Hamburg, Germany). Preparations were examined under a Zeiss Axioplan-2 microscope (Zeiss, Jena, Germany) and photographed using a color reversal film Agfa CTX 100. Microscopy with phase contrast resolution was used to show the localization of p65 in the kidney (Fig. 3). Semiquantitative scoring of ED-1–positive cells in the kidney was performed using computerized cell count program (KS 300 3.0; Zeiss). Fifteen different areas of each heart and kidney samples ($N = 5$ in all groups) were analyzed. The samples were examined without knowledge of the rats' identity.

Electrophoretic mobility shift assay

Tissue extracts and EMSA for the transcription factor NF-κB were performed as described earlier [25]. Briefly, frozen total kidneys were pulverized in liquid nitrogen with a pestle and mortar and were resuspended in 3 mL 50 mmol/L Tris (pH 7.4) containing a complete inhibitor tablet (Roche Boehringer) and 1 mmol/L Na-ortho-vanadate (Sigma Chemie, Deisenhofen, Germany). The suspension was centrifuged (4000 × *g*, 4 min, 4°C). The pellet was resuspended and lyzed for 30 minutes in whole cell lysate buffer [20 mmol/L HEPES, pH 7.9, 350 mmol/L NaCl, 20% glycerol, 1 mmol/L $MgCl_2$, 0.5 mmol/L ethylenediaminetetraacetic acid (EDTA), 0.1 mmol/L egtazic acid (EGTA), and 1% NP-40] and again centrifuged (13,000 × *g*, 10 min, 4°C). The supernatant was aliquoted and frozen in liquid nitrogen and stored at −80°C until use. The protein concentration for EMSA and Western blot was quantitated by the Bradford method. For EMSA, total kidney homogenates (50 μg) were incubated in a binding reaction medium [2 μg poly dI-dC, 1 μg bovine serum albumin (BSA), 1 mmol/L dithiothreitol (DTT), 20 mmol/L HEPES, pH 8.4, 60 mmol/L KCl, and 8% Ficoll] with 0.5 ng of 32P-dATP end-labeled

oligonucleotide, containing the NF-κB binding site from the multiple histocompatibility complex (MHC)-enhancer (H2K, 5′-GATCCAGGGCTGGGGATTCCCCATCTC CACAGG) at 30°C for 30 minutes. For AP-1 double-stranded oligonucleotides containing the consensus sequence for AP-1 (5′-GATCGAACTGACCGCCCGCC GCCCGT-3′; Santa Cruz Biotechnologies, Santa Cruz, CA, USA) were radiolabeled with γ-32P with the use of T4 polynucleotide kinase by standard methods and purified over a column. The DNA-protein complexes were analyzed on a 5% polyacrylamide gel 0.5% Tris buffer and were dried and autoradiographed. In competition assays, 50 or 100 ng unlabeled H2K oligonucleotides were used.

Immunocytochemistry

Rat aortic vascular smooth muscle cells (VSMCs) were obtained as described earlier. VSMCs were incubated with cerivastatin (5 μmol/L) or buffer for 20 minutes. Cells were then exposed to Ang II (10^{-7} mol/L), and ERK phosphorylation was assessed after one minute using confocal microscopy. Immediately after the experiments, the cells were fixed with 4% paraformaldehyde and were permeabilized with 80% methanol at −20°C and stained with a commercially available antibodies directed against p-ERK (Santa Cruz). Cells were then exposed to the secondary antibody FITC-conjugated antirabbit, at 1:100, 1% bovine serum albumin/phosphate-buffered saline; Dianova) for 60 minutes. The preparation was mounted with 50% glycerol under a glass cover slip on a Nikon-Diaphot (Tokyo, Japan) microscope. A Biorad MRC 600 confocal imaging system (Biorad Laboratories, Munich, Germany) with an argon/krypton laser was used. At least 10 to 18 cells from each of three experiments were examined under each experimental condition. The results were reproduced by two separate investigators, and multiple experiments were done. The observers were unaware of the experimental design and antibodies used.

Statistical analysis

Data are presented as means ± SEM. Statistically significant differences in mean values were tested by analysis of variance and Scheffé test. A value of $P < 0.05$ was considered statistically significant. The data were analyzed using Statview.

RESULTS

Renal histology and mortality dTGR developed hypertension, severe renal damage, and cardiac hypertrophy with focal necrosis. Nine of 20 untreated dTGR (45%) died before the end of the study at seven weeks. Cerivastatin showed a markedly reduced mortality (3 of 15; 20%), while none of the nontransgenic SD rats died before the end of the study ($P < 0.05$). Small vessels showed increased intimal and medial thickness as well as hyaline deposits. The renal tubules were frequently swollen and filled with proteinaceous material (Fig. 1A). Chronic treatment with cerivastatin prevented vascular injury in small renal vessels and extracellular matrix formation (Fig. 1B).

Effect of cerivastatin on blood pressure

Systolic blood pressure of cerivastatin-treated rats was significantly decreased (54 mm Hg) compared with untreated dTGR (147 ± 14 vs. 201 ± 6 mm Hg, $P < 0.001$; Fig. 2). dTGR showed a progressive increase in systolic blood pressure from five to seven weeks. After two weeks of treatment, cerivastatin prevented the increase in systolic blood pressure seen in dTGR. However, the blood pressure of cerivastatin-treated rats was significantly elevated compared with nontransgenic SD rats (147 ± 14 vs. 109 ± 2 mm Hg, $P < 0.001$, $N = 10$ to 17; Fig. 2).

Effect of cerivastatin on relative kidney weight, albuminuria, creatinine, and urea

There was a progressive increase in 24-hour albuminuria in untreated dTGR from five to seven weeks. Cerivastatin ameliorated but did not eliminate the development of albuminuria in dTGR (6.1 ± 2.5 vs. 17.5 ± 2.3 vs. 0.3 ± 0.1 mg/day for week 7, $P < 0.001$, $N = 7$ to 17; Fig. 3A). Plasma creatinine (0.45 ± 0.01 vs. 0.68 ± 0.05 vs. 0.49 ± 0.01 mg/dL, $P < 0.01$, $N = 8$ each; Fig. 3B) and plasma urea (49 ± 4 vs. 90 ± 22 vs. 45 ± 2 mg/mL, $P < 0.05$, $N = 8$ each; Fig. 3C) were significantly lower in cerivastatin-treated compared with untreated dTGR and were similar to SD rat levels. Plasma cholesterol levels in untreated dTGR were 2.84 ± 0.2 mmol/L. However, nontransgenic rats tended to have lower levels (2.3 ± 0.1 mmol/L at week 7, $P = 0.07$, $N = 7$). Treatment with cerivastatin did not significantly influence plasma cholesterol compared with dTGR and SD rats (2.5 ± 0.1 mmol/L at week 7, $P = 0.3$ and $P = 0.7$, respectively, $N = 8$ each; Fig. 3D). Relative kidney weight was significantly higher in dTGR than in cerivastatin-treated rats and SD rats (4.8 ± 0.1 vs. 4.3 ± 0.1 vs. 3.7 ± 0.1 mg/g body weight at week 7, $P < 0.01$, $N = 10$ to 15). Body weight of the rats were not different between dTGR and cerivastatin-treated rats (217 ± 6 vs. 232 ± 8 g at week 7, $P = 0.3$, $N = 10$ to 15). However, SD rats (264 ± 8 g) were slightly heavier compared with dTGR and cerivastatin-treated dTGR ($P < 0.05$ $N = 10$ to 15).

Cerivastatin reduced leukocyte infiltration and adhesion molecule expression

First, we analyzed the effects of cerivastatin on neutrophils and monocytes in our model. There was significant leukocyte infiltration in renal tissue of dTGR. Neutrophils (Fig. 4A, upper panels) were mostly present within

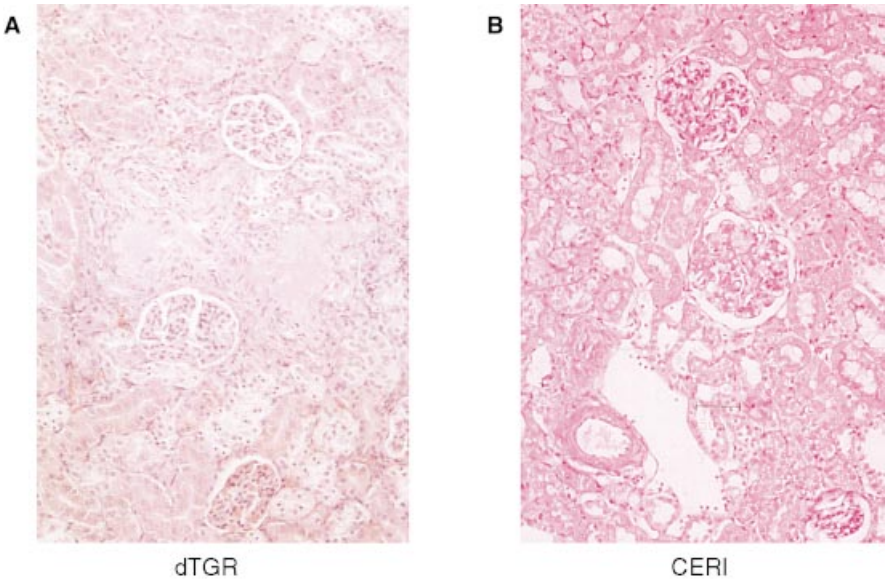

Fig. 1. Periodic acid-Schiff–stained section from a rat transgenic for human renin and angiotensinogen (*A*; dTGR) and cerivastatin-treated (*B*) kidneys. Small vessels showed increased intimal and medial thickness, as well as hyaline deposits; tubules were frequently swollen and filled with proteinaceous material. Chronic treatment with cerivastatin prevented vascular injury and extracellular matrix formation.

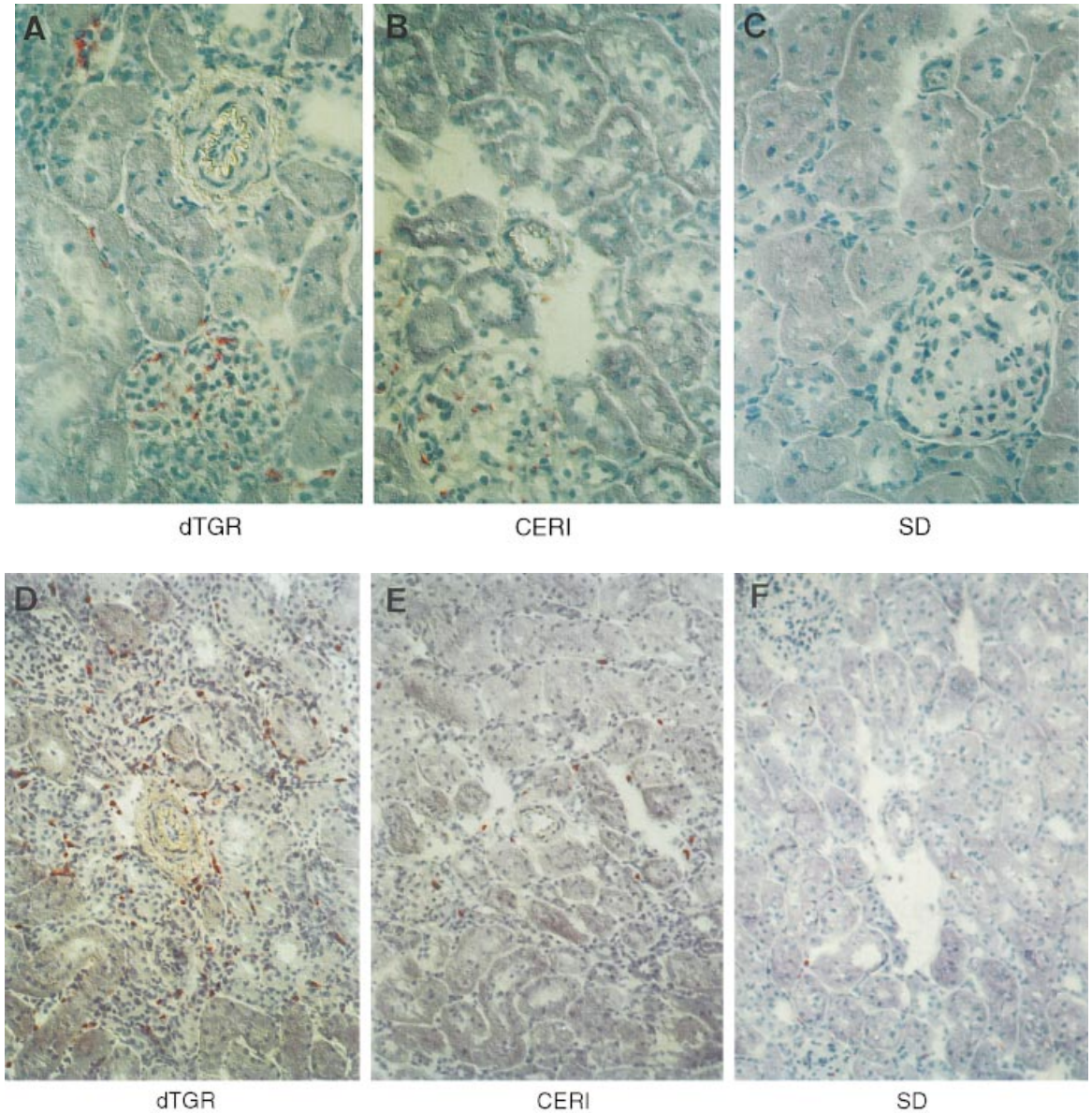

Fig. 4. Representative immunohistochemical photomicrographs of the infiltration of neutrophils (*A–C*) and ED-1–positive monocytic cells (*D–F*) in the kidneys of dTGR, dTGR treated with cerivastatin, and SD rats. Neutrophils predominantly infiltrated in the glomeruli, while ED-1–positive cells showed mainly perivascular and peritubular infiltration in untreated dTGR kidneys. Cerivastatin prevented the cellular infiltration of both neutrophils and monocytes/macrophages almost completely. Neutrophils and ED-1–positive monocytic cells are stained in red.

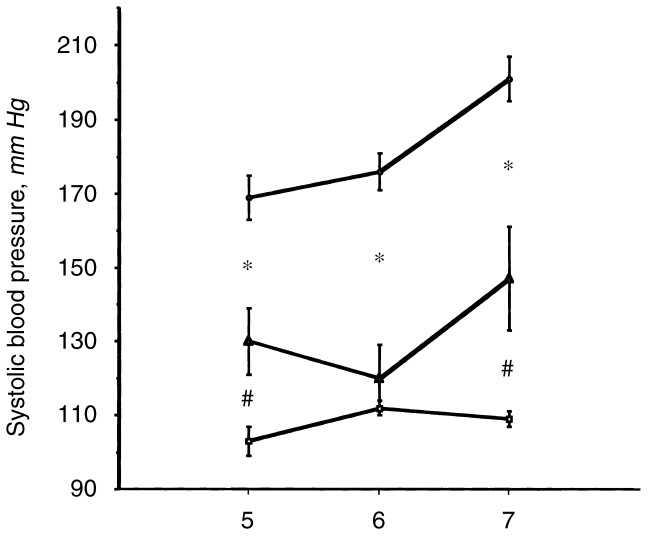

Fig. 2. Systolic blood pressure in dTGR (●), dTGR treated with cerivastatin (▲), and Sprague-Dawley (SD; □) rats. Systolic blood pressure of dTGR increased from weeks 5 to 7. Systolic blood pressure of cerivastatin-treated rats showed a lower blood pressure compared with untreated dTGR, but significantly higher compared to nontransgenic controls. Results are expressed as mean ± SEM of 10 to 17 animals per group. *$P < 0.01$ dTGR vs. cerivastatin-treated; #$P < 0.01$ cerivastatin-treated vs. SD.

the glomerulus and, to a lesser extent, in perivascular areas. In contrast, monocytes/macrophages were mostly localized in the perivascular space and between the tubules (Fig. 4D, lower panels). Treatment with cerivastatin prevented neutrophil infiltration almost completely. Cerivastatin also had an inhibitory effect on monocyte infiltration. Semiquantitative cell count analysis confirmed the significant reduction of monocyte/macrophage infiltration in the kidney after cerivastatin treatment ($P < 0.001$; Fig. 5).

We then investigated the effect of cerivastatin on the expression of adhesion molecules. The expression of ICAM-1 in the kidney (Fig. 6A) was increased in the intima, adventitia, and the perivascular space of the small vessels in untreated dTGR. Glomeruli and tubules showed increased ICAM-1 expression. Expression of ICAM-1 was markedly reduced by treatment with cerivastatin and was similar compared with the constitutive ICAM-1 expression in control animals at week 7. The expression of vascular cell adhesion molecule-1 (VCAM-1) in untreated dTGR was mostly observed in the intima of arterioles. As in the case of ICAM-1, treatment with cerivastatin reduced the up-regulation of VCAM-1, and no difference between treated animals and SD control animals could be observed (data not shown). These results demonstrate that treatment with cerivastatin reduced the infiltration of both neutrophils and monocytes and simultaneously inhibited the increased expression of adhesion molecules.

Effect of cerivastatin on iNOS expression

Next, we investigated the effects of cerivastatin on iNOS expression. These results are shown in Figure 7. We observed a strong increase in iNOS expression in the glomeruli (upper panels) and in the vessel wall of renal arterioles (lower panels compared with SD controls). Treatment with cerivastatin greatly reduced the iNOS immunoreactivity both in the blood vessels and the glomeruli. In contrast to iNOS, endothelial NOS was markedly increased in dTGR and cerivastatin-treated rats compared with SD rats.

Effect of cerivastatin on cell proliferation

In untreated dTGR, the number of Ki-67–positive cells in the kidney was significantly higher than that of SD rats. Cell proliferation was more dominant in the medulla of dTGR compared with cortex. Nevertheless, cerivastatin reduced vascular cell proliferation in both cortex and medulla (data not shown).

Effect of cerivastatin on p-ERK, AP-1, and Nuclear factor-κB activation

The possible intracellular mechanisms of the observed protective effects of cerivastatin were then analyzed. We first analyzed the activation of MAP kinase by using specific antibodies which only detect the phosphorylated, active form of extracellular signal regulated kinase (p-ERK). In untreated transgenic rats, an increase in phosphorylated ERK in the vessel wall, glomeruli, and the peritubular space was observed (Fig. 8). An even more pronounced increase was also present in the medulla (data not shown). Treatment with cerivastatin decreased, but did not abolished this staining pattern in the cortex and in the medulla.

We next investigated the activation of the transcription factors NF-κB and AP-1, which are important regulators of ICAM-1 and iNOS gene expression. EMSA was used for the detection of NF-κB and AP-1 DNA binding activity in the kidney. Both NF-κB (Fig. 9A) and AP-1 (Fig. 9B) showed a greatly increased activity in the kidneys of dTGR compared with SD rats. Cerivastatin treatment reduced renal DNA binding activity of NF-κB and AP-1 almost completely. An immunohistochemical analysis of the subunit p65 of NF-κB in the kidney was also performed. The expression of p65 was increased in the endothelium, smooth muscles cells of small vessels, infiltrated cells, glomeruli, and tubules of dTGR. Cerivastatin reduced p65 expression (data not shown).

Effect of cerivastatin on Ang II-induced ERK phosphorylation in vitro

To verify with certainty that cerivastatin indeed interferes with Ang II-induced ERK phosphorylation, in vitro experiments were performed. Ang II-induced ERK phosphorylation was analyzed with and without prior

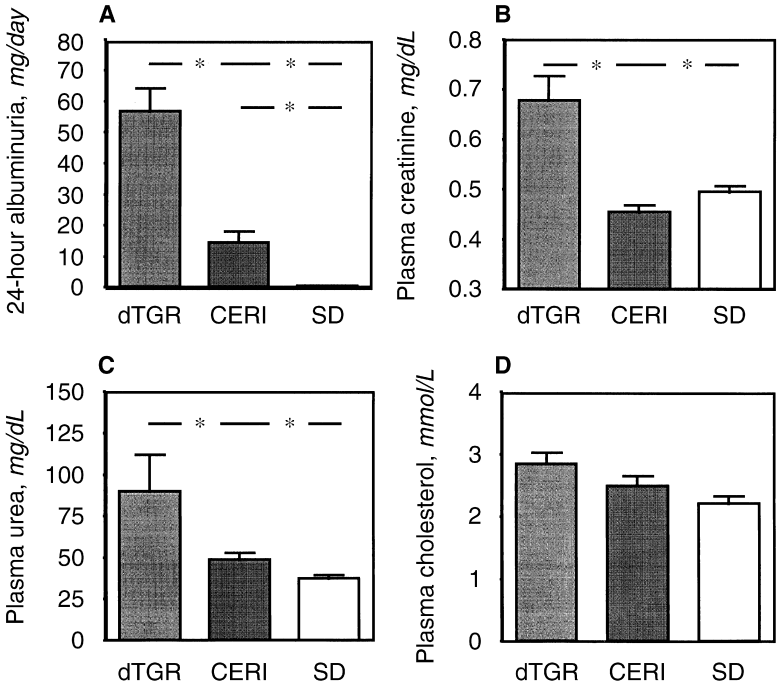

Fig. 3. (*A*) Twenty-four–hour urinary albumin excretion in dTGR, dTGR treated with cerivastatin, and SD rats. dTGR showed 100-fold increased albuminuria, which was reduced by 60% after cerivastatin treatment. Plasma creatinine (*B*) and plasma urea (*C*) levels were increased in dTGR, while the plasma levels were not elevated after cerivastatin treatment. Plasma cholesterol levels in untreated dTGR tended to higher levels ($P = 0.07$). Treatment with cerivastatin did not significantly influence plasma cholesterol compared with dTGR and SD rats ($P = 0.3$ and $P = 0.7$, respectively, *D*). Results are expressed as mean ± SEM of 8 to 17 animals per group ($^*P < 0.05$).

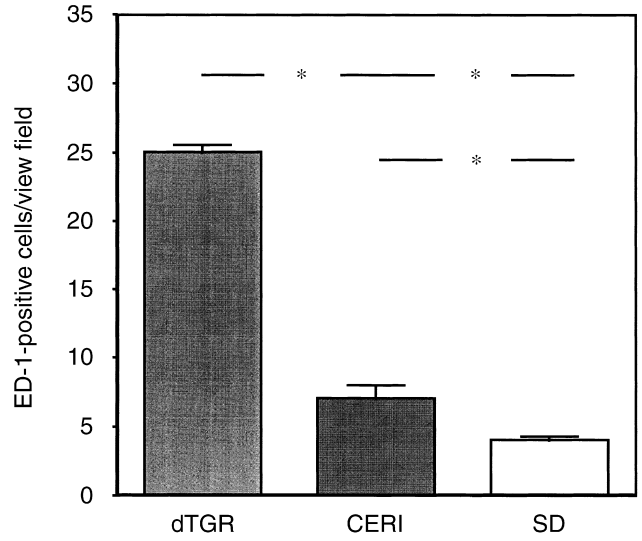

Fig. 5. Semiquantitative scoring of ED-1–positive monocytic cells in the kidney was performed using a computerized cell-count program. Fifteen different areas of each kidney were analyzed. Results are expressed as mean ± SEM of five animals per group ($^*P < 0.001$).

VSMC incubation with cerivastatin. VSMCs were incubated with cerivastatin (5 μmol/L) or buffer for 20 minutes. Cells were then exposed to Ang II (10^{-7} mol/L), and ERK phosphorylation was assessed after one minute using confocal microscopy. The results of these experiments are shown in Figure 10. Ang II induced a rapid increase in p-ERK immunoreactivity within one minute. This response was almost abolished by the prior incubation with cerivastatin ($N = 3$, $P < 0.01$). The inhibitory effect was also observed after longer cerivastatin incubation times (6, 12, and 24 hours).

DISCUSSION

We tested the hypothesis that in a lipid-independent transgenic animal model of Ang II-mediated organ damage, HMG-CoA reductase inhibition ameliorates renal failure and inhibits inflammatory changes such as adhesion molecule expression, cell infiltration, and iNOS expression. In addition, we investigated whether specific intracellular signaling pathways are influenced by cerivastatin. We showed that cerivastatin reduced MAP kinase activation, inhibited AP-1 and NF-κB binding activity, prevented inflammatory responses, and ameliorated renal damage. We selected a dose that was considered sufficiently high to lower total cholesterol in rats; however, even this relatively high dose, compared with human treatment, did not lower total cholesterol significantly. Our animal model features hypertension, albuminuria, severe inflammatory changes, cardiac hypertrophy, and focal necrosis in heart and kidney. Untreated dTGR have a 50% mortality at seven weeks [20, 22]. Earlier we showed that Ang II production in the kidneys and elsewhere is responsible for this severe vasculopathy [21]. Our findings suggest that cerivastatin influences the Ang II-induced cellular mechanisms directly, independent of changes in cholesterol.

Cerivastatin led to a decrease in blood pressure compared with nontreated animals. The blood pressure-low-

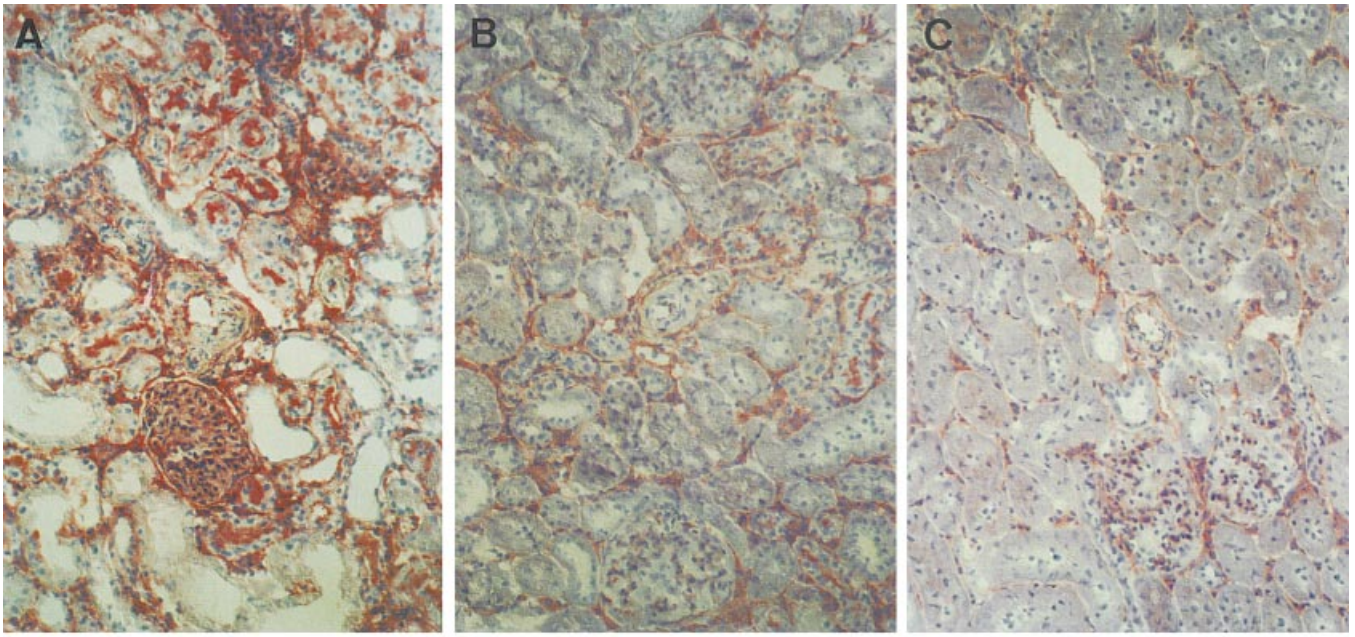

Fig. 6. Representative immunohistochemical photomicrographs of intercellular adhesion molecule-1 (ICAM-1) in the kidney of dTGR (*A*), cerivastatin-treated dTGR (*B*), and SD rats (*C*). The expression of ICAM-1 was increased in the intima, adventitia, and the perivascular space of the small dTGR vessels. Glomeruli and tubuli showed frequently increased ICAM-1 expression. Stimulation of ICAM-1 was markedly reduced by cerivastatin.

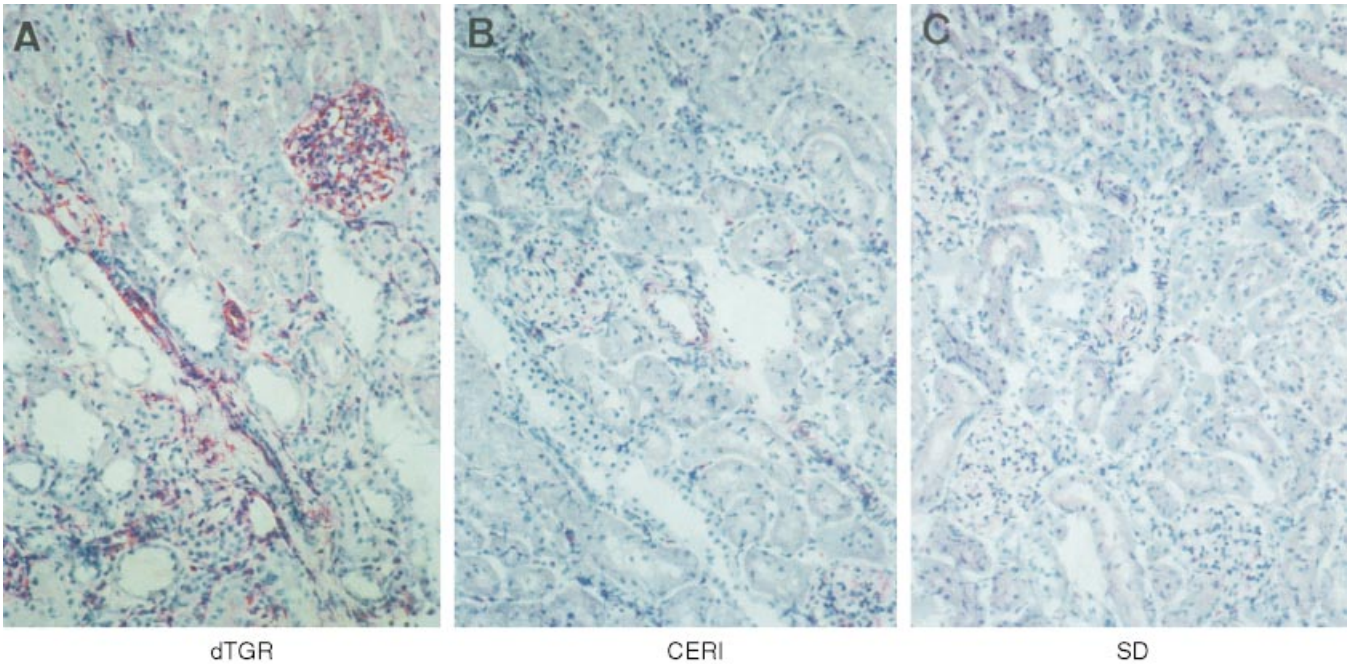

Fig. 7. Representative immunohistochemical photomicrographs of inducible nitric oxide synthase (iNOS) of kidneys from dTGR, cerivastatin-treated, and SD rats. iNOS expression was increased in glomeruli and the vessel wall of dTGR. Cerivastatin reduced the iNOS expression.

ering effect of statin treatment may be due to the prevention of renal injury. However, we cannot rule out a direct effect of statins on blood pressure. Recently, a reduction in blood pressure treatment by statins in hypercholesterolemic patients using angiotensin-converting enzyme inhibitors was reported [26]. A blood pressure-lowering effect of statins was also observed in animal models of hypertension. These results have recently been verified in a double-blind, crossover trial in humans [27]. The effect may be due to the inhibition of isoprenoid synthesis, which

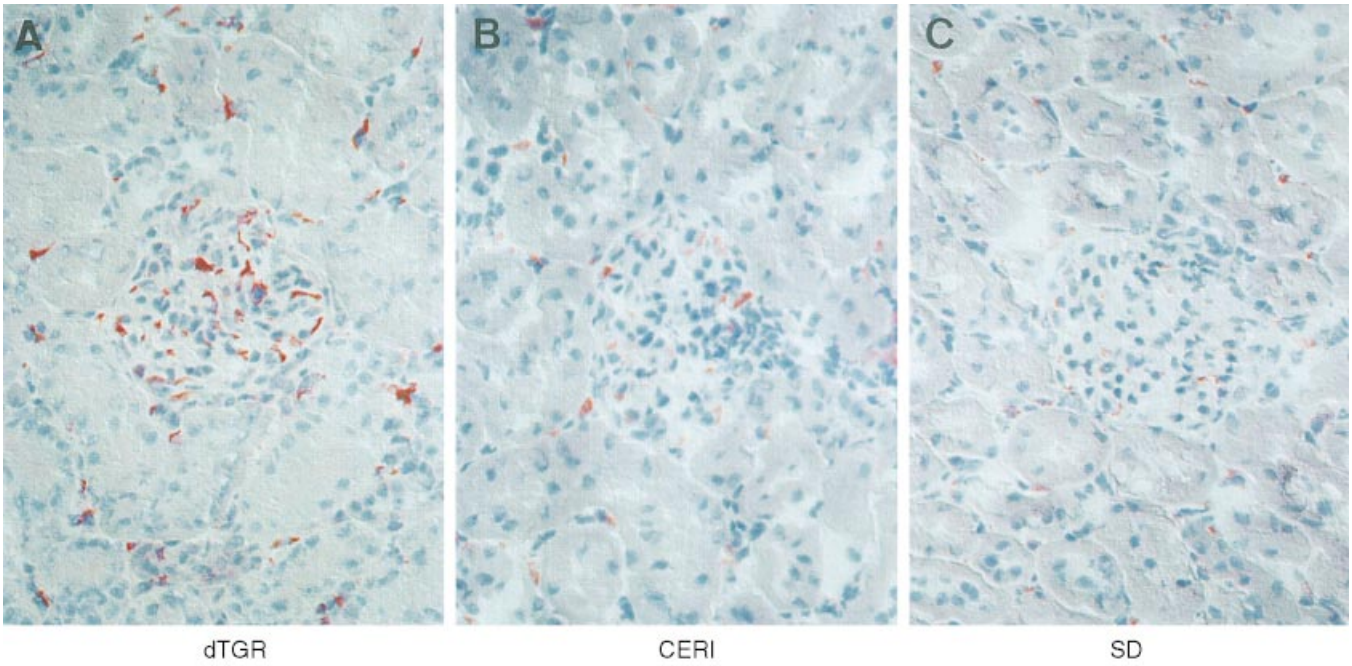

Fig. 8. Representative immunohistochemical photomicrographs of phosphorylated extracellular signal regulated kinase (p-ERK) in the kidney of dTGR (*A*), cerivastatin-treated dTGR (*B*), and SD rats (*C*). The expression of p-ERK was increased in the vessel wall, glomeruli, and interstitium of dTGR. Expression of p-ERK was markedly reduced by cerivastatin.

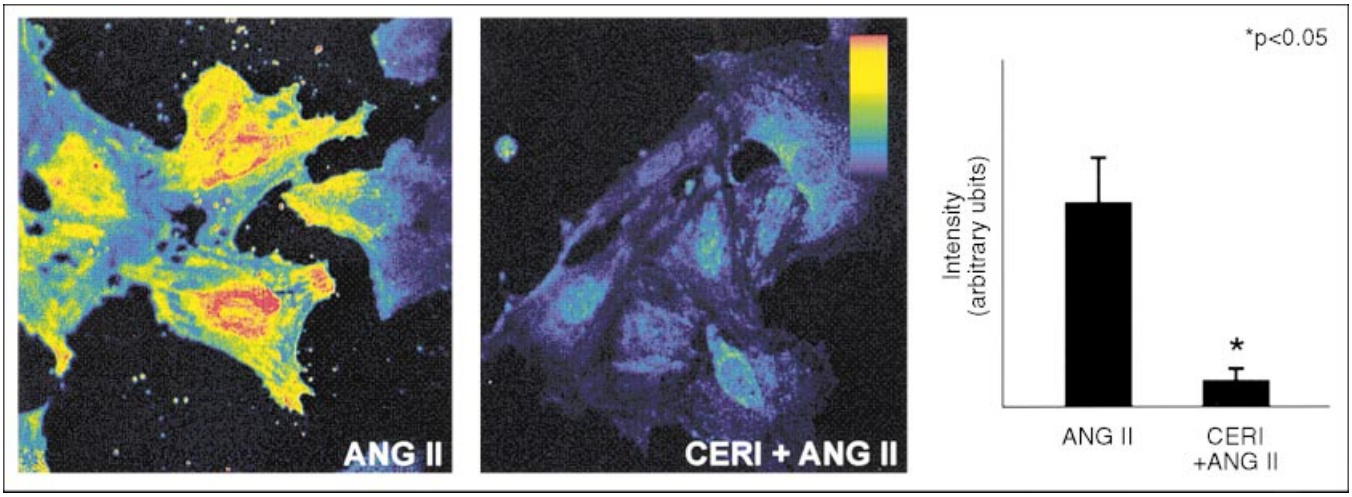

Fig. 10. Effects of cerivastatin on the angiotensin (Ang) II-induced phosphorylated extracellular signal regulated kinase (p-ERK) in vascular smooth muscle cells (VSMCs). Confocal micrographs demonstrate an increase in p-ERK immunoreactivity after exposure Ang II (10^{-7} mol/L) for one minute. Prior exposure of the VSMCs by cerivastatin (5 μmol/L) almost abolished the Ang II-induced p-ERK ($N = 3$, $P < 0.05$).

subsequently influences VSMC signaling [28]. The cerivastatin-mediated decrease in blood pressure may have contributed to the renoprotective effect. However, we do not believe that a blood pressure-lowering action of cerivastatin had a major effect, since effective antihypertensive triple treatment (hydralazine, reserpine, and hydrochlorothiazide) in our model only partially prevented tissue damage and did not reduce inflammation [29].

Cerivastatin treatment inhibited the inflammatory process in our animal model considerably. Neutrophil infiltration was almost abolished. Neutrophils are important mediators of injury in acute inflammatory renal diseases [30]. Cerivastatin also inhibited the expression of the endothelial cell adhesion molecule ICAM-1. Since ICAM-1 is responsible for neutrophil adhesion to the endothelium and subsequent infiltration [30], cerivastatin probably inhibited neutrophil infiltration via inhibition of ICAM-1. This assumption is supported by earlier findings from Guijarro et al, showing that statins inhibit the ICAM-1 expression in mesangial cells in vitro [31].

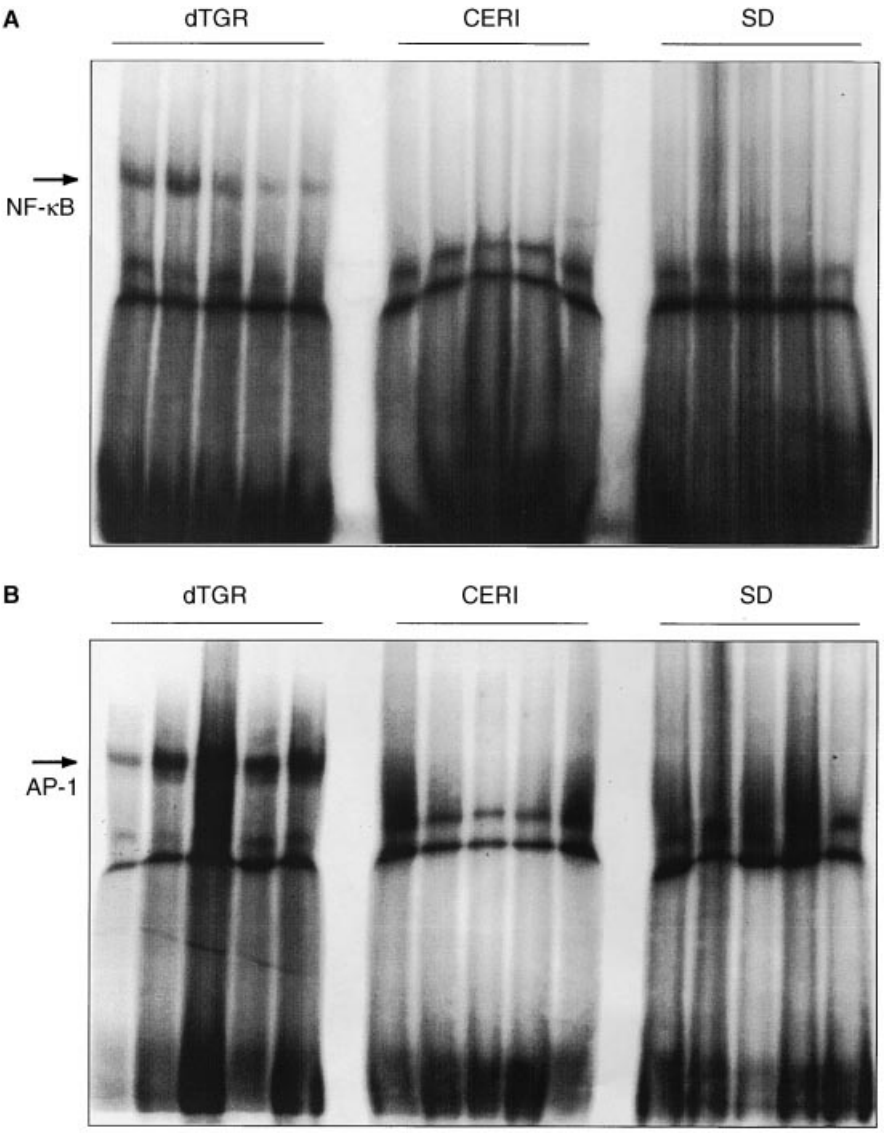

Fig. 9. Effects of cerivastatin on the activation of DNA binding nuclear factors in the kidney. Electrophoretic mobility shift assay (EMSA) for the detection of nuclear factor-κB (NF-κB; *A*) and activated protein-1 (AP-1; *B*) shows a higher DNA binding activity of dTGR kidney homogenates compared with SD rats. Cerivastatin treatment reduced levels of both NF-κB and AP-1 DNA binding activity. Each lane represents a single rat kidney homogenate. Specific DNA binding of NF-κB and AP-1 is indicated by the arrow. EMSA was performed three times independently with similar results.

We recently showed that down-regulation of ICAM-1 prevents acute renal failure and reperfusion injury in rat kidney [32].

Monocyte infiltration and the expression of the adhesion molecule VCAM-1 were reduced by cerivastatin treatment. Several reports have demonstrated the participation of monocyte/macrophages in the onset and progression of various renal diseases [33]. Since monocytes play a role in long-term pathological changes and chronic renal failure and have been associated with matrix accumulation and fibrosis [34], our findings suggest that cerivastatin has a direct influence on these processes. Statins improve long-term outcome in renal transplantation [35, 36], and the positive effect of statins on chronic vascular changes in the kidney may be partially due to their direct effects upon monocyte/neutrophil infiltration. We are presently investigating whether cytokines and growth factors released from these monocytes are also affected by statins. Since monocytes and their products play an important role in the pathogenesis of acute and chronic atherosclerotic syndromes, the beneficial effects of statins seen in patients with chronic vascular disease may be related in part to their effect on monocyte infiltration.

Cerivastatin greatly reduced iNOS expression in the dTGR. NO regulates numerous physiological processes, including smooth muscle contractility, platelet reactivity, and the cytotoxic activity of leukocytes. Because of the ubiquitous nature of NO, inappropriate release of this mediator has been linked to the pathogenesis of a number of disease states [37]. While NO serves beneficial roles as a messenger and host defense molecule, excessive NO production can be cytotoxic. The result of NO's reaction with reactive oxygen and nitrogen species leads

to peroxynitrite anion formation, protein tyrosine nitration, and hydroxyl radical production. Indeed, NO may contribute to the evolution of several commonly encountered renal diseases, including immune-mediated glomerulonephritis, postischemic renal failure, radiocontrast nephropathy, obstructive nephropathy, and acute and chronic renal allograft rejection [38]. Inhibitors of NOS are potentially beneficial in the treatment of conditions associated with an overproduction of NO, including inflammation [39]. It is possible that the inhibition of the increased NO expression by cerivastatin plays an important role in the anti-inflammatory effect of the drug.

Cerivastatin reduced the activation of the transcription factors NF-κB and AP-1. NF-κB is the main factor in the transcription of NOS, ICAM-1, and VCAM-1 [40, 41]. The molecular mechanisms whereby cerivastatin influenced Ang II-induced cell activation are not clear. Cerivastatin could influence cell activation through inhibition of NF-κB. Guijarro et al have previously shown that lovastatin inhibits lipopolysaccharide-induced NF-κB activation in human mesangial cells in vitro [31]. Ruiz-Ortega et al showed that Ang II stimulated NF-κB in mesangial cells and that activation of NF-κB in the renal cortex was reduced by angiotensin-converting enzyme inhibition [42]. Another possibility is the activation of NF-κB through oxygen free radicals. Reactive oxygen species represent an important signal transduction pathway inside the cell and also participate in the expression of adhesion molecules on the cell surface [43, 44]. Our results indicate that statins interfere with the MAP kinase activation proximal to NF-κB activation. Since MAP kinase phosphorylation and activation occur through the ras signaling pathway, statins may interfere with ras signaling. Such a mechanism has been proposed by several investigators [16, 45]. The postulated mechanisms involve ras farnesylation and ras cell membrane binding [16]. Farnesylated p21 ras may be critical for cellular signaling. Inhibitors of HMG-Co A reductase block the production of mevalonate and its metabolite, farnesol. Statins inhibit proliferation of many cell types. This inhibition can be overcome by the simultaneous addition of either mevalonate or farnesol, but not by exogenous low-density lipoprotein cholesterol [45–48].

In conclusion, we have demonstrated that treatment with cerivastatin in dTGR ameliorates Ang II-induced organ damage and influences cell adhesion, cell infiltration, and NOS expression, together with an inhibition of intracellular events such as NF-κB activation and ERK phosphorylation. In addition, our in vitro results suggest that the observed effect is directly mediated by the statin and not related to changes in either blood pressure or plasma cholesterol. These findings add to the recently described "pleiotropic" effects of the statins and may be relevant for their therapeutic efficacy in cardiovascular disease.

ACKNOWLEDGMENTS

This study was supported by a grant-in-aid from Bayer Inc., Leverkusen, Germany, and from Hoffmann-La Roche, Basel, Switzerland. E.M. was supported by the Alexander von Humboldt Foundation, the Finnish Foundation for Cardiovascular Research, and the Academy of Finland; E.M. and D.N.M were supported by the Klinisch-Pharmakologischer-Verbund Berlin-Brandenburg. Ms. Karin Dressler, Mathilde Schmidt, and Ms. Christel Lipka gave expert technical assistance. Joon-Keun Park, Dominik Muller, and Eero Mervaala contributed equally to this work.

Reprint reqeusts to Dr. Friedrich C. Luft, Franz Volhard Clinic, Wiltberg Strasse 50, 13125 Berlin, Germany.
E-mail: luft@fvk-berlin.de

REFERENCES

1. Guijarro C, Keane WF: Effects of lipids on the pathogenesis of progressive renal failure: Role of 3-hydroxy-3-methylglutaryl coenzyme A reductase inhibitors in the prevention of glomerulosclerosis. *Miner Electrolyte Metab* 22:147–152, 1996
2. Oda H, Keane WF: Recent advances in statins and the kidney. *Kidney Int* 56(Suppl 71):S2–S5, 1999
3. Kasiske BL, O'Donnell MP, Garvis WL, Keane WF: Pharmacological treatment of hyperlipidemia reduces glomerular injury in rat 5/6 nephrectomy model of chronic renal failure. *Circ Res* 62:367–374, 1988
4. O'Donnell MP, Kasiske BL, Kim Y, Schmitz PG, Keane WF: Lovastatin retards the progression of established glomerular disease in obese Zucker rats. *Am J Kidney Dis* 22:83–89, 1993
5. Harris KP, Purkerson ML, Yates J, Klahr S: Lovastatin ameliorates the development of glomerulosclerosis and uremia in experimental nephrotic syndrome. *Am J Kidney Dis* 15:16–23, 1990
6. Kasiske BL, O'Donnell MP, Kim Y, Atluru D, Keane WF: Cholesterol synthesis inhibitors inhibit more than cholesterol synthesis. *Kidney Int* 45(Suppl 45):S51–S53, 1994
7. Wheeler DC: Are there potential non-lipid-lowering uses of statins? *Drugs* 56:517–522, 1998
8. Bellosta S, Bernini F, Ferri N, Quarato P, Canavesi M, Arnaboldi L, Fumagalli R, Paoletti R, Corsini A: Direct vascular effects of HMG-CoA reductase inhibitors. *Atherosclerosis* 137 (Suppl):S101–S109, 1998
9. Corsini A, Arnaboldi L, Raiteri M, Quarato P, Faggiotto A, Paoletti R, Fumagalli R: Effect of the new HMG-CoA reductase inhibitor cerivastatin (BAY W 6228) on migration, proliferation and cholesterol synthesis in arterial myocytes. *Pharmacol Res* 33: 55–61, 1996
10. Kim S, Guijarro C, O'Donnell M, Kasiske B, Kim Y, Keane W: Human mesangial cell production of monocyte chemoattractant protein-1: Modulation by lovastatin. *Kidney Int* 48:363–371, 1995
11. Weber C, Erl W, Weber K, Weber P: Effects of oxidized low density lipoprotein, lipid mediators and statins on vascular cell interactions. *Clin Chem Lab Med* 37:243–251, 1999
12. Hernandez-Perera O, Perez-Sala D, Navarro-Antolin J, Sanchez-Pascuala R, Hernandez G, Diaz C, Lamas S: Effects of the 3-hydroxy-3-methylglutaryl-CoA reductase inhibitors, atorvastatin and simvastatin, on the expression of endothelin-1 and endothelial nitric oxide synthase in vascular endothelial cells. *J Clin Invest* 101:2711–2719, 1998
13. Luscher T, Tanner F, Noll G: Lipids and endothelial function: Effects of lipid-lowering and other therapeutic interventions. *Curr Opin Lipidol* 7:234–240, 1996
14. Guijarro C, Kim Y, Schoonover C, Massy Z, O'Donnell M, Kasisk W, Kashtan C: Lovastatin inhibits lipopolysaccharide-induced NF-kappaB activation in human mesangial cells. *Nephrol Dial Transplant* 11:990–996, 1996
15. Luft UC, Bychkov R, Gollasch M, Roullet J-B, McCarron DA, Hofmann F, Haller H, Luft FC: Farnesol, a new class of L-type Ca^{2+} channel blocker. *Arterioscler Thromb Vasc Biol* 19: 959–966, 1999
16. Bassa B, Roh D, Vazir N, Kirschenbaum M, Kamanna V: Effect of inhibition of cholesterol synthetic pathway on the activation of

Ras and MAP kinase in mesangial cells. *Biochim Biophys Acta* 1449:137–149, 1999
17. Pahan K, Sheikh FG, Namboodiri AM, Singh I: Lovastatin and phenylacetate inhibit the induction of nitric oxide synthase and cytokines in rat primary astrocytes, microglia, and macrophages. *J Clin Invest* 100:2671–2679, 1997
18. Kreuzer J, Watson L, Herdegen T, Loebe M, Wende P, Kubler K: Effects of HMG-CoA reductase inhibition on PDGF- and angiotensin II- mediated signal transduction: Suppression of c-Jun and c-Fos in human smooth muscle cells in vitro. *Eur J Med Res* 4:135–143, 1999
19. Lander HM, Ogiste JS, Teng KK, Novogrodsky A: p21ras as a common signaling target of reactive free radicals and cellular redox stress. *J Biol Chem* 270:21195–21198, 1995
20. Bohlender J, Fukamizu A, Lippoldt A, Nomura T, Dietz R, Menard J, Murakami K, Luft FC, Ganten D: High human renin hypertension in transgenic rats. *Hypertension* 29:428–437, 1997
21. Luft FC, Mervaala E, Muller D, Gross V, Park J-K, Schmitz C, Lippoldt A, Breu V, Dragun D, Dechend R, Schneider W, Ganten D, Haller H: Hypertension-induced end-organ damage: A new transgenic approach to an old problem. *Hypertension* 33: 212–218, 1999
22. Mervaala E, Muller D, Park J-K, Schmidt F, Breu V, Dragun D, Ganten D, Haller H, Luft F: Monocyte infiltration and adhesion molecules in a rat model of high human renin hypertension. *Hypertension* 33:389–395, 1999
23. Dragun D, Tullius SG, Park JK, Maasch C, Lukitsch I, Lippoldt A, Gross V, Luft FC, Haller H: ICAM-1 antisense oligodesoxynucleotides prevent reperfusion injury and enhance immediate graft function in renal transplantation. *Kidney Int* 54:590–602, 1998
24. Haller H, Maasch C, Dragun D, Wellner M, von Janta-Lipinski M, Luft FC: Antisense oligodesoxynucleotide strategies in renal and cardiovascular disease. *Kidney Int* 53:1550–1558, 1998
25. Mervaala EMA, Muller DN, Park J-K, Schmidt F, Dechend R, Ganten D, Haller H, Luft FC: Calcineurin inhibitors inhibit angiotensin II-induced cardiac hypertrophy. *Hypertension* 35:360–366, 2000
26. Sposito AC, Mansur AP, Coelho OR, Nicolau JC, Ramires JA: Additional reduction in blood pressure after cholesterol-lowering treatment by statins (lovastatin or pravastatin) in hypercholesterolemic patients using angiotensin-converting enzyme inhibitors (enalapril or lisinopril). *Am J Cardiol* 83:1497–1499, A8, 1999
27. Glorioso N, Troffa C, Filigheddu F, Dettori F, Soro A, Pinna Pargaglia P, Collatina S, Pahor M: Effect of the HMG-CoA reductase inhibitors on blood pressure in patients with essential hypertension and primary hypercholesterolemia. *Hypertension* 34: 1281–1286, 1999
28. Hughes AD: The role of isoprenoids in vascular smooth muscle: Potential benefits of statins unrelated to cholesterol lowering. *J Hum Hypertens* 10:387–390, 1996
29. Mervaala EMA, Muller DN, Schmidt F, Park J-K, Gross V, Bader M, Breu V, Ganten D, Haller H, Luft FC: Blood pressure-independent effects in rats with human renin and angiotensinogen genes. *Hypertension* 35:587–594, 2000
30. Linas SL, Whittenburg D, Parsons PE, Repine JE: Ischemia increases neutrophil retention and worsens acute renal failure: Role of oxygen metabolites and ICAM 1. *Kidney Int* 48:1584–1591, 1995
31. Guijarro C, Kim Y, Schoonover CM, Massy ZA, O'Donnell MP, Kasiske BL, Keane WF, Kashtan CE: Lovastatin inhibits lipopolysaccharide-induced NF-kappaB activation in human mesangial cells. *Nephrol Dial Transplant* 1:990–996, 1996
32. Dragun D, Lukitsch I, Tullius SG, Qun Y, Park JK, Schneider W, Luft FC, Haller H: Inhibition of intercellular adhesion molecule-1 with antisense deoxynucleotides prolongs renal isograft survival in the rat. *Kidney Int* 54:2113–2122, 1998
33. Cattell V: Macrophages in acute glomerular inflammation. (editorial) *Kidney Int* 45:945–952, 1994
34. Eddy AA: Experimental insights into the tubulointerstitial disease accompanying primary glomerular lesions. (editorial) *J Am Soc Nephrol* 5:1273–1287, 1994
35. Wheeler DC: Statins and the kidney. *Curr Opin Nephrol Hypertens* 7:579–584, 1998
36. Hobbs AJ, Higgs A, Moncada S: Inhibition of nitric oxide synthase as a potential therapeutic target. *Annu Rev Pharmacol Toxicol* 39: 191–220, 1999
37. Klahr S: The role of l-arginine in hypertension and nephrotoxicity. *Curr Opin Nephrol Hypertens* 7:547–550, 1998
38. Kone BC: Nitric oxide in renal health and disease. *Am J Kidney Dis* 30:311–333, 1997
39. Hecker M, Cattaruzza M, Wagner AH: Regulation of inducible nitric oxide synthase gene expression in vascular smooth muscle cells. *Gen Pharmacol* 32:9–16, 1999
40. Alexander RW: Theodore Cooper Memorial Lecture: Hypertension and the pathogenesis of atherosclerosis: Oxidative stress and the mediation of arterial inflammatory response: A new perspective. *Hypertension* 25:155–161, 1995
41. Guijarro C, Kim Y, Kasiske BL, Massy ZA, O'Donnell MP, Kashtan CE, Keane WF: Central role of the transcription factor nuclear factor-kappa B in mesangial cell production of chemokines. *Contrib Nephrol* 120:210–218, 1997
42. Ruiz-Ortega M, Bustos C, Hernandez-Presa MA, Lorenzo O, Plaza JJ, Egido J: Angiotensin II participates in mononuclear cell recruitment in experimental immune complex nephritis through nuclear factor-kappa B activation and monocyte chemoattractant protein-1 synthesis. *J Immunol* 161:430–439, 1998
43. Shono T, Ono M, Izumi H, Jimi SI, Matsushima K, Okamoto T, Kohno K, Kuwano M: Involvement of the transcription factor NF-kappaB in tubular morphogenesis of human microvascular endothelial cells by oxidative stress. *Mol Cell Biol* 16:4231–4239, 1996
44. Handel ML, Watts CK, Sivertsen S, Day RO, Sutherland RL: D-penicillamine causes free radical-dependent inactivation of activator protein-1 DNA binding. *Mol Pharmacol* 50:501–505, 1996
45. Wilson TW, Alonso-Galicia M, Roman RJ: Effects of lipid-lowering agents in the Dahl salt-sensitive rat. *Hypertension* 31:225–231, 1998
46. Martinez Gonzalez J, Vinals M, Vidal F, Llorente Cortes V, Badimon L: Mevalonate deprivation impairs IGF-I/insulin signaling in human vascular smooth muscle cells. *Atherosclerosis* 135: 213–223, 1997
47. Keane WF: Lipids and progressive renal failure. *Wien Klin Wochenschr* 108:420–424, 1996
48. O'Donnell MP, Kasiske BL, Massy ZA, Guijarro C, Swan SK, Keane WF: Isoprenoids and Ras: Potential role in chronic rejection. *Kidney Int* 52:S29–S33, 1995

3.5.2 Reduktion des Angiotensin II- und Aldosteron-induzierten Endorganschadens durch Lacidipin

Aus den Ergebnissen der dTGR- Behandlung mit MR-Blockern und der ADX-Studie ist zu schließen, dass weitere wirksame Inhibitoren in diesem Tiermodell sowohl Angiotensin II- als auch Aldosteroneffekte beeinflussen. In dieser Studie wurde der Kalzium-Kanal-Blocker Lacidipin untersucht. Kalzium-Kanal-Blocker hemmen den langsamen Kalzium-Einstrom in die Zellen und senken dadurch den peripheren Gefäßwiderstand. dTGR wurden von der 4. bis zur 7. Lebenswoche täglich mit 0,3 bzw. 3 mg/kg/KG Lacidipin behandelt. Während die höhere Lacidipindosis den Blutdruck signifikant senkte, war in der Gruppe, die mit der niedrigeren Dosis behandelt worden war, kaum ein Blutdruck-Unterschied feststellbar. Trotzdem beobachteten wir bei beiden Dosierungen eine deutliche und vergleichbare Nephroprotektion: Sowohl die Albuminurie als auch das Plasma-Kreatinin waren in beiden Behandlungsgruppen signifikant niedriger, verglichen mit den unbehandelten dTGR. Immunhistochemisch ging die Nephroprotektion mit einer reduzierten Expression des Adhäsionsmoleküls ICAM-1, mit weniger infiltrierten Zellen und einer geringeren Aktivität der Transkriptionsfaktoren AP-1 und NF-κB einher.

Schlussfolgerung: Die alleinige Behandlung mit dem Kalzium-Kanal-Blocker Lacidipin schützte im Tiermodell unabhängig von der Blutdrucksenkung vor den Folgen eines aktivierten RAAS. Die Lacidipin-Behandlung reduzierte dabei die Aktivität der für den Endorganschaden zentralen Transkriptionsfaktoren AP-1 und NF-κB.

Reprint 6

Fiebeler A*, Park JK*, Muller DN, Mervaala EM, Dechend R, Abou-Rebyeh F, Luft FC, Haller H. Lacidipine inhibits adhesion molecule and oxidase expression independent of blood pressure reduction in angiotensin-induced vascular injury.

***Hypertension*. 2002;39:685-9.**

Lacidipine Inhibits Adhesion Molecule and Oxidase Expression Independent of Blood Pressure Reduction in Angiotensin-Induced Vascular Injury

Joon-Keun Park, Anette Fiebeler, Dominik N. Muller, Eero M.A. Mervaala, Ralf Dechend, Faikah Abou-Rebyeh, Friedrich C. Luft, Hermann Haller

Abstract—Dihydropyridines can inhibit gene expression in-vitro and may have a protective vascular effect independent of blood pressure reduction. We tested the hypothesis that lacidipine prevents induction of inducible NO synthase (iNOS), influences leukocyte adhesion and infiltration, inhibits nuclear factor (NF)-κB transcription factor activity, and ameliorates end-organ damage in a transgenic rat model of angiotensin (Ang) II–dependent organ sclerosis. We treated rats transgenic for human renin and angiotensinogen (dTGR) from week 4 to 7 with lacidipine (0.3 or 3 mg/kg by gavage). Blood pressure was measured by tail cuff. Organ damage was assessed by histology and immunohistochemistry. Adhesion molecules and cytokines were analyzed by immunohistochemistry. Transcription factors were analyzed by mobility shift assays. Untreated dTGR developed moderate hypertension, cardiac hypertrophy, and severe renal damage with albuminuria. Lacidipine decreased blood pressure slightly at the low dose and substantially at the higher dose. However, both treatments reduced albuminuria and plasma creatinine to the same degree ($P<0.05$). Intercellular adhesion molecule-1 (ICAM-1) was markedly reduced by lacidipine as well as renal neutrophil and monocyte infiltration. Lacidipine reduced mitogen-activated protein (MAP) kinase phosphorylation and iNOS expression in both cortex and medulla. NF-κB and AP-1 were activated in dTGR but reduced by lacidipine. Lacidipine ameliorates Ang II-induced end-organ damage independent of blood pressure lowering, perhaps by inhibiting the MAP kinase pathway and NF-κB activation. **(*Hypertension*. 2002;39[part 2]:685-689.)**

Key Words: Angiotensin II ■ nitric oxide synthase ■ calcium antagonists ■ transcription ■ cell adhesion molecules

Dihydropyridines calcium antagonists ameliorate end-organ damage.[1,2] In a nephrectomy model[3] and in diabetic animals[4] the drugs retarded the progression of glomerular disease and inhibited the development of glomerulosclerosis in experimental hypertension.[5] The beneficial effects are a function of blood pressure reduction. However, dihydropyridines may influence the cellular mechanisms directly.[6–9] In vitro studies provide supportive evidence. For instance, dihydropyridines suppress mesangial cell growth and chemokine expression.[10,11] They also decreased vascular cell infiltrates and expression of adhesion molecules in endothelial cells.[12–14] Dihydropyridines inhibit the activation of the protein kinases in vitro.[15] Calcium signaling may be involved; however, we presented evidence indicating that other signal transduction systems such as protein kinase C are the drug targets.[11,15,16] Thus, dihydropyridines could influence cellular mechanisms of renal damage via the intracellular signaling pathways and reduce the activity of downstream signaling.[2,17–19] To test this hypothesis, we used an angiotensin (Ang) II-dependent transgenic rat model with both human renin and angiotensinogen genes. The rats develop moderate hypertension and severe renal and cardiac damage resulting in 50% mortality at age 7 weeks.[20,21,22]

Methods

All procedures, as outlined elsewhere, were done according to guidelines from the American Physiological Society and were approved by local authorities. The lacidipine dTGR groups (n=10 each) received the drug for 3 weeks by gavage once daily at two doses (0.3 or 3 mg/kg by gavage). Control dTGR (n=10) and SD rats (n=10) received vehicle (1% sodium carboxymethylcellulose). Systolic blood pressure was measured weekly by tail-cuff method under light ether anesthesia 20 hours after the last drug dose. Urine samples were collected over a 24-hour period. Rats were killed at age 7 weeks. The kidneys and hearts were washed with ice cold saline, blotted dry, and weighed. For immunohistochemistry, western blot, and analysis of nuclear factor (NF)-κB and AP-1, the tissues were snap-frozen in liquid nitrogen, for immunohistochemistry in isopentane (−35°C), and stored at −80°C. Our histology, immunohistochemistry, Western blotting analyses, and electrophoretic mobility shift assay techniques have been described in detail elsewhere.[23,24]

Received September 24, 2001; first decision November 7, 2001; revision accepted November 26, 2001.

Department of Nephrology, Medical School Hannover (J-K.P., A.F., F.A-R., H.H.), Germany; Franz Volhard Clinic, Medical Faculty of the Charité, Humboldt University of Berlin (D.N.M., R.D., F.C.L.), Germany; Institute of Biomedicine, University of Helsinki (E.M.A.M.), Finland.

J.-K.P. and A.F. contributed equally to this work.

Correspondence to Hermann Haller, MD, Medizinische Hochschule Hannover, Abt. Nephrologie, Carl-Neuberg-Straße 1, 30625 Hannover, Germany. E-mail haller.hermann@mh-hannover.de

Hypertension **is available at http://www.hypertensionaha.org**

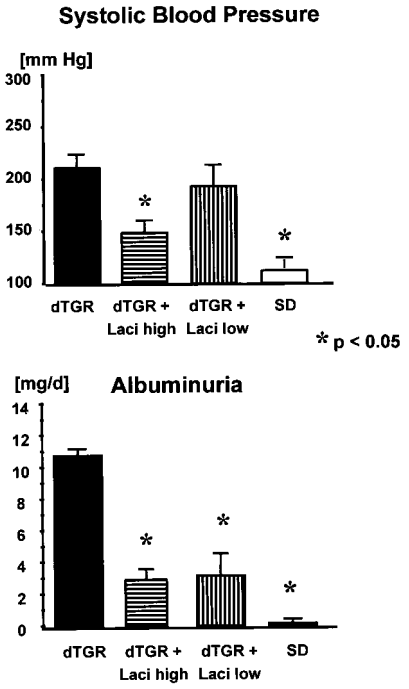

Figure 1. Systolic blood pressure in dTGR, dTGR treated with a high and a low dose of lacidipine, and SD rats (top). Twenty-four–hour urinary albumin excretion in dTGR, dTGR treated with lacidipine, and SD rats (bottom). Results are expressed as mean±SEM of 10 animals per group.

Data are presented as means±SEM. Statistically significant differences in mean values were tested by ANOVA and the Tukey multiple range test. A value of $P<0.05$ was considered statistically significant. The data were analyzed using SYSTAT® statistical software (SYSTAT Inc).

Results

Lacidipine was given at two dosages 0.3 mg/kg body (low lacidipine group) or 3 mg/kg body weight (high lacidipine group). Systolic blood pressure in the untreated transgenic animals at week 7 was 203±11 mm Hg, compared with 108±3 mm Hg in the wild-type SD control animals. Lacidipine in the high treatment group lowered blood pressure by 54% to 149±7 mm Hg ($P<0.001$) compared with the untreated group) as shown in Figure 1 (top). In contrast, treatment in the low lacidipine group lowered blood pressure by only 9% to 185±10 mm Hg ($P<0.05$) compared with the untreated group). The difference in blood pressure between the two groups was 36±14 mm Hg ($P<0.05$). Despite the significant difference in blood pressure between the two treatment groups, the lower dose of lacidipine showed the same effect on albumin excretion as the higher lacidipine (bottom). Albuminuria in the untreated transgenic animals was 11±0.2 mg/d compared with 0.3±0.01 mg/d in the SD controls ($P<0.01$). Lacidipine decreased albumin excretion to 3.1±0.2 mg/d in the low treatment group and to 3.6±0.03 mg/d in the high lacidipine group.

Vehicle-treated dTGR had severe renal damage with focal necrosis, and a 50% mortality at 7 weeks. Small vessels showed increased intimal and medial thickness as well as hyaline deposits. The renal tubules were frequently swollen and filled with proteinaceous material. Treatment with lacidipine prevented vascular injury in small renal vessels and extracellular matrix formation (data not shown). The beneficial effects of lacidipine were observed with both concentrations of lacidipine.

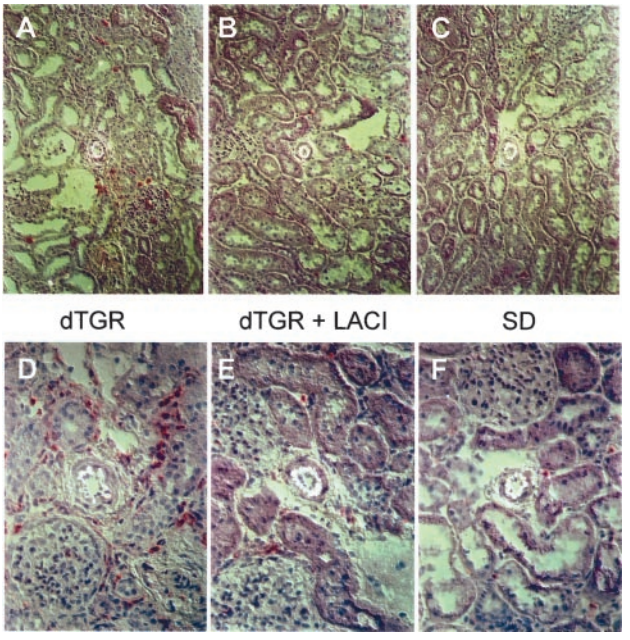

Figure 2. Representative immunohistochemical photomicrographs of neutrophils (HIS 48; top panels) and ED-1 positive monocytic cells (bottom panels) in the kidneys of dTGR, dTGR treated with lacidipine, and SD rats (positive cells are shown in red).

We quantitated the effects of lacidipine on neutrophils and monocytes as shown in Figure 2. Monocytes were present in the perivascular space and between the tubules. In contrast, granulocytes were mostly seen within the glomeuli and, to a lesser extent, in perivascular areas. Treatment with lacidipine prevented cell infiltration almost completely and only a few neutrophils were observed within glomeruli. Lacidipine had also an inhibitory effect on monocyte infiltration. Semiquantitative cell count analysis confirmed the significant reduction of both neutrophil and mononuclear cell infiltration after lacidipine treatment in kidney ($P<0.01$).

We next investigated the effect of lacidipine on the expression of adhesion molecules, as shown in Figure 3 (top panels). Intercellular adhesion molecule-1 (ICAM-1) expression in the kidney was increased in the intima, adventitia, and in the perivascular space of the small vessels in untreated dTGR. Glomeruli and tubules showed increased ICAM-1 expression. The ICAM-1 was significantly reduced by treatment with lacidipine at both doses. In contrast to ICAM-1 expression, vascular cell adhesion molecule-1 (VCAM-1) was mostly observed in the intima of arterioles and, to a lesser extent in the glomerular vascular poles, as well as in the peritubular capillaries (data not shown). As in the case of ICAM-1, treatment with lacidipine prevented the upregulation of VCAM-1 at both doses.

We next investigated the effects of lacidipine on iNOS expression as shown in Figure 3 (lower panels). We observed

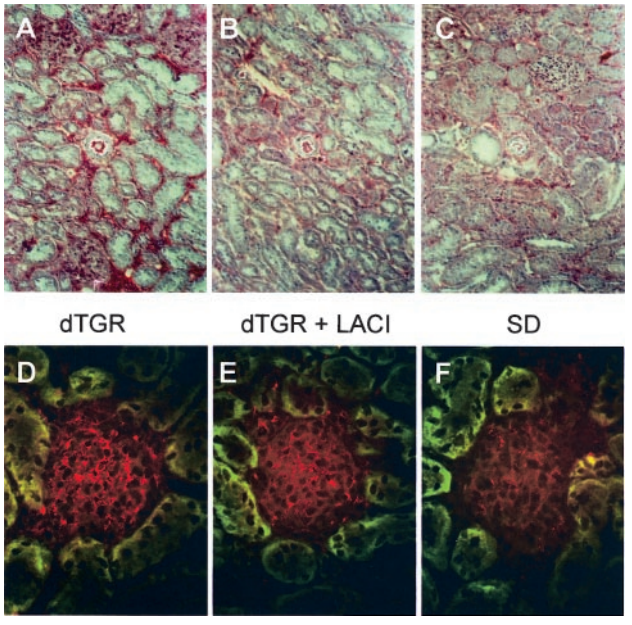

Figure 3. Representative immunohistochemical photomicrographs of ICAM-1 (top panels) and iNOS (bottom panels) in the kidney of dTGR and lacidipine-treated dTGR.

a strongly increased expression in the glomeruli and in the vessel wall of renal arterioles from dTGR. Treatment with lacidipine greatly reduced the iNOS immunoreactivity both in the blood vessels and the glomeruli at both doses.

Since matrix expression is involved in scarring, we analyzed the effects of lacidipine on the expression of collagen IV and fibronectin. In untreated dTGR, collagen IV was observed in the peritubular space, as shown in Figure 4.

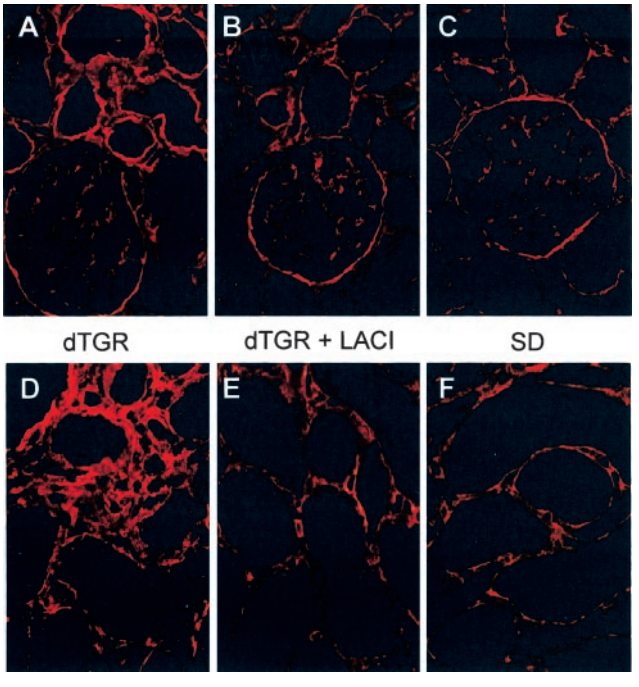

Figure 4. Representative immunohistochemical photomicrographs of collagen IV (top panels) and fibronectin (bottom panels) of kidneys from dTGR, lacidipine-treated, and SD rats.

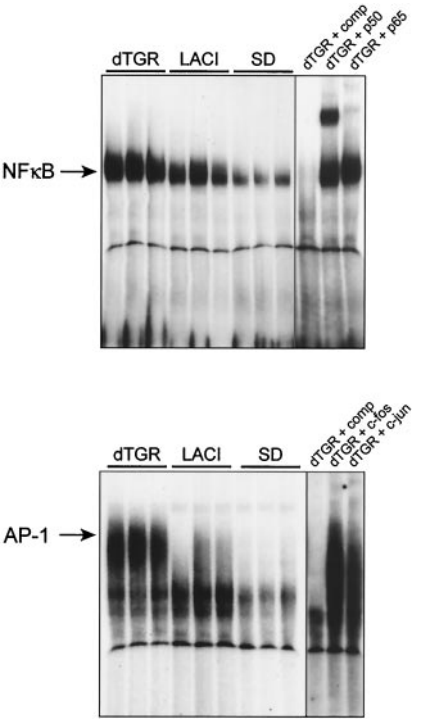

Figure 5. EMSA for NF-κB (top) and AP-1 (bottom) before and after treatment with lacidipine.

Treatment with lacidipine at both doses prevented the increased expression of collagen IV almost completely, and no significant difference between the lacidipine-treated animals and the SD control animals was observed at week 7. We also observed an increased expression of fibronectin in the renal interstitium. Lacidipine reduced the increased expression of fibronectin significantly at both doses.

We studied MAP kinase activation by using specific antibodies that only detect the phosphorylated, active form of the enzyme (p-ERK). In untreated dTGR, phosphorylated MAP kinase was increased in the glomeruli and in the peritubular space (data not shown). A similar increase was also present in the medulla. Treatment with lacidipine at either dose abolished this staining pattern both in the cortex and in the medulla.

We next analyzed the activation of the transcription factors NF-κB and AP-1 since both regulate ICAM-1 and iNOS gene expression, as shown in Figure 5. Both, NF-κB and AP-1 showed greatly increased activity in the kidneys of dTGR compared with SD rats. Lacidipine-treatment reduced the increased levels of NF-κB and AP-1 activity. This effect was evident at either dose.

Discussion

We tested the hypothesis that the lipophilic calcium antagonist lacidipine ameliorates renal failure and inhibits inflammatory changes independent of its blood pressure-lowering activities. We used a transgenic animal model of angiotensin II-mediated organ damage and analyzed the effects of lacidipine on adhesion molecule expression, cell infiltration, iNOS expression, and matrix molecule expression. In addition, we investigated whether specific intracellular signaling

pathways are influenced by lacidipine. We showed that lacidipine reduces NF-κB activation, prevents inflammatory responses, and altogether ameliorates renal damage. Our animal model features hypertension, albuminuria, severe inflammatory changes with renal damage and focal necrosis, and a 50% mortality at 7 weeks.[20] We have previously demonstrated that Ang II is responsible for these effects.[21] Our findings strongly suggest that lacidipine influences the angiotensin-induced cellular mechanisms directly in a blood pressure-independent manner.

Chronic treatment with a high dosage of lacidipine led to a decrease in blood pressure compared with animals treated with a lower concentration of the dihydropyridine. The decrease in blood pressure with lacidipine may have contributed to the reno-protective effect of the dihydropyridine. However, we do not believe that the blood pressure lowering effect of lacidipine had a major effect because effective antihypertensive treatment by hydralazine, reserpine, and hydrochlorothiazide in our model only partially prevented tissue damage and did not reduce inflammation.[22]

Treatment with the calcium antagonist lacidipine inhibited the inflammatory process in our animal model considerably. Lacidipine almost abolished neutrophil infiltration. We have previously shown that the specific inhibition of ICAM-1 prevents leukocyte infiltration in the kidney thus ameliorating tissue injury.[23,24] Neutrophils are important mediators of injury in many inflammatory diseases.[25,26] The prevention of neutrophil infiltration by lacidipine may partially explain the anti-inflammatory effects of dihydropyridines in our model. Furthermore, lacidipine inhibited the expression of the endothelial cell adhesion molecule ICAM-1. Because ICAM-1 is responsible for the neutrophil adhesion to the endothelium and subsequent infiltration,[25] it is most likely that lacidipine inhibited neutrophil infiltration via inhibition of ICAM-1. This assumption is supported by earlier findings from Cominacini and coworkers that lacidipine inhibits the ICAM-1 expression in endothelial cells in vitro.[13,16] Others have also demonstrated that dihydropyridines affect directly cell infiltration and macrophage activation in vivo.[27–29] We have recently shown that dihydropyridines also lead to down-regulation of ICAM-1 and VCAM and influence endothelial cell permeability.[30,31]

We also demonstrated that monocyte infiltration was reduced by lacidipine. Several reports have demonstrated the participation of monocyte/macrophages in the onset and progression of various renal diseases.[32] Since monocytes play a role in long-term pathological changes and chronic renal failure and have been associated with matrix accumulation and fibrosis,[33] our findings may implicate that lacidipine has a direct influence on these processes. It has recently been shown that dihydropyridines improve long-term outcome in renal transplantation,[34] and the positive effect of lacidipine on chronic vascular changes in the kidney may partially be due to its direct effects on monocyte/neutrophil infiltration.

Lacidipine greatly reduced iNOS expression in the dTGR. Nitric oxide (NO) regulates numerous physiological processes, including smooth muscle contractility, platelet reactivity, and the cytotoxic activity of leukocytes. Because of the ubiquitous nature of NO, inappropriate release of this mediator has been linked to the pathogenesis of a number of disease states.[35] While NO serves beneficial roles as a messenger and host defense molecule, excessive NO production can be cytotoxic. The result of NO's reaction with reactive oxygen and nitrogen species, leads to peroxynitrite anion formation, protein tyrosine nitration, and hydroxyl radical production. NO may contribute to the evolution of several commonly encountered renal diseases, including immune-mediated glomerulonephritis, postischemic renal failure, radiocontrast nephropathy, obstructive nephropathy, and acute and chronic renal allograft rejection.[36] NO synthase inhibitors are potentially beneficial in the treatment of conditions associated with an overproduction of NO, including inflammation.[37,38] It is therefore likely that the inhibition of the increased NO expression by lacidipine plays an important role in the anti-inflammatory effect of this compounds.

Lacidipine reduced the increased activity of the transcription factors NF-κB and AP-1 considerably. NF-κB is the main factor in the transcription of NOS, ICAM-1 and VCAM-1 and lacidipine could influence expression of these molecules through inhibition of NF-κB.[39] Cominachini and coworkers have previously shown that lacidipine inhibits lipopolysaccharide-induced NF-κB activation in human mesangial cells in vitro.[16] Activation of NF-κB could occur through several mechanims. Ruiz-Ortega et al showed that ANG II stimulated NF-κB in mesangial cells and that activation of NF-κB in the renal cortex was reduced by ACE inhibition.[40] Another possibility is the activation of NF-κB through oxygen free radicals. Reactive oxygen species represent an important signal transduction pathway inside the cell and also participate in the expression of adhesion molecules on the endothelial cells.[41,42] Our results indicate that dihydropyridines interfere with the MAP kinase activation proximal of NF-κB activation.

Mostly, the effects of dihydropyridines have been explained via their inhibitory effects on the L-type calcium channel. Recently, several other hypotheses have been postulated. We have observed an inhibitory effect of calcium antagonists on protein kinase C activity without any change in intracellular free calcium concentration.[19] The calcium antagonist-mediated effects on gene expression were observed at pharmacological concentrations that are one to two orders of magnitude lower than those required for inhibition of depolarization-induced opening of voltage sensitive L-type calcium channels. Similar observations have been made by other groups.[11,19] Recently, Orth et al investigated the effects of calcium antagonists in mesangial cells and could not associate the observed inhibitory effects on cell proliferation with changes in intracellular calcium.[12]

In summary, we have shown that the dihydropyridine lacidipine ameliorates angiotensin II–induced renal disease independent of its blood pressure lowering effect. In a model of severe organ damage with endothelial cell activation, leukocyte infiltration and sclerosis, we observed an inhibitory effect of lacidipine on adhesion molecule expression, leukocyte infiltration, iNOS activation and matrix molecule expression. We could also demonstrate that intracellular pathways such as MAP kinase and activation of transcription factors were influenced by lacidipine. It remains open whether the

observed effects are mediated by calcium channel inhibition or whether other cellular effector mechanisms play a role in the beneficial therapeutic effect of lacidipine.

Acknowledgments

This study was supported by a grant-in-aid from Boehringer-Ingelheim., Germany. We thank Professor Gaviraghi from Glaxo-Wellcome for the compound and critical advice during the study. E.M. was supported by the Alexander von Humboldt Foundation, the Klinisch-pharmakologischer Verbund Berlin-Brandenburg, the Finnish Foundation for Cardiovascular Research, and the Academy of Finland. Ms Christel Lipka and Ms Mathilde Schmidt gave expert technical assistance.

References

1. Epstein M. Calcium antagonists and renal disease. *Kidney Int*. 1998;54: 1771–1784.
2. Haller H. Calcium antagonists and cellular mechanisms of glomerulosclerosis and atherosclerosis. *Am J Kidney Dis*. 1993;21:26–31.
3. Hamaguchi A, Kim S, Wanibuchi H, Iwao H. Angiotensin II and calcium blockers prevent glomerular phenotypic changes in remnant kidney model. *J Am Soc Nephrol*. 1996;7:687–693.
4. Miric G, Dallemagne C, Endre Z, Margolin S, Taylor SM, Brown L. Reversal of cardiac and renal fibrosis by pirfenidone and spironolactone in streptozotocin-diabetic rats. *Br J Pharmacol*. 2001;133:687–694.
5. Sabbatini M, Vitaioli L, Baldoni E, Amenta F. Nephroprotective effect of treatment with calcium channel blockers in spontaneously hypertensive rats. *J Pharmacol Exp Ther*. 2000;294:948–954.
6. Blaheta RA, Hailer NP, Brude N, Wittig B, Oppermann E, Leckel K, Harder S, Scholz M, Weber S, Encke A, Markus BH. Novel mode of action of the calcium antagonist mibefradil (Ro 40–5967): potent immunosuppression by inhibition of T-cell infiltration through allogeneic endothelium. *Immunology*. 1998;94:213–220.
7. Schiffrin EL. Small artery remodeling in hypertension: can it be corrected? *Am J Med. Sci*. 2001;322:7–11.
8. Nayler WG. Calcium channels and their involvement in cardiovascular disease. *Biochem Pharmacol*. 1992;43:39–46.
9. Moreyra AE, Gelpi RJ, Mosca SM, Cingolani HE. Chronic administration of nicardipine attenuates myocardial stunning in isolated rabbit hearts. *J Mol Cell Cardiol*. 1994;26:979–984.
10. Orth SR, Nobiling R, Bonisch S, Ritz E. Inhibitory effect of calcium channel blockers on human mesangial cell growth: evidence for actions independent of L-type Ca2+ channels. *Kidney Int*. 1996;49:868–879.
11. Roth M, Keul R, Emmons LR, Horl WH, Block LH. Manidipine regulates the transcription of cytokine genes. *Proc Natl Acad Sci U S A*. 1992;89: 4071–4075.
12. Alexander JJ, Miguel R, Piotrowski JJ. The effect of nifedipine on lipid and monocyte infiltration of the subendothelial space. *J Vasc Surg*. 1993;17:841–847.
13. Cominacini L, Pasini AF, Pastorino AM, Garbin U, Davoli A, Rigoni A, Campagnola M, Tosetti ML, Rossato P, Gaviraghi G. Comparative effects of different dihydropyridines on the expression of adhesion molecules induced by TNF-alpha on endothelial cells. *J Hypertens*. 1999;17: 1837–1841.
14. Bellosta S, Bernini F. Lipophilic calcium antagonists in antiatherosclerotic therapy. *Curr Atheroscler Rep*. 2000;2:76–81.
15. Hempel A, C. Maasch U, Heintze C, Lindschau R, Dietz FC, Luft, and H. Haller. High glucose concentrations increase endothelial cell permeability via activation of protein Kinase C alpha. *Circ Res*. 1997;81:363–371.
16. Cominacini L, Garbin U, Fratta Pasini A, Paulon T, Davoli A, Campagnola M, Marchi E, Pastorino AM, Gaviraghi G, Lo Cascio V. Lacidipine inhibits the activation of the transcription factor NF-kappaB and the expression of adhesion molecules induced by pro-oxidant signals on endothelial cells. *J Hypertens*. 1997;15:1633–1640.
17. Matsumori A, Nunokawa Y, Sasayama S. Nifedipine inhibits activation transcription factor NF-κB. *Life Sci*. 2000;67:2655–2661.
18. Hayashi M, Yamaji Y, Nakazato Y, Saruta T. The effects of calcium channel blockers on nuclear factor kappa B activation in the mesangium cells. *Hypertens Res*. 2000;23:521–525.
19. Block LH, Emmons LR, Vogt E, Sachinidis A, Vetter W, Hoppe J. Ca2+-channel blockers inhibit the action of recombinant platelet-derived growth factor in vascular smooth muscle cells. *Proc Natl Acad Sci U S A*. 1989;86:2388–2392.
20. Bohlender J, Fukamizu A, Lippoldt A, Nomura T, Dietz R, Menard J, Murakami K, Luft F, Ganten D. High human renin hypertension in transgenic rats. *Hypertension*. 1997;29:428–437.
21. Luft F, Mervaala E, Muller D, Gross V, Park J-K, Schmitz C, Lippoldt A, Breu V, Dragun D, Dechend R, Schneider W, Ganten D, Haller H. Hypertension-induced end-organ damage: a new transgenic approach to an old problem. *Hypertension*. 1999;33:212–218.
22. Mervaala E, Muller DN, Schmidt F, Park JK, Gross V, Bader M, Breu V, Ganten D, Haller H, Luft FC. Blood pressure-independent effects in rats with human renin and angiotensinogen genes. *Hypertension*. 2000;35: 587–594.
23. Dragun D, Tullius SG, Park J-K, Maasch C, Lukitsch I, Lippoldt A, Gross V, Luft FC, Haller H. ICAM-1 antisense oligodesoxynucleotides prevent reperfusion injury and enhance immediate graft function in renal transplantation. *Kidney Int*. 1998;54:590–602.
24. Haller H, Maasch C, Dragun D, Wellner M, von Janta-Lipinski M, Luft FC. Antisense oligodesoxynucleotide strategies in renal and cardiovascular disease. *Kidney Int*. 1998;53:50–58.
25. Brady HR. Leukocyte adhesion molecules: potential targets for therapeutic intervention in kidney diseases. *Curr Opin Nephrol Hypertens* 1993;2:171–182.
26. Linas SL, Whittenburg D, Parsons PE. Repine JE: Ischemia increases neutrophil retention and worsens acute renal failure: role of oxygen metabolites and ICAM 1. *Kidney Int*. 1995;48:1584–1591.
27. Donetti E, Fumagalli R, Paoletti R, Soma MR. Direct antiatherogenic activity of isradipine and lacidipine on neointimal lesions induced by perivascular manipulation in rabbits. *Pharmacol Res*. 1997;35:417–422.
28. Corsini A, Accomazzo MR, Canavesi M, Sartani A, Testa R, Catapano AL, Fumagalli R, Paoletti R, Bernini F. The new calcium antagonist lercanidipine and its enantiomers affect major processes of atherogenesis in vitro: is calcium entry involved? *Blood Press Suppl*. 1998;2:18–22.
29. Hailer NP, Blaheta RA, Harder S, Scholz M, Encke A, Markus BH. Modulation of adhesion molecule expression on endothelial cells by verapamil and other Ca++ channel blockers. *Immunobiology*. 1994;15: 38–51.
30. Haller H, Lindschau C, Quass P, Luft FC. Low-density lipoprotein induces vascular adhesion molecule expression on human endothelial cells. *Hypertension*.1995:511–516.
31. Haller H. Endothelial function. General considerations. *Drugs*. 1997; 53(suppl 1):1–10.
32. Cattell V. Macrophages in acute glomerular inflammation. *Kidney Int*. 1994;45:945–952.
33. Eddy AA. Experimental insights into the tubulointerstitial disease accompanying primary glomerular lesions. *J Am Soc Nephrol*. 1994;5: 1273–1287.
34. Rodicio JL. Calcium antagonists and renal protection from cyclosporine nephrotoxicity: long-term trial in renal transplantation patients. *J Cardiovasc Pharmacol*. 2000;35(3 suppl 1):S7–S11.
35. Hobbs AJ, Higgs A, Moncada S. Inhibition of nitric oxide synthase as a potential therapeutic target. *Annu Rev Pharmacol Toxicol*. 1999;39: 191–220.
36. Klahr S. The role of L-arginine in hypertension and nephrotoxicity. *Curr Opin Nephrol Hypertens* 1998;7:547–550.
37. Kone BC. Nitric oxide in renal health and disease. *Am J Kidney Dis*. 1997;30:311–333.
38. Hecker M, Cattaruzza M, Wagner AH. Regulation of inducible nitric oxide synthase gene expression in vascular smooth muscle cells. *Gen Pharmacol*. 1999;32:9–16.
39. Alexander RW. Theodore Cooper Memorial Lecture. Hypertension and the pathogenesis of atherosclerosis. Oxidative stress and the mediation of arterial inflammatory response: a new perspective. *Hypertension*. 1995; 25:155–161.
40. Ruiz-Ortega M, Bustos C, Hernandez-Presa MA, Lorenzo O, Plaza JJ, Egido J. Angiotensin II participates in mononuclear cell recruitment in experimental immune complex nephritis through nuclear factor-kappa B activation and monocyte chemoattractant protein-1 synthesis. *J Immunol*. 1998;161:430–439.
41. Shono T, Ono M, Izumi H, Jimi SI, Matsushima K, Okamoto T, Kohno K, Kuwano M. Involvement of the transcription factor NF-kappaB in tubular morphogenesis of human microvascular endothelial cells by oxidative stress. *Mol Cell Biol*. 1996;16:4231–4239.
42. Handel ML, Watts CK, Sivertsen S, Day RO, Sutherland RL. D-penicillamine causes free radical-dependent inactivation of activator protein-1 DNA binding. *Mol Pharmacol*. 1996;50;501–505.

3.6 Renin-Angiotensin-Aldosteron-System im Gas6-/Axl-Weg

3.6.1 Stimulierung der Synthese von Gas6 und Axl durch Angiotensin II und Aldosteron in vitro

Bereits 1999 wurde von Melaragno gezeigt, dass Angiotensin II die Synthese der Rezeptortyrosinkinase Axl und ihrem Liganden Gas6 stimuliert. Wir untersuchten, ob die NADPH-Oxidase für diese Angiotensin II-induzierte Synthesesteigerung wichtig ist, und zeigten, dass sowohl die Untereinheit p22phox als auch p47phox für die Synthese von Axl und Gas6 funktionieren müssen. Neuere eigene Ergebnisse belegen, dass auch Aldosteron eine Neusynthese von Axl und Gas6 vermittelt (**Abb. 13**).

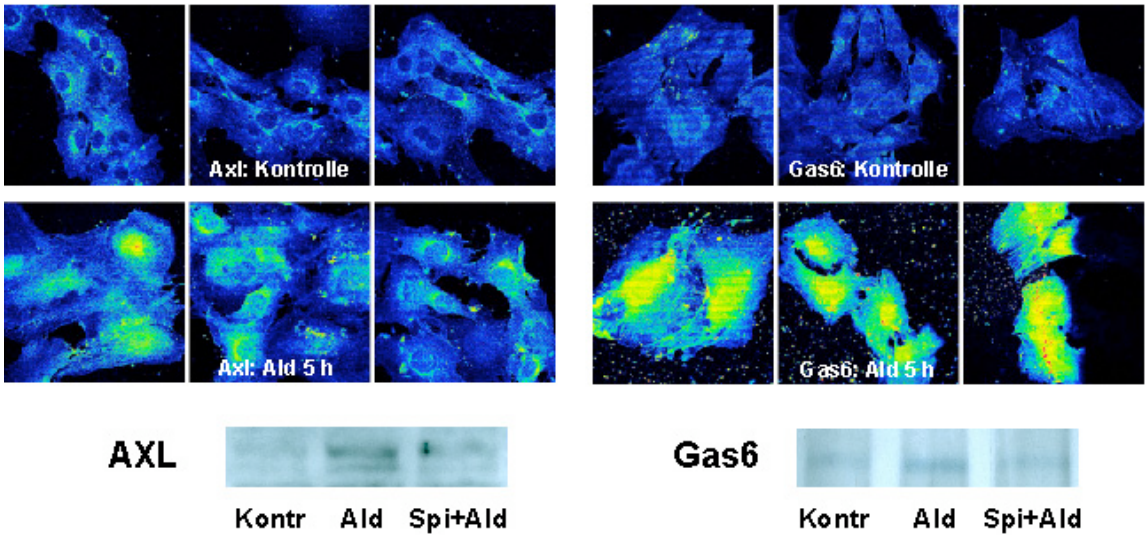

Abbildung 13: Axl und Gas6-Expression in glatten Muskelzellen; Glatte Muskelzellen aus der Aorta von NMRI-Mäusen wurden mit Aldosteron (Ald; 10^{-9}M) für 5 Stunden stimuliert; Oben ist die Proteinexpression von Kontrollen und Aldosteron-stimulierten Zellen mittels Immunhistochemie gezeigt. Unten sieht man einen Westernblot mit der Proteinexpression vor (Kontrolle) und 5 Stunden nach Stimulation und in Gegenwart von Spironolakton (Spi, 10^{-6}M).

3.6.2 Gas6 und Axl als zentrale Mittlerproteine bei verschiedenen Nierenerkrankungen

Wir konnten zeigen, dass in Nieren von unbehandelten dTGR die Proteine Gas6 und Axl im Vergleich zu Losartan-behandelten dTGR überexprimiert sind (**Abb. 14**).

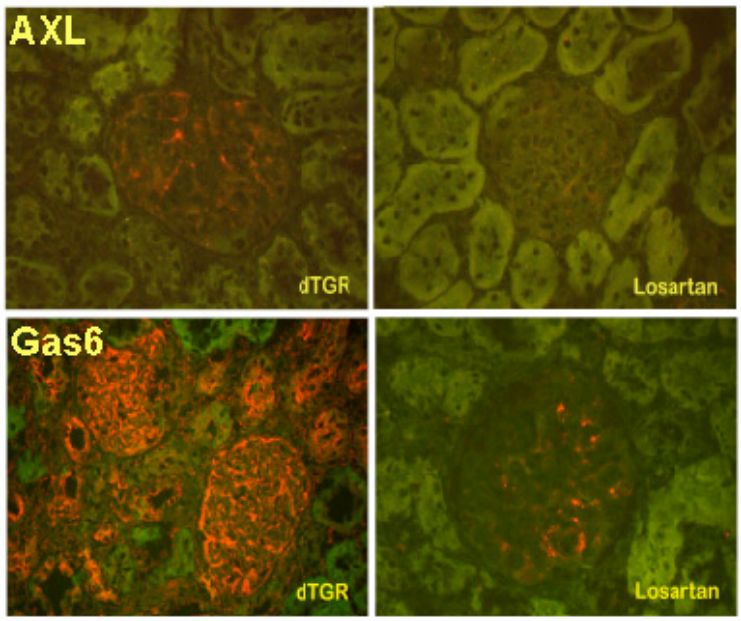

Abbildung 14. Axl- und Gas6-Expression in der Niere von dTGR und Losartan-behandelten dTGR. Expression von Axl und Gas6 in Nieren von 7 Wochen alten dTGR und dTGR, welche von der 4. bis zur 7. Woche mit Losartan behandelt wurden.

Das RAAS wird bei verschiedenen Nierenerkrankungen lokal aktiviert. Ein grundsätzlicher Therapieansatz zur Reduktion der Proteinurie unabhängig von ihrer Genese besteht in der Blockade der Angiotensin II-Wirkung. Wir verglichen humane Nierenbiopsien von Patienten mit verschiedenen Nierenerkrankungen (IgA-Nephropathie, akute Lupusnephritis, ANCA-assoziierte Nephritis, akute vaskuläre Rejektion) mit gesunden Nieren auf die Expression von Axl und Gas6. Die Axl- und Gas6-Überexpression trat unabhängig von der Grundkrankheit bei allen akuten

Nierenerkrankungen im Gefäßsystem, in den Glomeruli und in den distalen Tubuli auf.

Schlussfolgerung: Der Signalweg von Axl und Gas6 wird bei akuten Nierenerkrankungen aktiviert. Das RAAS und eine funktionstüchtige NADPH-Oxidase sind für die Regulation von Axl und Gas6 *in vitro* entscheidend. Aldosteron stimuliert wie Angiotensin II die Synthese der Rezeptortyrosinkinase Axl und ihres Liganden Gas6. Diese krankheits- unspezifische Expressionsregulation ist möglicherweise ein Hinweis auf einen weiteren wichtigen Signalweg in der Entwicklung von Nierenerkrankungen und kommt damit für eine therapeutische Intervention in Frage.

Reprint 7

Fiebeler A, Park JK, Muller DN, Lindschau C, Mengel M, Merkel S, Banas B, Luft FC, Haller H. Growth arrest specific protein 6/Axl signaling in human inflammatory renal diseases.

***Am J Kidney Dis*. 2004;43:286-95.**

Growth Arrest Specific Protein 6/Axl Signaling in Human Inflammatory Renal Diseases

Anette Fiebeler, MD, Joon-Keun Park, PhD, Dominik N. Muller, PhD, Carsten Lindschau, PhD, Michael Mengel, MD, Saskia Merkel, MD, Bernhard Banas, MD, Friedrich C. Luft, MD, and Hermann Haller, MD

• ***Background:*** **Growth arrest-specific gene 6 (Gas6) and its binding partner, the receptor tyrosine kinase Axl, are important mediators in experimental nephritis. The authors tested whether the Gas6/Axl signaling pathway participates in human renal diseases.** ***Methods:*** **The authors compared 26 human renal specimens from patients with IgA nephritis, acute diffuse immune complex glomerulonephritis, acute lupus nephritis, antineutrophil cytoplasmic antibody—associated glomerulonephritis, acute transplant rejection, and normal renal tissue. Because reactive oxygen species are pivotal in inflammation, the authors tested whether the Axl/Gas6 expression is influenced by NADPH oxidase in vitro.** ***Results:*** **Gas6 and Axl immunofluorescence was barely detectable in normal kidney. However, in disease Axl was copiously expressed in the small vessel media, glomeruli, distal tubules, and collecting ducts. Similarly, Gas6 was upregulated in the small vessel intima and media, all segments of the renal tubules, the brush border, and glomeruli. Gas6 and Axl upregulation was a prominent but nonspecific finding in these renal diseases. Cultured rat vascular smooth muscle cells and immortalized human mesangial cells were stimulated with angiotensin (Ang) II (1×10^{-7} mol/L) for 6 or 18 hours. Confocal microscopy and Western blot showed Ang II–dependent Gas6 and Axl expression. An antisense probe against the p22 phox unit of NADPH-oxidase suppressed Ang II–induced Gas6 and Axl expression. In addition, in p47 phox knockout cells Ang II–induced Gas6 and Axl expression were blocked.** ***Conclusion:*** **GAS6/Axl signaling is involved in human renal disease. The Ang II–induced Gas6 and Axl expression may be dependent on NADPH-oxidase. Gas6 and Axl are important signaling molecules in human renal disease and may be potential therapeutic targets.** ***Am J Kidney Dis*** **43:286-295.**

INDEX WORDS: Gas6; angiotensin; kidney; signal transduction; NADPH oxidase.

THE ABBREVIATION "Axl" comes from the Greek word *anexelekto* "the uncontrolled." The molecule, also known as *Ark, Ufo,* and *Tyro7,* was initially isolated from 2 patients with chronic myelogenous leukemia and is expressed in monocytes and myeloic leukemias.[1-3] Together with Sky (also named *Rse, Brt, Tif, Dtk, Etk, Tyro3*) and Mer, Axl belongs to a group of 3 structurally related receptor tyrosine kinases. In triple knockout mice deficient in all 3 kinases, severe autoaggressive states are observed. The growth arrest specific protein 6 (Gas6) is a ligand for Axl, Sky, and Mer. Gas6 is structurally related to protein S and is a vitamin K–dependent protein.[4] Gas6 was identified as an upregulated protein in serum-starved NIH 3T3 cells.[5,6] Similarly, ip-E1A cells are protected from serum deprivation–induced apoptosis when they overexpress Axl.[7] Both Gas6 and Axl promote cell survival in different cell types. Recently, Gas6 and Axl were shown to be upregulated in an animal model of anti-Thy1–induced glomerulonephritis. Injection of the extracellular domain of Axl conjugated with the Fc portion of human IgG1 (Axl-Fc) abolished the typical glomerular changes of Thy1 glomerulonephritis.[8] In addition, Gas6 was found to be overexpressed in a rat model of renal transplantation.[9] Even more compelling are recent findings showing that Gas6 gene–disrupted mice are resistant to nephrotoxic nephritis.[10] When these mice are outfitted with recombinant wild-type Gas6, the propensity for nephrotoxic nephritis is restored. These observations suggest that Axl/Gas6 signaling plays a fundamental role in inflammatory renal disease. However, the relevance of this signaling path-

From the Helios Klinikum-Berlin, Franz Volhard Clinic at the Max Delbrück Center, Medical Faculty of the Charité, Humboldt University of Berlin, Berlin; the Department of Pathology and Internal Medicine-Nephrology, Hannover University Medical School, Hannover; and the Department of Internal Medicine-Nephrology, University Medical School, Regensburg, Germany.

Received July 7, 2003; accepted in revised form October 20, 2003.

A.F. and J.-K.P. contributed equally to this article.

Address reprint requests to Anette Fiebeler, MD, HELIOS Clinic Berlin, Franz Volhard Clinic at the Max Delbrueck Center, Wiltberg Str. 50, 13125 Berlin, Germany. E-mail: fiebeler@fvk-berlin.de

0272-6386/04/4302-0005$30.00/0

doi:10.1053/j.ajkd.2003.10.016

way to various human renal diseases is unknown. We performed a biopsy study of human renal diseases. We found that GAS6/Axl is an early disease mediator. To elucidate possible common mechanisms, we also performed in vitro studies involving angiotensin (Ang) II-induced NADPH oxidase stimulation.

METHODS

Renal Specimens

Human renal specimens were obtained from paraffin-embedded samples taken for diagnostic procedures and collected in the pathology department of the Hannover University School of Medicine. Patients were selected randomly according to typical clinical presentation and the pathologic findings in the renal biopsy at the time of their diagnosis. Samples from patients with various forms of glomerulonephritis, vasculitis, and posttransplant rejection were selected. Normal human renal tissue was obtained from kidneys harboring malignant tumors. Immunohistochemical studies were performed as described earlier.[11] Antibodies were purchased against Axl and Gas6 (Santa Cruz), secondary AB double antigoat-Cy 3.

Cell Culture

Vascular smooth muscle cells (VSMCs) from rat and mouse aorta preparations (homozygous p47phox-/- mice and control mice were a gift from Dr Steven M. Holland at National Institutes of Health) or immortalized human mesangial cells (MCs) were grown on coverslips and stimulated with Ang II 10^{-7} mol/L for 6 hours as outlined earlier.[12] After fixation with 4% paraformaldehyde (10 minutes) and permeabilization with methanol, the cells were stained for Axl and Gas6. For antisense experiments, cells were incubated in serum-free medium for 12 hours and then transfected with oligonucleotides for 24 hours. The sequences were as follows: antisense 5′ GAT CTG CCC CAT GGT GAG GAC C3′; sense 5′ GGT CCT CAC CAT GGG GCA GAT C3′; scramble 5′CCG ACG TGG ATA CGG CTC ACT G′. After medium change, cells were stimulated with Ang II 10^{-7} mol/L for 6 hours.

Immunohistochemistry

Confocal microscopy was performed as described earlier.[12] At least 50 to 80 cells from each of at least 3 experiments were examined under each experimental condition. Examination was conducted by 2 different investigators on a blinded basis, without knowledge of the origin of the specimens. Quantification was done with histogram function in the MRC laser sharp software. The subcellular regions were outlined manually, and the calculated mean fluorescence intensity was obtained for the delineated regions. Data are presented as the mean fluorescence intensity in the respective cell area.

RESULTS

Expression of Axl and Gas6 in Human Renal Tissue

Tissue from 23 individuals was included in the study. Table 1 summarizes the clinical and pathologic findings. Normal specimens from patients undergoing nephrectomy for malignant tumors served as controls.

Figures 1 and 2 show representative photomicrographs from normal and diseased renal tissue from patients with IgA nephropathy, lupus nephritis, and renal transplant rejection stained for Gas6 and Axl. Small vessels and glomeruli are shown. The normal glomeruli, which showed erythrocytes with autofluorescence in their capillaries, had little or no staining for Axl or Gas6. In the various diseases, Axl staining was mainly detected in the media of small vessels, in the glomeruli with a mesangial staining pattern, distal tubules, and collecting ducts. Gas6 was upregulated in the intima and media of small vessels, all segments of the tubules, along the brush border, and in the glomeruli with a mesangial staining pattern. Thus, Axl staining was detected in the vessel wall, in the glomerular capillary loops, and in the tubules. Gas6 staining was observed in a similar, colocalizing distribution. The protein expression of Gas6 and Axl did not appear to be disease specific but correlated to the degree of tissue damage of the biopsy. The data suggest that the Axl/Gas6 complex is involved in acute inflammatory renal diseases.

Ang II–Dependent Expression of Axl and Gas6 in VSMC and MC

We tested cultured VSMCs from rat and mouse aorta and immortalized human MCs. The cells were stimulated with Ang II (1×10^{-7} mol/L) for 6 hours or 18 hours (for Gas6 and Axl, respectively) and compared with control unstimulated cells. Figure 3 shows Gas6 expression in VSMCs. Immunofluorescent confocal microscopy and Western blot showed Gas6 expression with Ang II stimulation in the cytoplasmatic as well as the nuclear compartment (Fig 3A: VSMC; Fig 3B: MC). Gas6 was not expressed in quiescent cells. We next tested whether reactive oxygen species production might be involved in this expression. We reasoned that Ang II might function by stimulat-

Table 1. Demographic and Clinical Patient Data

Diagnosis	Age	Sex	Creatinine (mg/dL)	Creatinine Clearance (mL/min)	Proteinuria (g/L; g/d)	Blood Pressure (mm/Hg)	Histopathology
IgA Nephropathy	42	M	1.5	44	3 g/d	130/80	Mesangioproliferative GN with secondary FSGS
	51	M	ND	130	8.8 g/d	125/80	Mesangioproliferative GN with secondary FSGS
	35	M	1.4	ND	Positive	120/75	Mesangioproliferative GN with secondary FSGS
SLE Nephritis	54	F	0.9	93	12 g/L	140/85	Immuncomplex GN with secondary FSGS
	30	M	0.7	129	0.29 g/d	150/90	Immuncomplex GN with secondary FSGS
	27	M	1.0	102	1.97 g/d	120/60	Immuncomplex GN with secondary FSGS
Acute transplant rejection	29	M	4.9	25	0.43 g/d	120/80	Tubulointerstitial rejection
	54	M	4.2	25	0.39 g/d	110/80	Vascular and tubulointerstitial rejection
	29	F	1.8	46	0.88 g/d	130/90	Tubulointerstitial rejection
	27	M	8.7		ND	220/120	Vascular and tubulointerstitial rejection
	50	M	4.5	21	0.43 g/d	150/95	Tubulointerstitial rejection
	39	M	2.6	ND	ND	160/80	Vascular and tubulointerstitial rejection
	36	M	ND	ND	ND	ND	Vascular and tubulointerstitial rejection
	13	F	ND	ND	ND	ND	Vascular and tubulointerstitial rejection, thrombotic microangiopathy as recurrent disease
Immuncomplex GN	31	M	2.4	56	3.68 g/d	130/80	Mesangioproliferative GN with secondary FSGS
	63	M	2.5	29	1.66 g/d	120/70	Endocapillary proliferating GN with secondary FSGS
	7	F	ND	ND	ND		Endocapillary proliferating GN with secondary FSGS
Membranous GN	79	F	1.0	59	5.8 g/L	130/80	Membranous GN II-III (Ehrenreich + Churgh)
	68	M	1.6	ND	Positive	135/80	Membranous GN I-II (Ehrenreich + Churgh), diffuse diabetic GN
	60	F	1.9	33	6.5 g/d	190/100	Membranous GN III (Ehrenreich + Churgh)
ANCA-positive GN	30	F	2.2	31	7.68 g/d	140/90	Crescentic GN
	68	M	1.6	47	0.87 g/d	150/90	Crescentic GN with secondary glomerulosclerosis
	20	M	2.5	ND	5.28 g/L	140/70	Crescentic GN
Normal kidney	66	M	ND	ND	ND	ND	ND
	65	M	ND	ND	ND	ND	ND
	70	M	ND	ND	ND	ND	ND

NOTE. To convert creatinine in mg/dL to μmol/L, multiply by 88.4; creatinine clearance in mL/min to mL/s, multiply by 0.01667.

Abbreviations: GN, glomerulonephritis; FSGS, focal segmental glomerulosclerosis; SLE, systemic lupus erythematosis; ANCA, antineutrophil cytoplasmatic antigen; ND, not done.

ing NADPH oxidase. Cultures of VSMCs and MCs were transfected with p22phox antisense (or sense as a negative control) for 3 hours before stimulating the cells with Ang II (1×10^{-7} mol/L) for 6 hours. Antisense p22phox had no influence on the expression level of Gas6 or Axl in unstimulated cells. In Ang II–stimulated cells, antisense p22phox blocked the upregulation of Gas6 expression, whereas sense control had no effect (shown by immunohistochemistry and Western blotting). Figure 4 shows similar studies for Axl in VSMCs (Fig 4A) and MCs (Fig 4B). Immunofluorescent confocal microscopy showed that Ang II stimulated Axl expression. The effect was blocked by antisense to p22phox but not by sense or scrambled control. Western blotting confirmed these findings. In p47 knockout cells, Ang II (1×10^{-7} mol/L) failed to induce Axl or Gas 6 expression. Figure 5A and B show no effect of Ang II on Gas6 or Axl expression in mouse VSMCs of p47 knockout cells compared with wild-type cells, as analyzed by immunofluorescent confocal microscopy.

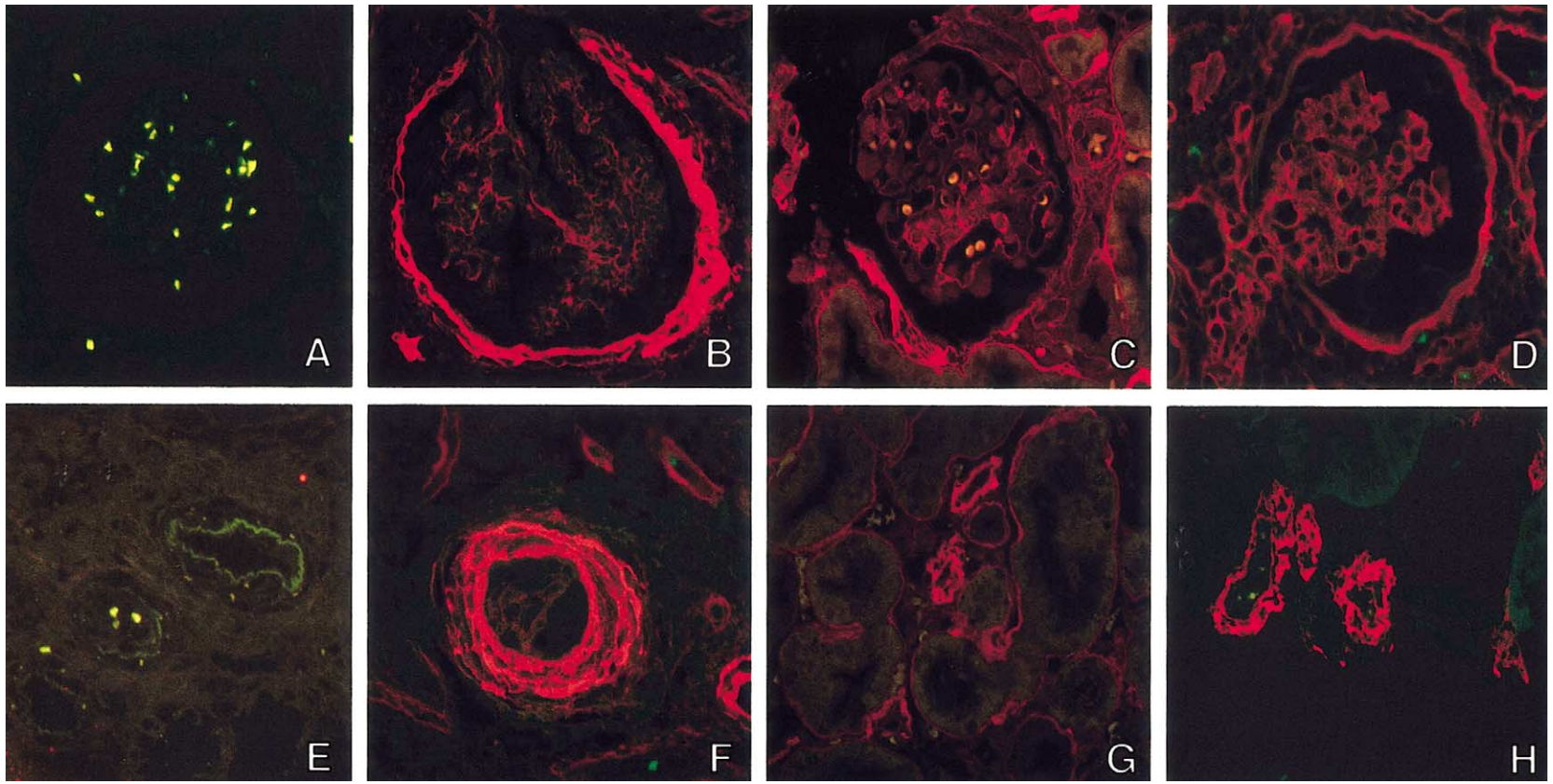

Fig 1. Gas6 expression in normal and diseased renal tissue (A, B, E, F from nephrectomy; C, D, G, H from renal biopsy) in the glomeruli (A-D) and the arterial vessels (E-H): (A and E) normal kidney; (B and F) acute vascular and cellular rejection; (C and G) IgA nephropathy; (D and H) lupus nephritis.

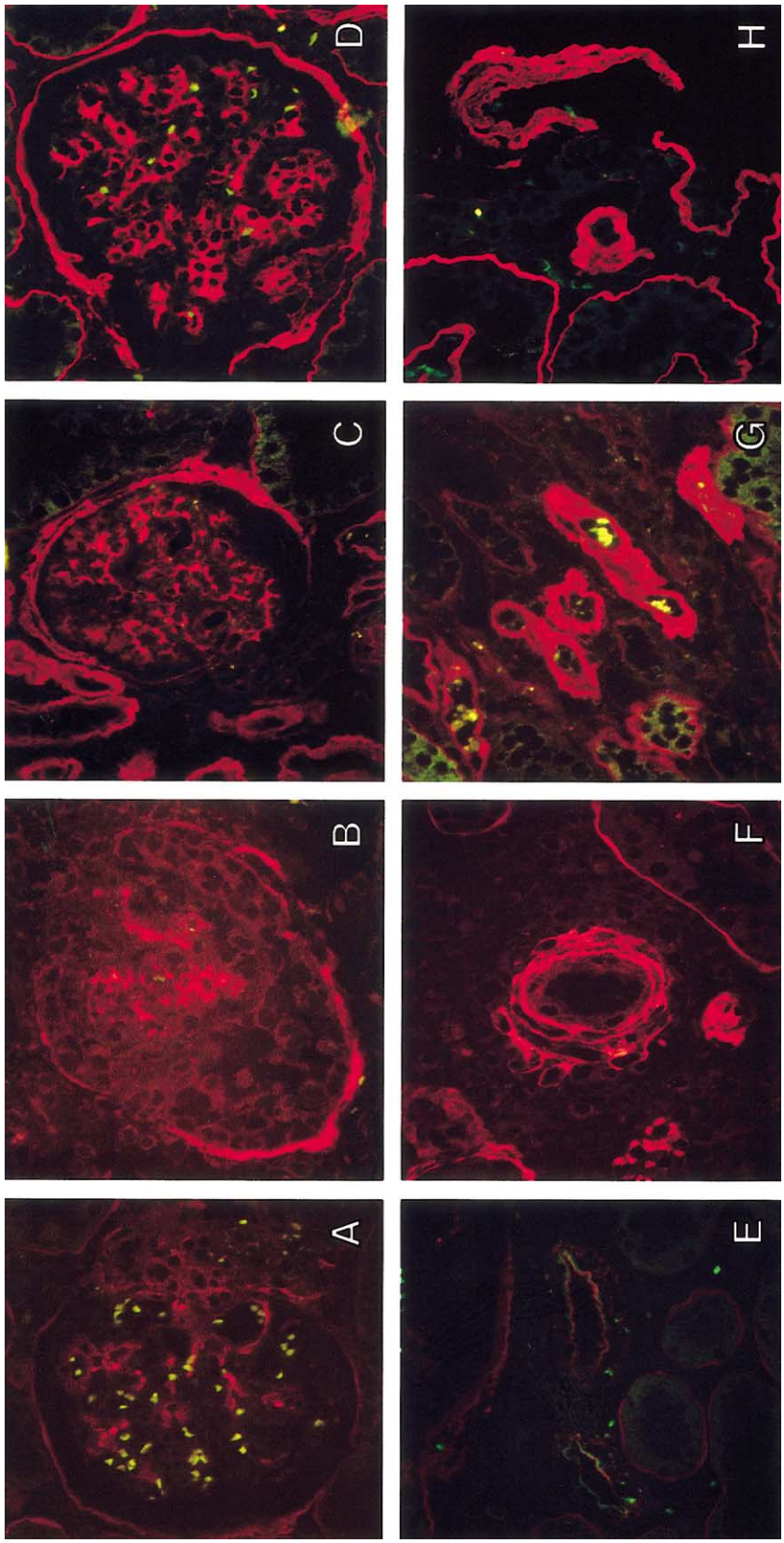

Fig 2. Axl expression in normal and diseased renal tissue (A, B, E, F from nephrectomy; C, D, G, H from renal biopsy) in the glomeruli (A-D) and the arterial vessels (E-H): (A and E) normal kidney; (B and F) acute vascular and cellular rejection; (C and G) IgA nephropathy; (D and H) lupus nephritis.

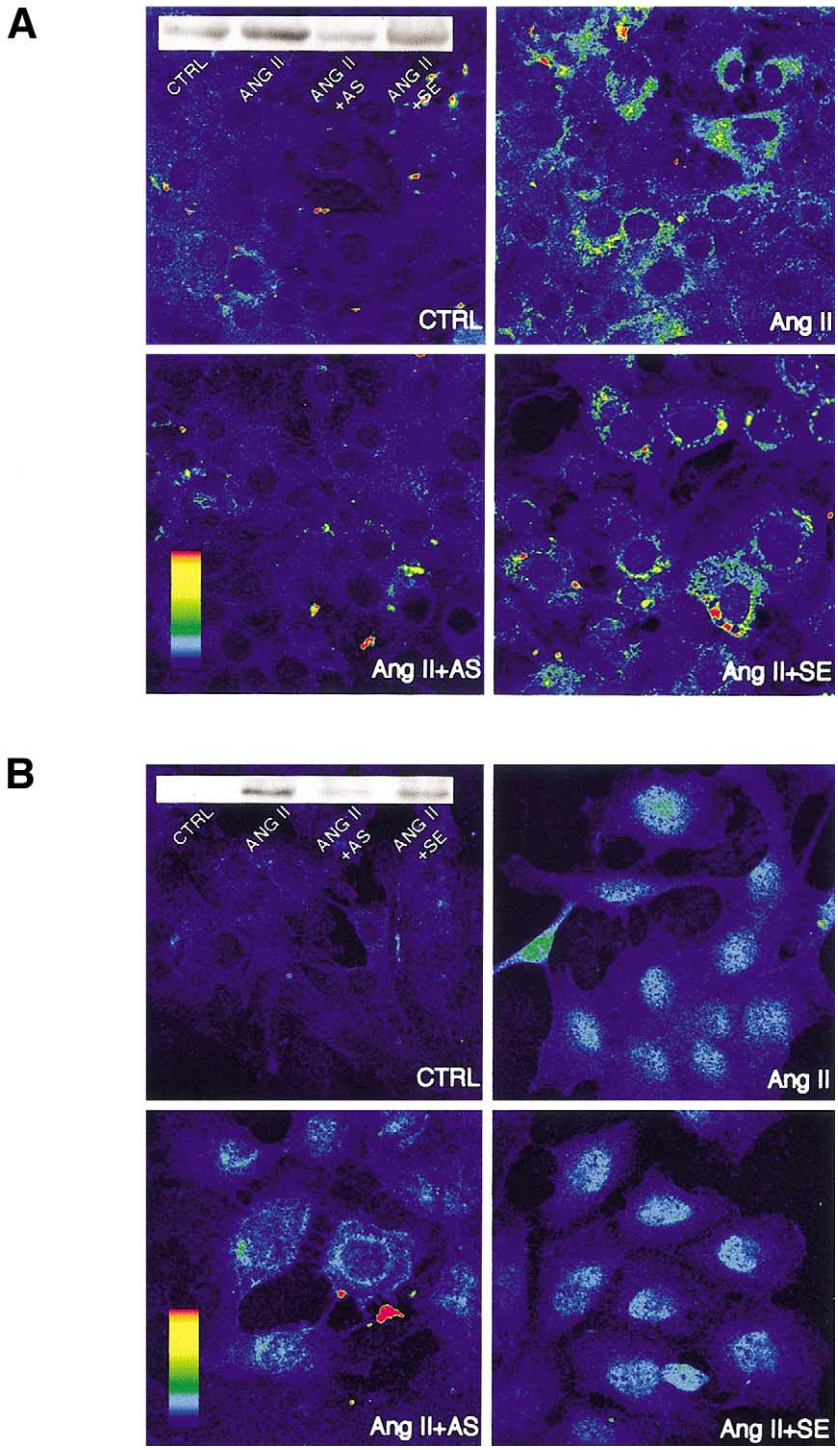

Fig 3. Confocal microscopy as well as Western blot confirm the crucial role for p22phox for Ang II–induced Gas6 expression in VSMCs (A) and MCs (B): CTRL (untreated cells), Ang II (angiotensin II, 10^{-7}mol/L, 6 hours), Ang II + AS (cells transfected with p22phox antisense oligonucleotides before Ang II stimulation), Ang II + SE (cells transfected with p22phox sense oligonucleotides before Ang II stimulation), Ang II + SC (cells transfected with p22phox scrambled oligonucleotides before Ang II stimulation).

DISCUSSION

This study describes the expression of Gas6 and Axl in human renal diseases and normal renal tissue. Interestingly, both proteins were copiously expressed in inflammatory renal diseases of various etiologies. We found that the Gas6/Axl pathway is activated in all forms of acute renal diseases tested. Gas6/Axl also partici-

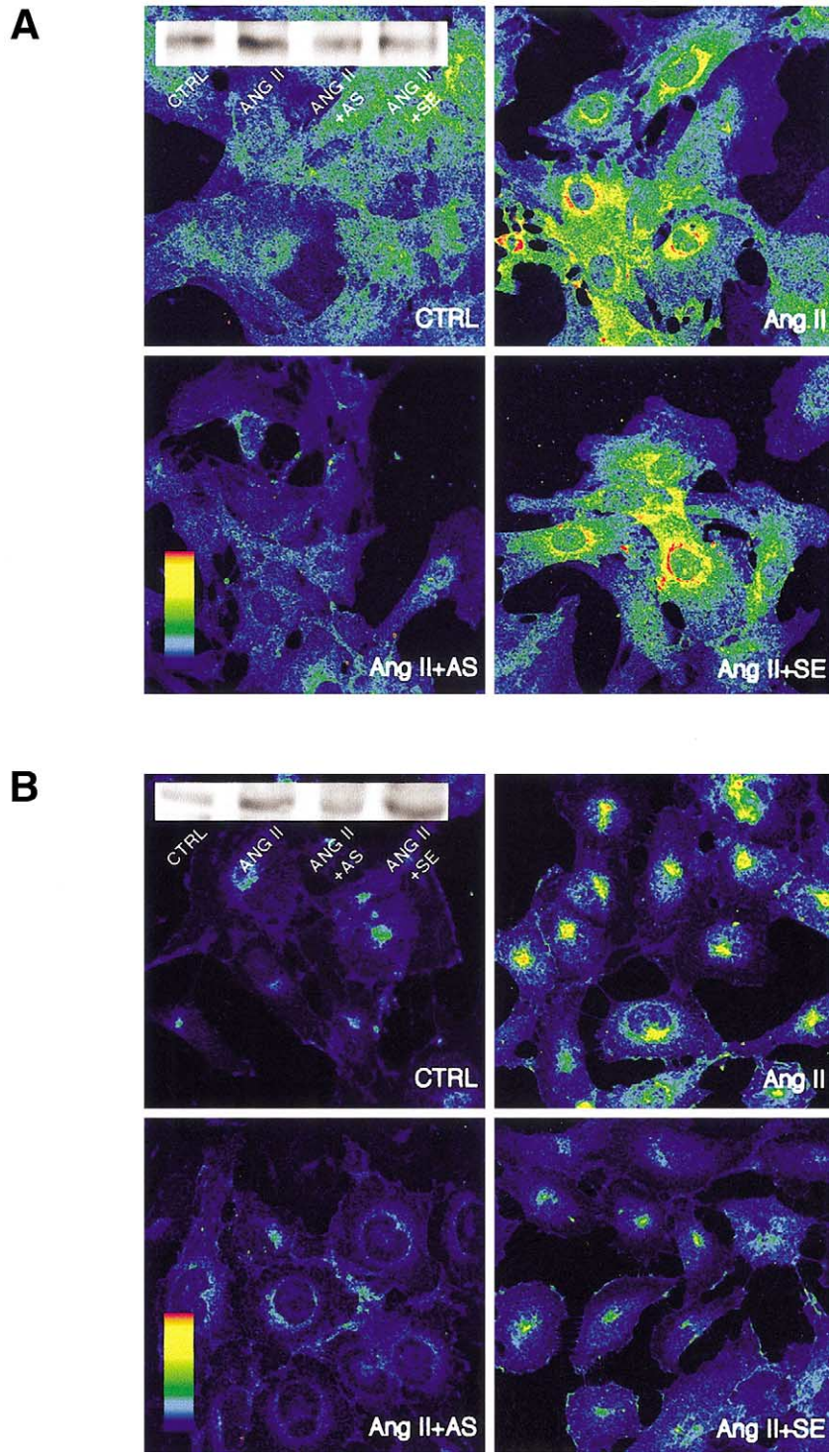

Fig 4. Confocal microscopy (A) as well as Western blot (B) confirm the crucial role for p22phox for Ang II–induced Axl expression in VSMCs (A) and MCs (B): CTRL (untreated cells), Ang II (Ang II, 10^{-7}mol/L, 18 hours), Ang II + AS (cells transfected with p22phox antisense oligonucleotides before Ang II stimulation), Ang II + SE (cells transfected with p22phox sense oligonucleotides before Ang II stimulation), Ang II + SC (cells transfected with p22phox scrambled oligonucleotides before Ang II stimulation).

pated in acute cellular and vascular transplant rejection. We then performed in vitro studies to gain insight into a possible common activating mechanism. Inflammatory cells are intimately involved in all the diseases we studied. We therefore selected reactive oxygen species and chose to stimulate the NADPH oxidase in VSMCs with Ang II. We found that Ang II rapidly elicits

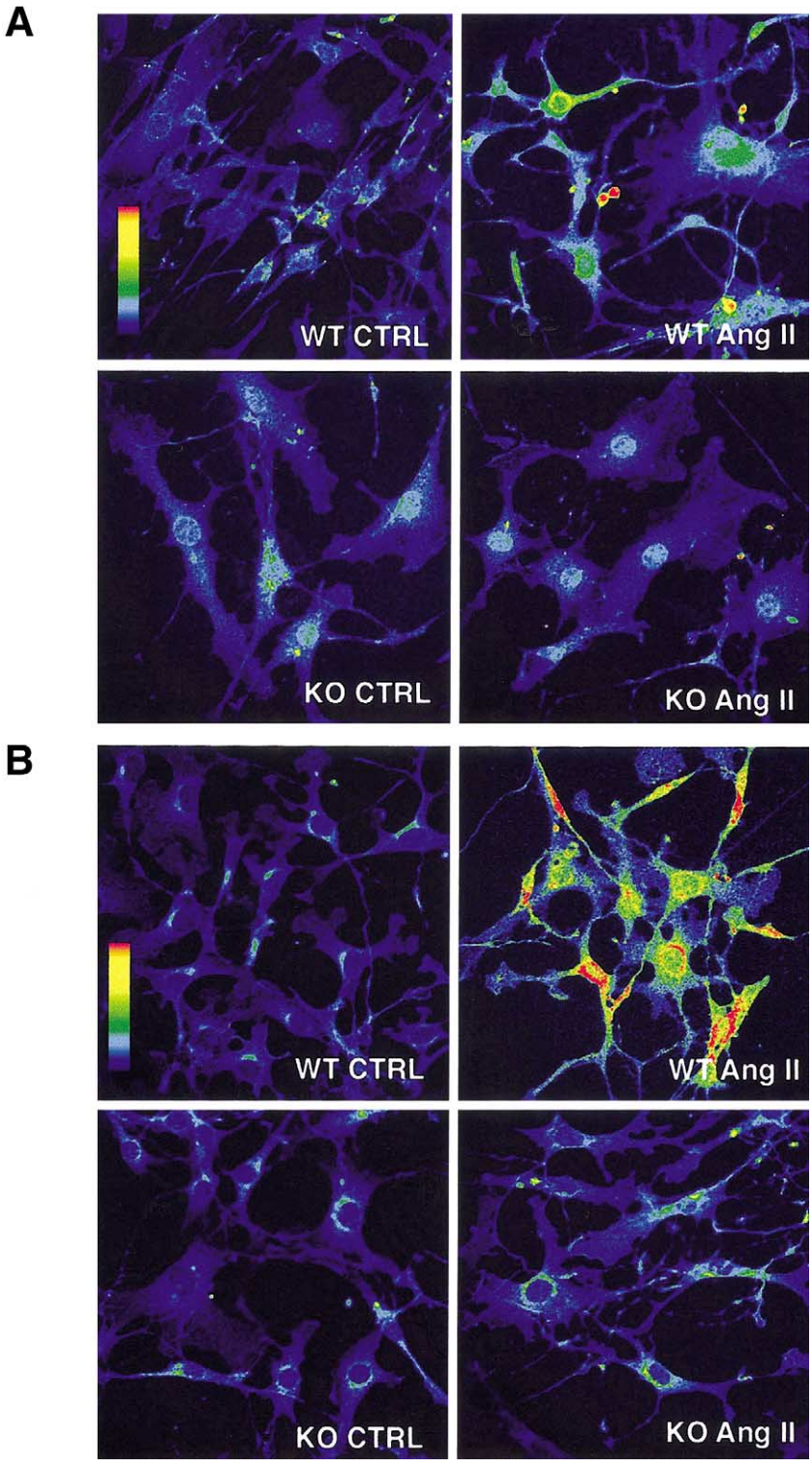

Fig 5. Confocal microscopy confirms the crucial role for NADPH oxidase for Ang II–induced Gas6 (Ang II, 10^{-7}mol/L; 6 hours), and Axl (Ang II, 10^{-7}mol/L; 18 hours) expression in VSMCs: Gas6 (A) and Axl (B) are induced by Ang II in wild-type (WT) but not in p47 knockout (KO) cells.

Gas6/Axl expression in these cells but only if the NADPH oxidase is functioning. These findings suggest that reactive oxygen species may be important for the stimulation of Gas6 and Axl.

Axl remained an "orphan" receptor until Varnum et al[4] and Stitt et al[13] showed that Gas6 is the ligand for the Axl receptor. Axl was shown to potentiate the growth response of VSMCs to G protein–coupled receptor agonists, including Ang II.[14] Subsequently, Melaragno et al[14] established the importance of the Gas6/Axl system in vascular cell function when they performed carotid injury studies in rats. Their studies led them to conclude that Gas6/Axl is an early downstream event after vascular injury that may suppress apoptosis and stimulate VSMC migration and proliferation. That Gas6, true to its name, *growth arrest–specific gene*, inhibits apoptosis, led to studies investigating possible mechanisms.[6] Gas6 was shown to activate src and the phosphatidylinositol-3-OH kinase (PI3K).[15] PI3K signals via Akt to inhibit the degradation of the nuclear factor kappa-B (NF-κB), the transcription factor that facilitates survival.[16] Subsequently, the dependence of Gas6 antiapoptosis on NF-κB activation has been documented in detail.[17] NF-κB is involved in all inflammatory glomerular and vascular diseases.[18] NF-κB is activated by numerous mechanisms; however, the role of reactive oxygen species is particularly prominent.[19]

Interestingly, Gas6 is a vitamin K–dependent growth factor whose action is inhibited by the anticoagulant warfarin.[5,20] Gas6 activities depend on g-carboxylation of glutamate residues on the Gas6 N terminus.[20] Yanagita et al[21] have shown that warfarin and the extracellular domain of Axl can both inhibit mesangial cell proliferation and ameliorate the Thy1 model of glomerulonephritis.[8] These novel observations underscore the notion that Gas6 is a prominent therapeutic target. Yanagita et al[10] then studied Gas6 gene–disrupted mice and found that the mice were astoundingly resistant to the development of nephrotoxic nephritis. The mice were "rescued" from their resistance by the replacement of Gas6. Whereas the use of warfarin in clinical studies in advanced disease did have some beneficial effects for the outcome of glomerulonephritis,[22] similar clinical studies inhibiting g-carboxylation of proteins at an early stage of glomerular damage have not been performed. Yin et al[9] showed increased Gas6 expression in rat kidneys during acute rejection, acute tubular necrosis, and chronic allograft nephropathy, as well as increased Axl expression during acute tubular necrosis. The experimental data from animal studies, coupled with data from Yin and the information we report here, underscore the fundamental importance of Gas6/Axl signaling in inflammatory renal disease.

Mutant mice, deficient in Axl and the 2 other structurally related receptor tyrosine kinases, Tyro3 and Mer, exhibit hyperproliferation of their continuously activated B and T cells. As a result, they have hyperplastic secondary lymphoid tissue and have autoimmunity. The mice exhibit lesions similar to those observed in rheumatoid arthritis, lupus erythematosus, and pemphigus vulgaris. Their antigen-presenting dendritic cells express elevated levels of activation markers. In triple-mutant mice lacking all 3 receptor tyrosine kinases, namely Axl, Mer, and Sky, an increased proliferation of all B and T cells also takes place (T $>$ B-cells, CD4 $>$ CD8 cells). Furthermore, a chronic-activated protein C hyperactivity and typical features of autoimmunity have been shown.[23] These findings point to a role of the 3 receptor-tyrosine kinases and their interaction in controlling immune and inflammatory mechanisms.

Hafizi et al[24] recently confirmed the involvement of PI3K and Grb2 in the Axl signaling cascade with a large-scale yeast-2 hybrid screen. They identified SOCS-1 and Nck2 as binding partners for Axl and characterized a new protein, which they termed *C1-TEN*, the C1 domain-containing phosphatase and TENs in homologue. C1-TEN is an intracellular protein with multiple interaction domains and an almost universal expression pattern with highest levels in heart, kidney, and liver. Thus, a series of new signaling molecules currently are being identified that are relevant to Gas6/Axl.

We performed cell culture experiments to study the Ang II–-induced expression of the Axl-Gas6 pathway further. We selected Ang II as a stimulant purposely knowing that Ang II stimulates Gas6/Axl in VSMCs and also because of the relevance that Ang II has for the progression of any renal disease.[25] Ang II stimulates Gas6 and Axl in mesangial cells, as well. Furthermore, we were aware that blockage of the NADPH oxidase prevents Ang II–induced superoxide generation in vitro, which might act as second messenger

for long-term responses[26] and in the signaling cascade to activate Gas6 and Axl expression.

Our findings are admittedly preliminary and descriptive. The numbers of patients studied in each group were small, and the degree of kidney damage varied within the groups. Final conclusions to relate expression pattern of Gas6 and Axl to the disease type cannot be drawn for certain. To ultimately prove evidence of the Gas6/Axl pathway in Ang II–induced renal damage, a blocking experiment will have to be done in vitro. We are engaged in such studies. However, because Gas6/Axl signaling has a profound effect on experimental nephritis, and because Gas6 may be a promising target that can be influenced with agents already available, we suggest that Gas6/Axl are clinically relevant molecules.

ACKNOWLEDGMENT

The authors thank P. Quass, G. N′diaye, and M. Schmidt for their excellent technical assistance.

REFERENCES

1. O'Bryan JP, Frye RA, Cogswell PC, et al: Axl, a transforming gene isolated from primary human myeloid leukemia cells, encodes a novel receptor tyrosine kinase. Mol Cell Biol 11:5016-5031, 1991

2. Janssen JWG, Schulz AS, Steenvoorden ACM, et al: A novel putative tyrosine kinase receptor with oncogenic potential. Oncogene 6:2113-2120, 1991

3. Neubauer A, Fiebeler A, Graham DK, et al: Expression of axl, a transforming receptor tyrosine kinase, in normal and malignant hematopoiesis. Blood 84:1931-1941, 1994

4. Varnum BC, Young C, Elliott G, et al: Axl receptor tyrosine kinase stimulated by the vitamin K-dependent protein encoded by growth-arrest-specific gene 6. Nature 373: 623-626, 1995

5. Manfioletti G, Brancolini C, Avanzi G, Schneider C: The protein encoded by a growth arrest-specific gene (gas6) is a new member of the vitamin K-dependent proteins related to protein S, a negative coregulator in the blood coagulation cascade. Mol Cell Biol 13:4976-4985, 1993

6. Goruppi S, Ruaro E, Schneider C: Gas6, the ligand of Axl tyrosine kinase receptor, has mitogenic and survival activities for serum starved NIH3T3 fibroblasts. Oncogene 12:471-480, 1996

7. Lee WP, Liao Y, Robinson D, Kung HJ, Liu ET, Hung MC: Axl-gas6 interaction counteracts E1A-mediated cell growth suppression and proapoptotic activity. Mol Cell Biol 19:8075-8082, 1999

8. Yanagita M, Arai H, Ishii K, et al: Gas6 regulates mesangial cell proliferation through Axl in experimental glomerulonephritis. Am J Pathol 158:1423-1432, 2001

9. Yin JL, Pilmore HL, Yan YQ, et al: Expression of growth arrest-specific gene 6 and its receptors in a rat model of chronic renal transplant rejection. Transplantation 73:657-660, 2002

10. Yanagita M, Ishimoto Y, Arai H, et al: Essential role of Gas6 for glomerular injury in nephrotoxic nephritis. J Clin Invest 110:239-246, 2002

11. Muller DN, Mervaala EM, Dechend R, et al: Angiotensin II (AT(1)) receptor blockade reduces vascular tissue factor in angiotensin II-induced cardiac vasculopathy. Am J Pathol 157:111-122, 2000

12. Haller H, Quass P, Lindschau C, Luft FC, Distler A: Platelet-derived growth factor and angiotensin II induce different spatial distribution of protein kinase C-alpha and -beta in vascular smooth muscle cells. Hypertension 23:848-852, 1994

13. Stitt TN, Conn G, Gore M, et al: The anticoagulation factor protein S and its relative, Gas6, are ligands for the Tyro 3/Axl family of receptor tyrosine kinases. Cell 80:661-670, 1995

14. Melaragno MG, Wuthrich DA, Poppa V, et al: Increased expression of Axl tyrosine kinase after vascular injury and regulation by G protein-coupled receptor agonists in rats. Circ Res 83:697-704, 1998

15. Goruppi S, Ruaro E, Varnum B, Schneider C: Requirement of phosphatidylinositol 3-kinase-dependent pathway and Src for Gas6-Axl mitogenic and survival activities in NIH 3T3 fibroblasts. Mol Cell Biol 17:4442-4453, 1997

16. Datta SR, Brunet A, Greenberg ME: Cellular survival: A play in three Akts. Genes Dev 13:2905-2927, 1999

17. Demarchi F, Verardo R, Varnum B, Brancolini C, Schneider C: Gas6 anti-apoptotic signaling requires NF-kappaB activation. J Biol Chem 25:25, 2001

18. Luft FC: Angiotensin, inflammation, hypertension, and cardiovascular disease. Curr Hypertens Rep 3:61-67, 2001

19. Griendling KK, Sorescu D, Ushio-Fukai M: NAD(P)H oxidase: Role in cardiovascular biology and disease. Circ Res 86:494-501, 2000

20. Nakano T, Kawamoto K, Kishino J, Nomura K, Higashino K, Arita H: Requirement of gamma-carboxyglutamic acid residues for the biological activity of Gas6: Contribution of endogenous Gas6 to the proliferation of vascular smooth muscle cells. Biochem J 323:387-392, 1997 (pt 2)

21. Yanagita M, Ishii K, Ozaki H, et al: Mechanism of inhibitory effect of warfarin on mesangial cell proliferation. J Am Soc Nephrol 10:2503-2509, 1999

22. Zimmerman SW, Moorthy AV, Dreher WH, Friedman A, Varanasi U: Prospective trial of warfarin and dipyridamole in patients with membranoproliferative glomerulonephritis. Am J Med 75:920-927, 1983

23. Lu Q, Lemke G: Homeostatic regulation of the immune system by receptor tyrosine kinases of the Tyro 3 family. Science 293:306-311, 2001

24. Hafizi S, Alindri F, Karlsson R, Dahlback B: Interaction of Axl receptor tyrosine kinase with C1-TEN, a novel C1 domain-containing protein with homology to tensin. Biochem Biophys Res Commun 299:793-800, 2002

25. Remuzzi G, Ruggenenti P, Perico N: Chronic renal diseases: Renoprotective benefits of renin-angiotensin system inhibition. Ann Intern Med 136:604-615, 2002

26. Griendling KK, Minieri CA, Ollerenshaw JD, Alexander RW: Angiotensin II stimulates NADH and NADPH oxidase activity in cultured vascular smooth muscle cells. Circ Res 74:1141-1148, 1994